



<https://theses.gla.ac.uk/>

Theses Digitisation:

<https://www.gla.ac.uk/myglasgow/research/enlighten/theses/digitisation/>

This is a digitised version of the original print thesis.

Copyright and moral rights for this work are retained by the author

A copy can be downloaded for personal non-commercial research or study,  
without prior permission or charge

This work cannot be reproduced or quoted extensively from without first  
obtaining permission in writing from the author

The content must not be changed in any way or sold commercially in any  
format or medium without the formal permission of the author

When referring to this work, full bibliographic details including the author,  
title, awarding institution and date of the thesis must be given

Enlighten: Theses

<https://theses.gla.ac.uk/>  
[research-enlighten@glasgow.ac.uk](mailto:research-enlighten@glasgow.ac.uk)

AN INVESTIGATION OF SOME TECHNIQUES FOR THE  
LOCALISATION OF IONIZING RADIATION.

by

JAMES HOUGH

DEPARTMENT OF NATURAL PHILOSOPHY  
UNIVERSITY OF GLASGOW

PRESENTED AS A THESIS FOR THE DEGREE OF Ph.D.  
IN THE UNIVERSITY OF GLASGOW

NOVEMBER, 1970

ProQuest Number: 10868056

All rights reserved

INFORMATION TO ALL USERS

The quality of this reproduction is dependent upon the quality of the copy submitted.

In the unlikely event that the author did not send a complete manuscript and there are missing pages, these will be noted. Also, if material had to be removed, a note will indicate the deletion.



ProQuest 10868056

Published by ProQuest LLC (2018). Copyright of the Dissertation is held by the Author.

All rights reserved.

This work is protected against unauthorized copying under Title 17, United States Code  
Microform Edition © ProQuest LLC.

ProQuest LLC.  
789 East Eisenhower Parkway  
P.O. Box 1346  
Ann Arbor, MI 48106 – 1346

## CONTENTS

	<u>Page</u>
Preface	
Acknowledgements	
Chapter I	Detectors for the Localisation of Ionizing Radiation. 1
Chapter II	The Fundamental Limitation to the Position Resolution of some Electronic Detectors. 18
Chapter III	Principle and Design of some Proportional Counter Systems. 29
Chapter IV	Proportional Counters for Position Sensitivity in One Dimension. 45
Chapter V	The Performance of the One Dimensional Counter Systems. 60
Chapter VI	A Proportional Counter for Position Sensitivity in Two Dimensions. 69
Chapter VII	Conclusion 91
Appendix	The Possible Operation of a Pulse Counter with an Organic Liquid Filling.
References	

## PREFACE.

This thesis contains an account of the experimental work performed by the author at the University of Glasgow during the period between October 1967 and September 1970.

The research carried out was on the development and study of position sensitive proportional counters and was initiated by Dr. R.W.P. Drever.

The first chapter of this thesis is a discussion of the type of experimental problems which require the spatial distribution of ionizing radiation to be investigated and of the different methods of obtaining position information. The possible advantages of a proportional counter system for the localisation of charged particles and low energy x-rays are pointed out.

In the following chapter, the main factors which limit the position resolution of any electrical detector are outlined, with particular emphasis on the effect of the thermal diffusion of the charge carriers in semiconductor counters, proportional counters and spark chambers.

The material for these two chapters was taken mainly from the literature, although the application of diffusion theory to the calculation of the position resolution in the different detectors was the work of the author.

Chapter III includes a general description of the method of charge division on a resistive electrode for obtaining position information from a counter; and the limitations to position linearity

and resolution which result from the use of this method (as reported in the literature) are discussed. The electronic system required for a position sensitive proportional counter is described and the design and development by the author of a high precision ratio circuit for this work is outlined.

The next chapter is an account of the experimental measurements of resolution and linearity performed by the author on proportional counters which were sensitive to position in one dimension. The position resolutions for single electrons, alpha particles and x-rays were measured, and the experimental resolution for single electrons is compared with the limitations from gas diffusion theory in Chapter V. The data for this comparison was partly drawn from the literature; but one of the methods used for calculating the electron diffusion in a gas mixture was devised by the author. The interpretation of the performance of these detectors, in Chapter V, is also that of the writer.

Chapter VI deals with the building and operation of a two dimensional position sensitive proportional counter which uses a new method of obtaining the counter signal - from electrodes placed between the anode and the cathode. This method was proposed by Dr. Drever. The counter frame used for this work had been designed initially by him, but a number of important modifications to it were made by the author. The development of the counter and the investigation of its performance were the entire responsibility of the author.

The appendix to this thesis is an account of an attempt to

observe proportional counter or Geiger counter operation in a cylindrical detector filled with liquid hexane. This work was initiated and carried out by the writer.

#### Acknowledgements.

The author would like to thank Professor P.I. Dee for his interest and encouragement throughout this work.

The work was carried out under the supervision of Dr. R.W.P. Drever, and the author is grateful to him for his help and stimulating advice.

He would also like to express his gratitude to Dr. K.W.D. Ledingham and Mr. A.L. Cockroft for many useful discussions.

Considerable technical assistance was given by Mr. A. McKellar, Mrs. E. Taylor, Mr. J.T. Lloyd, and by the workshop staff under Mr. J. Baird, and the stores staff under Mr. R.E. Donaldson.

The author wishes to acknowledge financial support from the University of Glasgow during the period when the work described here was carried out.

## Chapter I.

### DETECTORS FOR THE LOCALISATION OF IONIZING RADIATION.

#### Introduction

The development of different methods of radiation detection has allowed many advances to be made in different scientific fields - from the determination of nuclear properties to the visualisation of organs in the human body treated with radioactive tracer material.

In particular, radiation detectors which give an electrical output signal for the entry of a particle or photon have been of value, because of their capabilities for fast data collection and display in an experiment. Unfortunately, these instruments - such as the ionization chamber and the proportional, Geiger, scintillation and semiconductor counters - give no information as to the spatial distribution of the radiation detected and, as will be discussed below, this limits their usefulness for many applications.

There are three main classes of experiment where the position of the incident radiation in a detector system should be known -

- a) Scattering experiments in nuclear physics.
- b) Spectrometer applications.
- c) The image formation of radiation distributions.

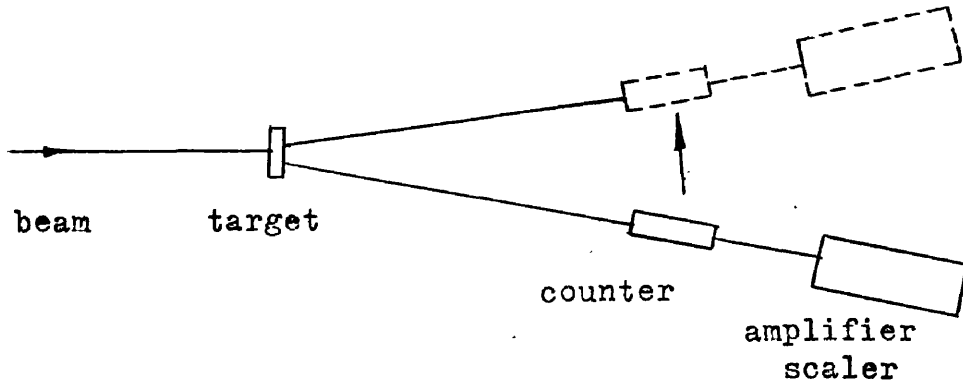
Scattering Experiments. Suppose an experiment for the scattering of a beam of particles or photons from a target is to be carried out. This may be to determine the nuclear cross section of a particular target

material for a given energy of particles, or to determine the polarisation of the incident beam; but, in general, it is the angular distribution of the scattered particles or photons which is measured in the experiment. Techniques for making this type of measurement have included the use of nuclear emulsions or the photographic output from a spark chamber. However, neither of these methods gives immediately usable information and, in both cases, the expenditure of labour on the scanning and measuring of the emulsions or plates is a serious disadvantage. An electrical detecting system eliminates both these factors.

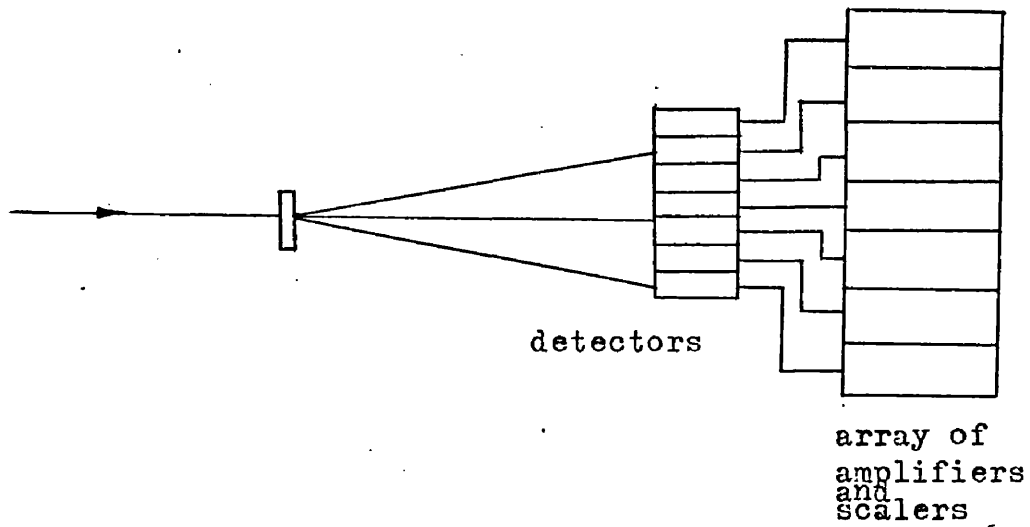
Although a single electrical counter is suitable for finding the number of particles scattered from a beam at a given angle as, for example, a function of the beam energy, there are difficulties if an angular distribution has to be obtained. For, in this case, the counter must be moved to different angles and the count rate measured at each angle (as in Fig.1-1(a).) The total measurement time becomes long (especially if the count rate is low) and the results are dependent on the long term stability of both the incident particle beam and the detecting equipment. For angular distributions it is best to make measurements on all angles of interest at the same time. One method of doing this is to have an array of detectors each with its own electronics and readout facility, which is usually a scaler - Fig.1-1(b). However, if the angular range to be covered is large and high angular resolution is required, the complexity and cost of the equipment becomes excessive and the reliability of the system falls. Thus there is a need in this

SIMPLE SCATTERING EXPERIMENT.

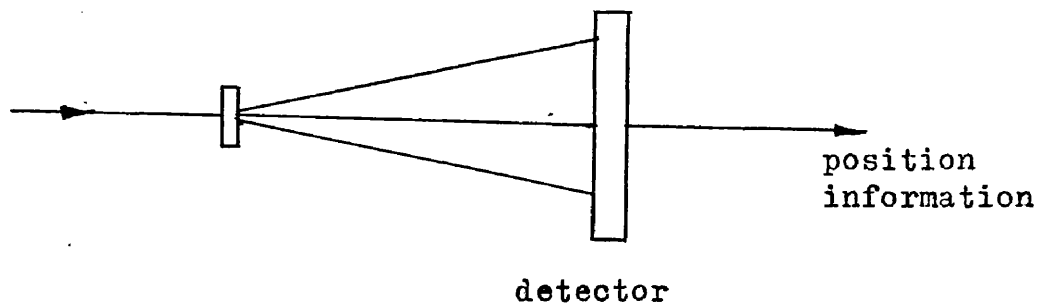
- a) Movement of a single counter to different angles.



- b) The use of an array of detectors.



- c) The use of a position sensitive detector.

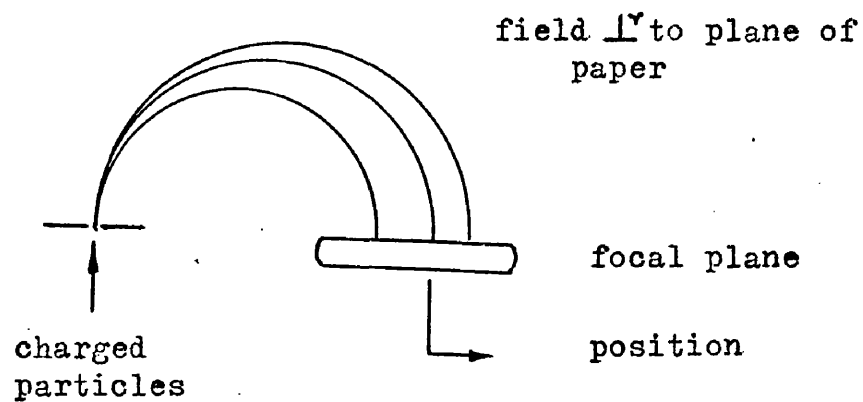


type of experiment for a detector which gives direct position information with a simple electronic readout system and which provides fast data collection and display - Fig.1-1(c). Information in one dimension is usually sufficient for most applications; but the utilisation of a detector to give the position of the scattered particles in two dimensions would make better use of the scattered beam and would allow simpler alignment of the target and detector.

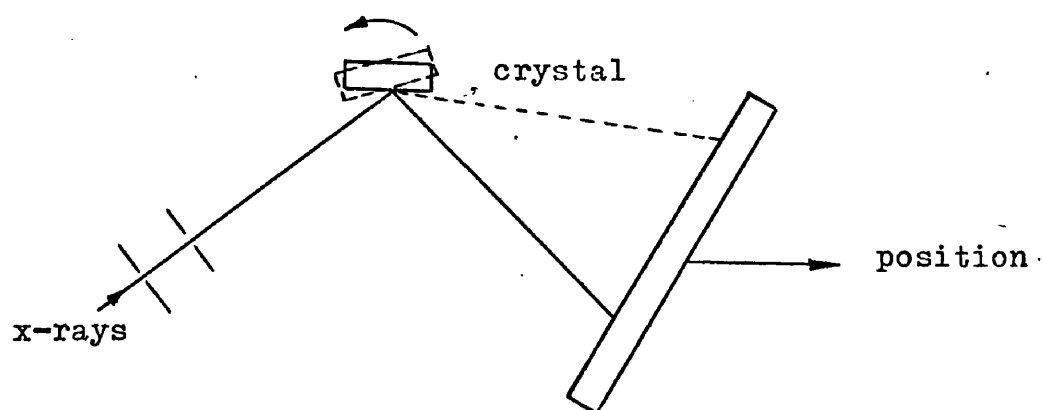
Spectrometer Applications. Another similar problem is encountered in the analysis of the output of spectrometers, which deflect particles or photons of different energy to different positions in space. This dispersion of different energies is obtained by magnetic effects for charged particles and by diffraction for x-rays and ultra-violet radiation. Most magnetic spectrometers for charged particles (electrons, protons, alpha particles, etc.) deflect particles of different energy on to different points on a focal line or plane, and some type of detection system which is position sensitive in one dimension must be placed on this focal surface to measure the distribution of the radiation. The possible detecting systems are the same as those for scattering experiments which were discussed above, and the same disadvantages of these standard methods are encountered again. Thus, in this case also, a detector which gives direct position information in one dimension is of considerable value (see Fig.1-2(a)).

Such a detector system can also simplify the analysis of x-ray spectra from a crystal or a powder sample, or ultra-violet spectra from a grating, as a direct measurement of the diffracted intensity at

a) POSITION SENSITIVE DETECTOR FOR FOCAL PLANE OF  
MAGNETIC SPECTROMETER.



b) POSITION SENSITIVE DETECTOR FOR CRYSTAL SPECTROMETER  
FOR X-RAYS.



different positions can then be made. Fig.1-2(b) shows a possible arrangement for the diffraction of x-rays at a crystal surface, the crystal being rocked through a range of angle to cover the required spectral range.

In certain applications, such as the examination of crystal structure by the diffraction of monochromatic x-rays by a powder sample or by the diffraction of a continuous x-ray spectrum by a single crystal, the diffracted beam carries information in two dimensions. Thus, in order to obtain full information on the distribution of intensity with position, a method of detection which is sensitive in two dimensions is required. This will be discussed below.

Imaging Experiments. Many of the applications of ionizing radiation in the biological and medical field require the image formation of the spatial intensity of x-rays or charge particles - for instance, in the examination of crystal structure as was mentioned above; in x-ray radiography; and in the visualisation of certain organs in the body by the addition of radioactive tracer materials, which are usually gamma ray emitting.

The normal photographic methods of x-ray shadow radiography do not allow 'in vivo' studies, where the movement of some part of the body may be of interest, and they do not give accurate intensity information. However, an electronic recording technique can overcome these disadvantages.

Gamma ray imaging of a surface can be accomplished by the scanning of a single detector (which is well collimated so that a small

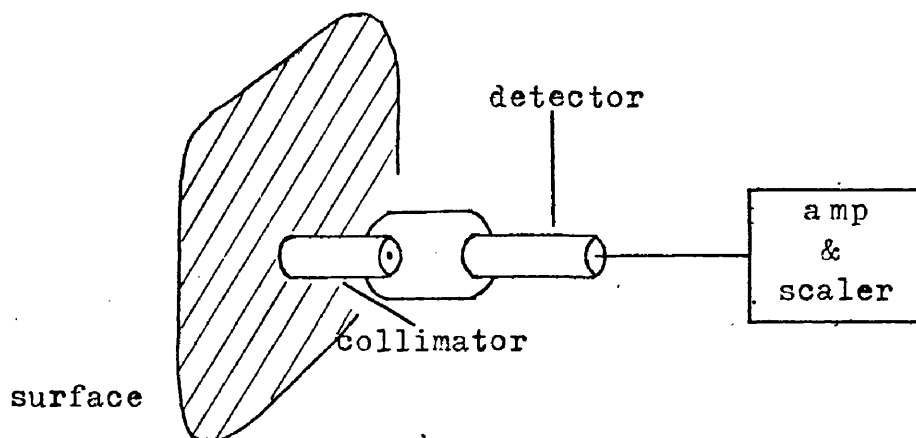
part of the surface only is viewed at each position) over the area of interest, or by having an array of detectors each with its own electronic channel (see Figs. 1-3(a and b)). Again the problems of measurement time and complexity of apparatus are very relevant and improvements can be made by the use of a simple position detecting system.

At present, there is a strong interest in x-ray astronomy and in the imaging of soft x-ray sources such as solar flares. This can be achieved with an x-ray focussing telescope as used by Giacconi et al (1960, 63) in which the x-rays are reflected at grazing incidence, first from a paraboloidal and then a hyperboloidal surface to give an image of about 1cm diameter. With the carriage of such devices in rockets, satellites or balloons, which may not be recoverable, electronic detection of the focussed x-ray flux is a considerable advantage in that the information obtained can be conveyed to earth by telemetry. One method of building up the image of an x-ray source is to use a collimated detector at the centre of the focal plane of the telescope so that it only views a small element of the telescope's field. This arrangement is shown in Fig. 1-4(a). The full image can be obtained by scanning the telescope over the required area of sky. However, this scanning would not be necessary if an electronic counter with the capability of giving the position co-ordinates of a detected photon was placed in the focal plane of the telescope.

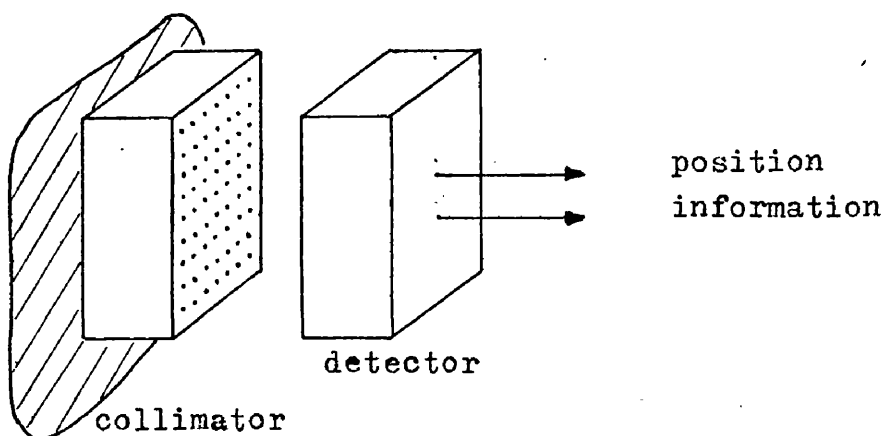
The same type of electrical counting technique would be of value in the x-ray telescope suggested by Young (1963) and Mertz (1965), in which the x-ray image of an area of sky can be reconstructed from the

IMAGE INFORMATION OF A RADIATION DISTRIBUTION.

- a) Single detector and collimator scanned over gamma ray emitting surface.

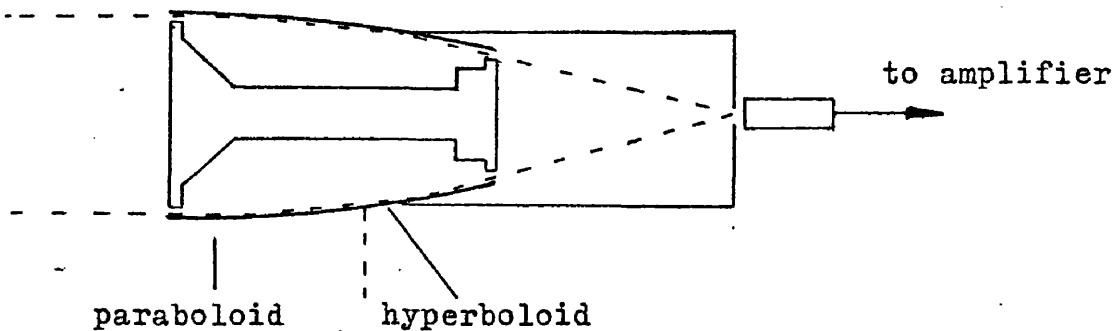


- b) Image of the surface with a multichannel collimator and a two dimensional position sensitive detector.

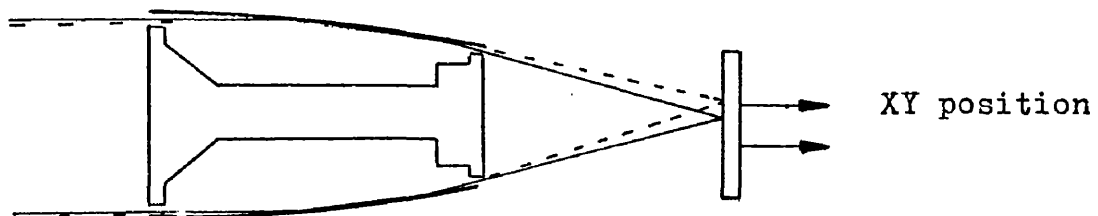


X RAY IMAGE FORMATION WITH A FOCUSING TELESCOPE.

- a) Counter collimated to view only a small part of the field. Image formed by scanning over area of interest.



- b) Inverted image formed by position sensitive detector.



shadow pattern of a Fresnel zone plate viewing the area.

The position location in two dimensions of charge particles is also of importance in the profile analysis of secondary charged particle beams from accelerators, and in the analysis of chromatograph plates for the detection of particular substances which have been tagged with radioactive tracer. In each of these cases the replacement of the standard detection methods of a single counter or array of counters with a detector giving direct position information can lead to a simplification of the apparatus and experimental procedure.

These examples illustrate some of the applications where relatively simple position sensitive electrical detectors are of use; and in the following section a review of the different designs of such detectors is given.

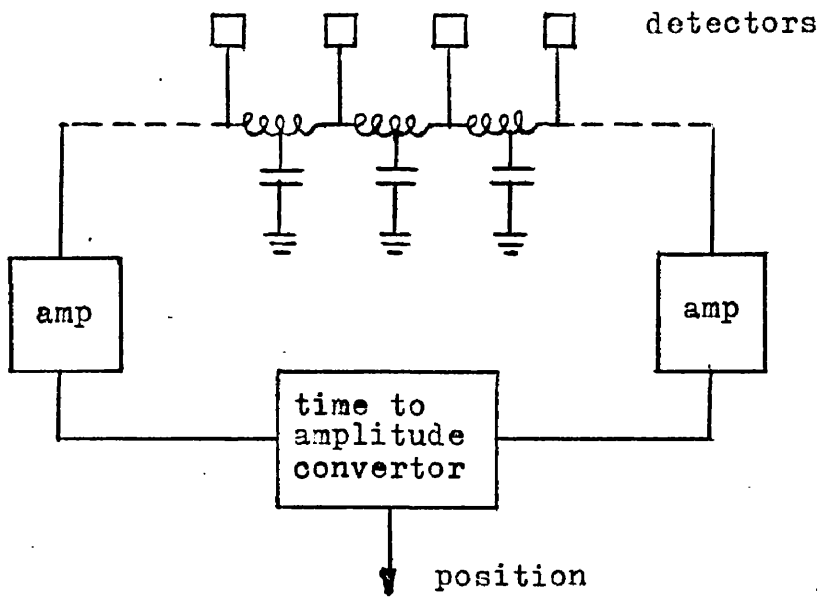
Methods of Obtaining Position Information.1) From an array of detectors.

As has been mentioned before, the spatial distribution of ionizing radiation can be obtained from an array of individual detectors each with its own amplifier or photomultiplier and associated electronics. If the requirement for the large number of amplifiers etc. can be overcome, such a system is suitable for the applications already discussed. Methods of obtaining a direct output signal from such an array of detectors in one dimension have been introduced.

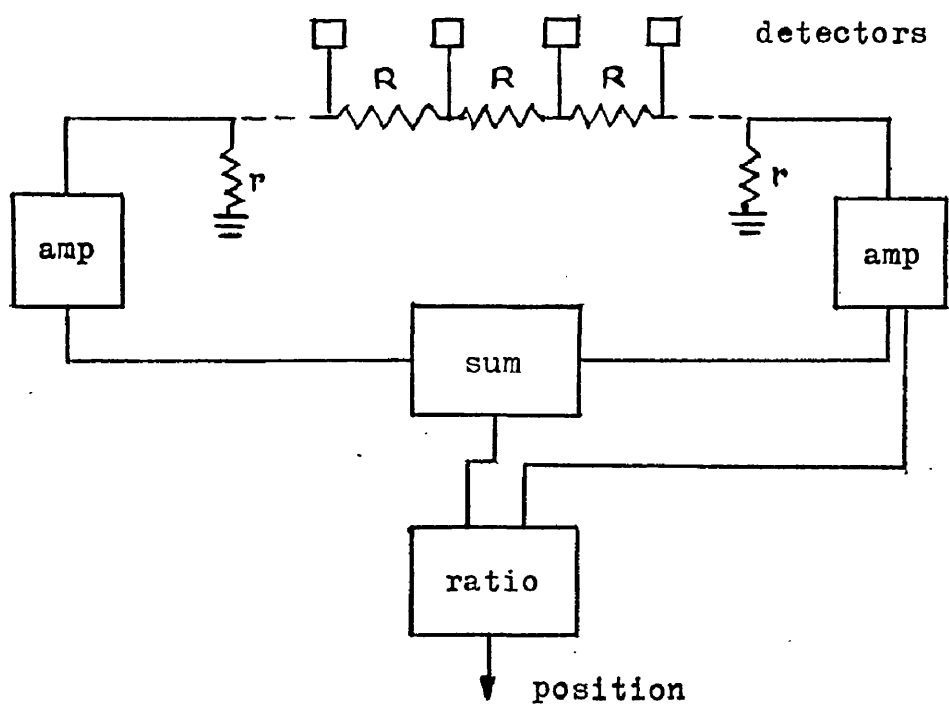
One of these is the connection of each counter to a different point on a delay line such that the delays between the counters are equal. The detector which has recorded the entry of a charged particle or photon can then be determined from the time difference between the signals reaching the two ends of the line. Such a system, as shown in Fig.1-5(a), has been constructed by Bilaniuk (1961), with 20 surface barrier semiconductor detectors each 2mm wide, for applications in either the focal plane of a magnetic spectrometer or for the measurement of the angular distribution of alpha particles from nuclear reactions.

A similar principle has been used in spark chambers, with wire planes as the electrodes, for high energy nuclear scattering experiments. Each wire acts as an independent chamber and is connected to a point on the delay line, which can be of the standard electromagnetic type or can be a magnetostrictive line. The spark current from

a) DELAY LINE READOUT FOR AN ARRAY OF DETECTORS.



b) RESISTIVE LINE READOUT.



a wire induces a longitudinal deformation pulse in the magnetostrictive material and, since this pulse moves with the speed of sound in the material, the delay per unit length is greater than in a typical electromagnetic line. Thus the resulting accuracy of position measurement is better. Position resolutions of 0.7mm full width at half maximum (FWHM) in two dimensions in chambers of up to 50cm side have been achieved by Perez-Mendez et al (1965,67) in this way. A separate wire plane and delay line was used for each dimension.

Alternatively, an attenuating line can be used. One such arrangement is shown in Fig.1-5(b) where the signal outputs of  $N$  detectors are joined by equal resistances  $R$  and are grounded at both ends through small resistances  $r$ . Then, for a particle entering the  $m^{\text{th}}$  detector and producing a total pulse height  $E$  in the system, the output across the resistance  $r$  at one end is proportional to  $E \cdot m/N$ . If the spread in the pulse height ( $E$ ) is small, the position is given by the signal from one end alone. However, if there is a large spread in pulse height, the output must be normalised by dividing the signal from one end by the total signal ( $E$ ) to determine the counter which has detected the event.

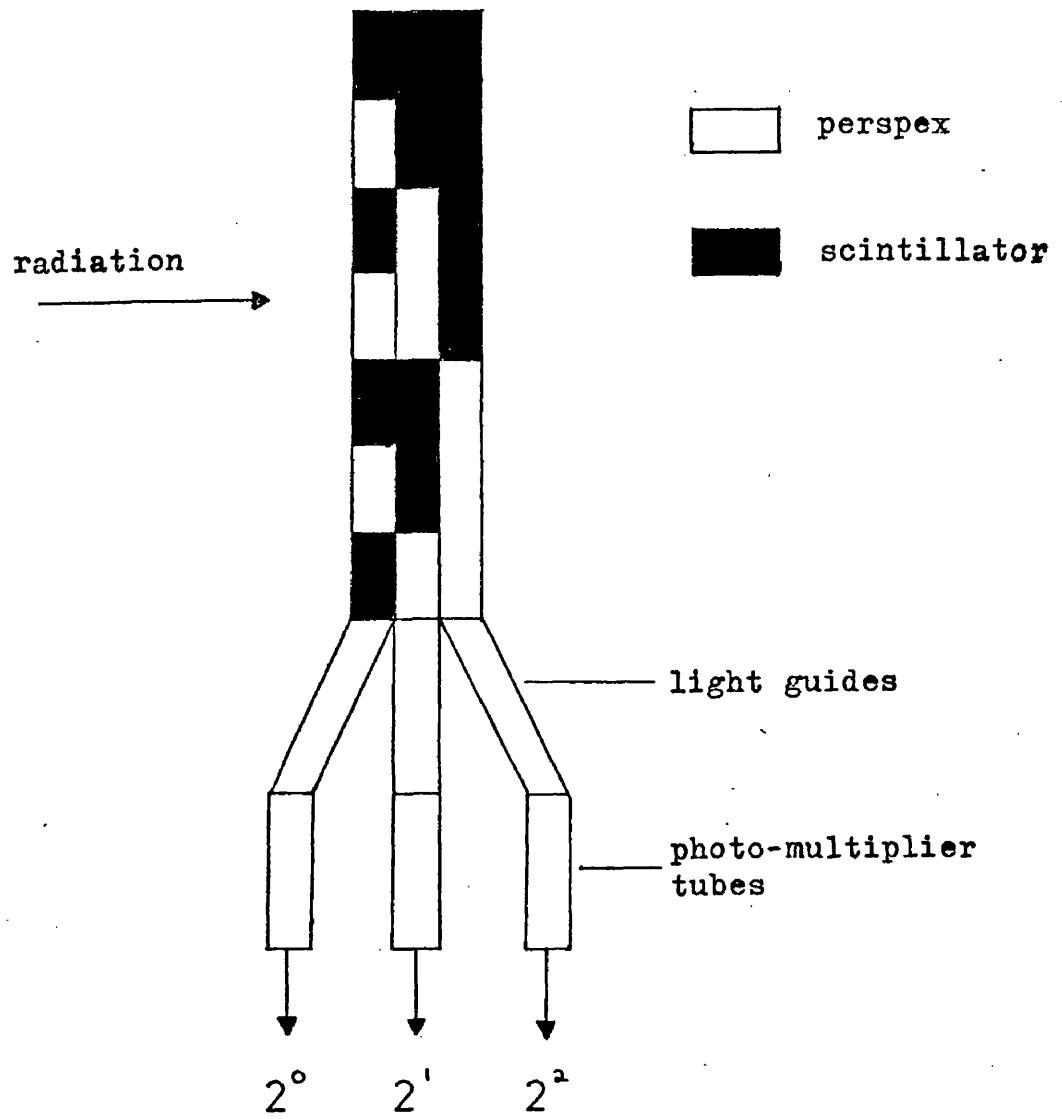
Both of these methods are of use only when there is an electrical signal which can be applied directly to the delay or attenuating line. Therefore, in the case of an array of scintillator crystals, a separate photomultiplier is still required for each counter. To some extent this defeats the simplicity of the system.

In certain cases, the number of output channels can be reduced

by binary coding the output signals from the detectors. This requires the addition of the signals from different detectors in different sub-groups. For spark chambers this can be carried out with magnetic cores, as used by Pullan et al (1966), and for scintillators by combining the light from different parts of the detector before the photomultipliers. Fig.1-6 shows the principle behind a scintillator system proposed by Alvarez (1960) for particles which traverse the total thickness of the detector. For position location to one of seven sections, the detector is constructed in three layers with alternate sections in each layer of scintillator and perspex. Each of the layers is viewed by a photomultiplier and gives a binary co-ordinate of position. An analogue position signal can be obtained from a binary to analogue converter. In general, for  $N$  sections, the number of multipliers,  $m$ , is given approximately by  $2^m = N+1$ . A similar system using a single layer of crystal and coupled to the multipliers through a special binary coded mask has been developed by Elbek & Nakamura (1961) for the focal plane of a magnetic spectrometer.

For the acquisition of bidimensional information, it is possible to reduce the problem of obtaining the output from each detector individually to one of separately reading the  $X$  and  $Y$  co-ordinates of the counter which has recorded the entry of a particle. If there are  $N$  counters in the array, the number of channels is reduced from  $N$  to  $2\sqrt{N}$ , i.e.  $\sqrt{N}$  along the  $X$  direction and  $\sqrt{N}$  along the  $Y$  direction. This can be achieved for arrays of Geiger, proportional or semiconductor counters by adding the signals from the counter anodes in rows in one

BINARY OUTPUT FROM SCINTILLATOR ARRAY.



direction, and from the cathodes in columns in the other direction.

A two dimensional semiconductor counter of this type was constructed by Hofker et al (1966). The individual detectors were formed on a single silicon crystal and rows of gold were deposited on one face of the crystal and columns of aluminium deposited on the other. The crystal was of 1.5cm diameter, and 88 separate surface barrier detectors, each of 1.37mm square, were formed between the strips of metal. This detector was for use as a counter telescope in angular distribution experiments.

For an array of scintillator crystals, the addition to give orthogonal rows and columns is carried out by having two light guides from each crystal - one for a row and one for a column. All the guides, from a particular row or column, are taken to one photomultiplier tube. This design was used by Bender & Blau (1963) in their autofluoroscope for the bidimensional image formation of gamma ray sources in medical applications. An area of 15cm by 23cm was covered with 293 crystals each 1.12cm square. 34 photomultipliers were required.

## 2) Position information from a single detector.

There is another class of detector comprising those counters which themselves give position information. The principle behind these is usually similar to that for the readout of an array of counters except that the delay or attenuation is part of the detectors' construction.

For example, in a spark chamber, the delay may result from the

finite speed of the sound from a discharge in the gas filling; and by timing the sound wave from the spark reaching transducers at the sides of the chamber, Maglic & Kirsten (1962) and Jones et al (1964) have achieved resolutions in two dimensions of 0.7mm FWHM in detectors of 50cm side.

In a Geiger counter the discharge propagates along its length at a speed of the order of 10cm per microsecond, and the position of entry of a charged particle or photon can be determined from the time difference between the start of the pulse from the counter anode and the discharge reaching a sensitive probe at one end of the counter. Frank (1951) obtained a resolution of 2cm FWHM in a 50cm long Geiger counter in this way.

Attenuation methods have been used for spark chambers, semiconductor detectors, Geiger counters and gas proportional counters. In each case, one of the electrodes is of resistive material and is effectively grounded at both ends either by small resistors or by charge sensitive preamplifiers which have a low input impedance. The situation is similar to that of Fig.1-5(b) except that the counter electrode is a continuous resistor. The signal from one end is given by  $E \cdot x/L$  where  $E$  is the signal produced on the stray capacity of the counter of length  $L$  at a distance of  $x$  from one end. If the spread of the total signal is small, as is the case for spark chambers and often for semiconductor detectors, the position is given directly by the signal from one end. However, if there is a spread of pulse heights the position must be obtained from the ratio of the signal from one end

to the total signal. This technique has been applied to spark chambers by Charpak (1963) to give position resolution of the order of 0.5mm in 50cm.

Surface barrier (and p-n) semiconductor detectors using this principle have been built by a number of workers, e.g. Lauterjung et al (1963), Bock et al (1966), Melzer et al (1968) and Owen & Awcock (1967,68); and Owen & Awcock have extended the technique to sensitivity in two dimensions by using the second counter electrode as a resistive line connected in an othogonal direction to the first one. A disadvantage of the normal surface barrier detector is its small sensitive thickness (less than 1mm) so that energetic protons or electrons may not be stopped in the depletion layer. Therefore, the technique has been applied to a surface barrier lithium drifted detector with a depletion layer up to 3mm thick by Ludwig (1965). A disadvantage of the resistive electrode method is the high noise level which is generated by the resistance of the signal electrode. This will be discussed more fully in connection with a proportional counter system in Chapter III, but it should be pointed out that this restricts these semiconductor counters to the detection of energies above a few hundred keV. For 5.5 MeV alpha particles in the maximum length of detector, which is restricted to about 5cm by non-uniformities in the silicon, a resolution of 0.6mm limited by electronic noise has been obtained by Melzer (1968).

A position sensitive Geiger counter yielding a resolution of 2cm FWHM in 70cm has been demonstrated by McDicken (1967) and a proportional counter giving 1.2mm FWHM in a length of 30cm by

Kuhlmann et al (1966). In each case the position was obtained from the ratio of the signal from one end of the counter to the total signal.

Other systems for measuring the spatial distribution of radiation are in existence. For instance, the digitisation of the position of the discharge in a spark chamber by means of a vidicon tube viewing the chamber. This system, as proposed by Gelernter (1961), should allow a position resolution of about 1mm in 1 metre.

Direct position information in two dimensions from a single scintillator crystal can be obtained by coupling the crystal to a number of photomultiplier tubes and weighting the output from each tube according to its position. In this way Anger (1963,66) in a gamma ray camera for medical applications achieved a resolution of better than 1cm for x-rays of 100 to 500 keV in a crystal of 29cm diameter coupled to 19 photomultiplier tubes.

Resolutions of better than 1mm over areas of several hundred square cm can be achieved with a screen of small crystals coupled to an image intensifier tube, and systems of this type are in extensive use for medical x-ray radiography (see Clark (1963)). However there are difficulties in the operation of these systems, mostly as a result of the loss of light in the optical coupling between stages, and this is a serious limitation to their use in many applications. The image intensifiers do not give a direct electrical readout, but this can be obtained from a vidicon tube viewing the intensified image.

#### The Detector Systems.

A position sensitive detector for application to the problems

discussed earlier in this chapter should have the following properties -

- a) High position resolution over the length or area used in an experiment.
- b) The capability for fast data collection, analysis and display.
- c) Simplicity and low cost of information readout.
- d) A high efficiency for the radiation to be detected.
- e) The capability for determining the energy deposited in the detecting medium.

The relative importance of these points depends on the particular experimental problem for which the detector is to be used, but it is unlikely that any one design of detector will satisfy all the requirements at the same time.

Scintillation counters have a high efficiency for x and gamma rays and charged particles; although this efficiency for x and gamma rays depends on the type and the geometry of the crystals and falls with increasing photon energy. They have a count rate capability of greater than  $10^6$ /sec. and can determine the energy deposited in them. However, if an array of scintillators is used as a position sensitive detector, the position resolution is always limited by the size of the individual crystals to a few mm; if such resolution is to be attained over a length of the order of 10cm the electronics required are rather complicated. A single crystal viewed by a number of photomultipliers gives the same order of resolution and the electronic system is not much simpler. However, in some cases, the use of a

scintillator image intensifier system may overcome these problems - giving better position resolution with a simpler readout; although in most situations the difficulties of optical coupling outweigh the advantages.

Semiconductor counters show the same order of count rate capability and provide energy resolution, but there are restrictions to their use also. For instance, the high electronic noise which is present in most surface barrier detectors and all the counters with a resistive electrode, makes them of little use for soft x-rays. Also if an array of separate detectors is used the resolution is limited to about 1mm; and if a resistive electrode detector is used, the sensitive area is usually smaller than 5cm by 5cm because of the available size of low cost silicon crystals of uniform resistivity. It would be possible to design a low noise cooled system of individual lithium drifted detectors for x-ray measurements but the cost would be very high.

Some gas filled counters do not have the disadvantages mentioned above of the solid state detectors but they have other disadvantages. The most important of these is their low efficiency for high energy x-rays and gamma rays. This can be improved to some extent by the choice of a filling gas of high atomic number, at high pressure, and the use of a lead converter screen in front of the counters for gamma rays above 1 MeV. However, the gas filled counters are most suited to the detection of charged particles, for which they are about 100% efficient, and of low energy x-rays.

Geiger counters come into this category but their position resolution appears to be limited to a few cm by the mechanism of the spread of the discharge and they provide no energy resolution. Spark chambers give high position resolution, but their count rate of around  $10^3/\text{sec.}$  is relatively poor, they have no energy resolving capability and in most cases they require their electric field to be externally triggered. This latter factor is a serious disadvantage as it prevents these chambers from being used for the detection of charged particles or x-ray photons which are stopped in the detecting medium. In order to overcome this, Pullan et al (1966) have introduced a chamber with a constantly applied electric field for the location of low energy beta particles from chromatograph plates. The position is obtained from binary coding the signals from multiwire electrodes. Unfortunately, the system is insensitive for 10 milliseconds after each spark and the spurious counting rate tends to be high. A more interesting system has been developed by Lansiaart et al (1966) for the detection of x-rays in a spark chamber. A grid is placed between the spark chamber plates and is used as a proportional counter to trigger the chamber. This device has only been operated with an optical or photographic output, but the method should be applicable to chambers with an electrical readout, wire planes as the cathode and the anode giving information in two dimensions.

At the time when the author's research commenced, it seemed that the scintillation counters, semiconductor detectors and spark chambers all had serious restrictions on their use; and it was thought

that many of the disadvantages of these systems would not be encountered if position information was taken from a gas proportional counter. The gas proportional counter has been used for many years for the detection and energy measurement of x-rays (in the range 200 eV to 50 keV) and charged particles, at count rates of up to  $10^6$ /sec. It requires no external triggering and has been shown by Kuhlmann et al (1966) to provide position information at high resolution, in one dimension, with a relatively simple readout system. Certainly, the detection efficiency of such a counter for high energy x-rays and gamma rays is low, and in this respect position sensitive proportional counters could not compare with the scintillation detectors for gamma ray imaging. However, it is envisaged that their main use would be for the detection of x-rays (below 50 keV) and of charged particles.

Thus, the work which is described in this thesis was undertaken -

- a) To examine the factors which govern the position resolution of a gas proportional counter.
- b) To demonstrate the operation of such counters in one dimension using a resistive electrode to give position information for charged particles and low energy x-rays.
- c) To extend the position sensitivity of a proportional counter to a second dimension and to demonstrate its use for the formation of x-ray shadow images.

This extension to a second dimension uses a new method of collecting the detector signal on induction electrodes placed between the anode and the cathode.

Chapter II.THE FUNDAMENTAL LIMITATIONS TO THE POSITION  
RESOLUTION OF SOME ELECTRONIC DETECTORS.Introduction

The resolution of a position sensitive detector of radiation is limited by a number of basic factors which are common to almost all designs, but whose relative importance depends on the application of the detector. It will be realised that in the case of counter arrays these effects may often be masked by the finite size of the individual elements.

There are four factors which limit the position resolution of any detector and these are -

- a) The direction and collimation of the incident beam of radiation.
- b) Noise in the associated electronics.
- c) The interaction of the radiation with the detecting medium.
- d) The internal characteristics of the detector.

As far as the direction and collimation of the radiation is concerned, this is something which, in principle, can be improved to any desired extent and so will not be considered further. The noise in the electronics is not really fundamental in most cases, except perhaps for the resistive electrode type of counter and this case will be considered in detail in Chapter III.

However, the interaction of the radiation with the detecting medium is fundamental and important in its effect on the resolution. Depending on the type of radiation, the primary electrons may have

considerable energy and so the track of a particle in a counter can be effectively broadened either by the formation of delta rays (primary electrons which have enough energy to ionize further atoms) or by the thermal diffusion of the primary electrons, due to their relatively high energy with respect to the atoms or molecules of the medium. In particular, with x-rays or gamma rays, and depending on the photon energy, the resolution may be limited by the distance travelled by the photoelectrons released from the atoms of the medium, or by the range of the Compton electrons and re-emitted x-rays, or by the distance travelled by the positron electron pairs formed and their annihilation gamma rays. In these cases of the spreading of primary ionization, the only way to optimise the resolution is to use a medium of relatively high density. Another problem encountered is the multiple scattering of high energy particles (e.g. electrons) in the detecting medium and this can considerably degrade the resolution.

It can be realised that the effects of these interactions with the detecting medium on the resolution are very dependent on the type and energy of the radiation and so have to be calculated for each individual case.

However, the conditions of use do not affect the internal characteristics of a detector very much; and since these characteristics are intrinsic in any measurements made with a detector, it is worth considering the methods by which they limit the resolution. It seems that, for both semiconductor and gas filled counters, thermal diffusion of the charge carriers is the principle cause of resolution

limitation of this type; although in certain gas filled counters the resolution may be deteriorated by the effect of ultra-violet photons released in the detection process. Unfortunately, it is difficult to calculate the magnitude of this latter effect, but this will be mentioned again later in connection with the gas proportional counter.

The following section of this chapter describes the magnitude of the thermal diffusion effect in a semiconductor counter, a gas proportional counter and a spark chamber. It is of interest to compare the limitations of each.

#### The Effect of the Diffusion of the Charge Carriers on Different Counters.

Ionizing radiation entering either a semiconductor or a gas filled counter liberates charge carriers which drift under the influence of an electric field to suitably placed electrodes, and thus allow the presence of the radiation to be detected. During this drift of the positive charge carriers towards the cathode and the negative ones towards the anode, the charge distribution in space will change; and in general it is the positions of the centres of charge of the distributions reaching the collecting electrodes which are of interest in position sensitive detectors.

Suppose that an ionizing particle deposits  $N$  ion pairs (or electron hole pairs) somewhere in such a detector and that they are located within a small element of space. When no electric field is present and if recombination is neglected the particles of each

distribution will obey the diffusion equation.

$$\frac{\partial \rho_{\pm}}{\partial t} = D_{\pm} \nabla^2 \rho_{\pm} \quad 2.1$$

Where  $\rho_{\pm}$  are the densities of the particles and

$D_{\pm}$  are the diffusion coefficients of the particles in each distribution.

The solution of this equation is

$$\rho_{\pm} = \frac{N}{(4\pi D_{\pm} t)^{3/2}} \cdot \exp. - \frac{(x^2 + y^2 + z^2)}{4 D_{\pm} t} \quad 2.2$$

Where  $t$  is the time which has elapsed since the diffusion began and  $N$  is the number of particles diffusing.

When extended to particles moving in the  $Z$  direction under the influence of an electric field, Llewellyn-Jones (1966) has shown that the equation becomes

$$\rho_{\pm} = \frac{N}{(4\pi D_{\pm} t)^{3/2}} \cdot \exp. - \frac{[x^2 + y^2 + (z \pm W_{\pm} t)^2]}{4 D_{\pm} t} \quad 2.3$$

Where  $W_{\pm}$  are the relative velocities of the positive and negative charge carriers.

Equation 2.3 is a Gaussian distribution.

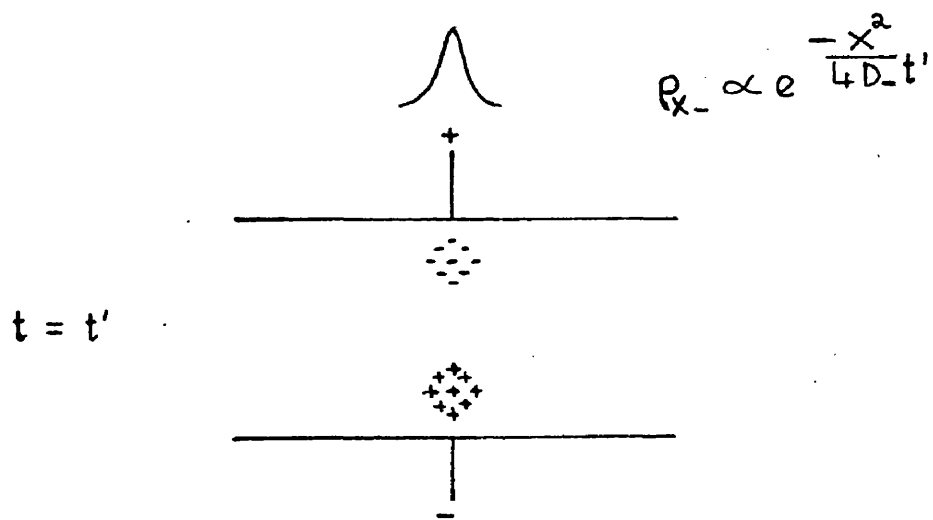
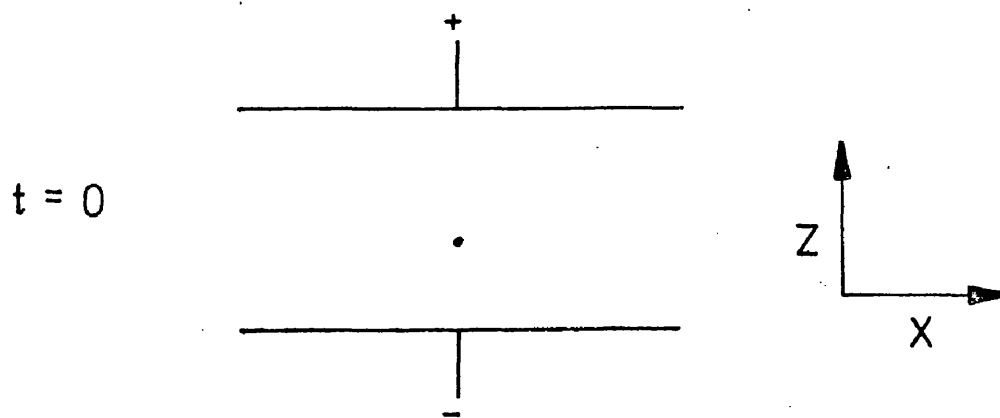
For the charge carriers drifting in the  $Z$  direction in a detector, as in Fig.2-1, the charge distributions in either the  $X$  or  $Y$  direction are Gaussian, of

$$FWHM_{+} = 2 \sqrt{4 D_{+} t_{+} \log_e 2} = 2 \sqrt{4 D_{+} \frac{L_{+}}{W_{+}} \log_e 2} \quad 2.4$$

and

$$FWHM_{-} = 2 \sqrt{4 D_{-} t_{-} \log_e 2} = 2 \sqrt{4 D_{-} \frac{L_{-}}{W_{-}} \log_e 2} \quad 2.5$$

DIFFUSION OF THE CHARGE CARRIERS IN A DETECTOR.



where  $\ell_{\pm}$  are the distances in the Z direction drifted by the positive and negative carriers at velocity  $W_{+}$  and  $W_{-}$  respectively.

However, it is usually the mean position, in either the X or the Y direction, of each charge distribution which is of interest in a position sensitive detector; and this has a Gaussian dependence on position of FWHM  $\epsilon^{+}$  or  $\epsilon^{-}$  where

$$\epsilon^{+} = 2 \sqrt{4 \frac{D_{+}}{W_{+}} \ell_{+} \log_e 2} / \sqrt{N} \quad 2.6$$

$$\epsilon^{-} = 2 \sqrt{4 \frac{D_{-}}{W_{-}} \ell_{-} \log_e 2} / \sqrt{N} \quad 2.7$$

N being the number of carriers diffusing in each case.

In principle, the diffusion limitation to the position resolution of the detector is given by a combination of  $\epsilon^{+}$  and  $\epsilon^{-}$ , each being weighted according to its contribution towards the total signal; but in some cases it may only depend on the diffusion of one sign of carrier.

Before the application of this theory to any design of counter it should be remembered that it has been assumed that the N ion pairs are liberated within a small element of space, and so a further summation over a number of elements must be carried out if the diffusion of a track of primary ionization is to be calculated.

#### Diffusion in a Silicon Surface Barrier Detector.

According to Sharpe (1964), the diffusion coefficients for electrons and holes in a condensed medium are given by

$$D_{\pm} = \frac{kT}{e} \mu_{\pm} \quad 2.8$$

where  $k$  is the Boltzmann constant,  $T$  is the absolute temperature,  $e$  is the electron charge and  $\mu_{\pm}$  are the charge carrier mobilities.

For silicon

$$\mu_- = 1300 \text{ cm}^2/\text{volt sec.} \quad \mu_+ = 500 \text{ cm}^2/\text{volt sec}$$

and so

$$\begin{aligned} D_+ &= 12.9 \text{ cm}^2/\text{sec.} && 2.9 \\ D_- &= 33.6 \text{ cm}^2/\text{sec.} && 2.10 \end{aligned} \quad \text{at room temperature}$$

For a typical surface barrier detector the collection time of the carriers may be 10 to 100 nanoseconds, so that for  $N$  electron hole pairs

$$\epsilon^+ \approx \frac{1.2 \times 10^{-2} \text{ mm}}{\sqrt{N}} \quad \text{to} \quad \frac{3.8 \times 10^{-2} \text{ mm}}{\sqrt{N}} \quad 2.11$$

$$\text{while } \epsilon^- \approx \frac{2 \times 10^{-2} \text{ mm}}{\sqrt{N}} \quad \text{to} \quad \frac{6.3 \times 10^{-2} \text{ mm}}{\sqrt{N}} \quad 2.12$$

In a resistive electrode type of detector (e.g. Owen & Awcock (1967)), where the position, in a direction perpendicular to the electric field, is essentially being continuously measured during the full diffusion time of the charge carriers, the FWHM of the mean position is probably of the order of  $\epsilon^+ / 2$  or  $\epsilon^- / 2$ . It can be seen from the figures above that, for all practical applications, the diffusion limitation to resolution in such a counter is negligible. In practice, it is the electronic noise from the resistive electrode which is the main limiting factor.

#### Diffusion in Gas Filled Chambers.

Gas filled position sensitive detectors tend to be rather more complicated than the semiconductor detector, since they usually

involve some type of internal amplification of the ionization deposited in them.

a) The Proportional Counter.

The gas proportional counter is characterised by the fact that the primary electrons liberated undergo a multiplication process in a high electric field in the gas, the spatial extent of the discharge being limited to a small region. Since the geometry of the detector usually is chosen so that the multiplication only occurs very close to the anode, the signal pulse on the anode is mainly due to the positive ions, produced in the avalanche region, moving away from the anode. However, the total diffusion limitation must include a) the diffusion of the electrons in the drift region, b) the diffusion of the electrons in the avalanche region, and c) the diffusion of the positive ions as they drift away from the anode. There is no need to consider the primary positive ions in this case as they play a negligible part in the detection process.

The typical magnitude of the diffusion quantities are calculated for a 3cm diameter proportional counter fitted with a 10  $\mu\text{m}$  diameter anode wire and filled with methane gas at atmospheric pressure. The quantity  $D/W$  is a function of the electric field at unit pressure - i.e.  $E/P$  - and since  $E/P$  is a function of the distance from the central wire ( $r$ ) in cylindrical geometry,  $D/W$  is also a function of  $r$ . So, for the drift region

$$\bar{\epsilon}_{\text{drift}} = 4 \sqrt{\log_e 2 \cdot \int \frac{D}{W} (r) dr} / \sqrt{N} \quad 2.13$$

where the integration is over the distance drifted by the  $N$  electrons. For a typical electric field, to achieve the required gain from the counter, it can be shown from the data of Cochran & Forester (1968) for methane that

$$\int \frac{D}{W} dr = 5 \times 10^{-4} \text{ cm}^2 \quad 2.14$$

and so

$$\bar{\epsilon}_{\text{drift}} = 0.75 / \sqrt{N} \text{ mm} \quad 2.15$$

for electrons drifting from the cathode towards the anode.

In the avalanche region, the value of the electric field per unit pressure is high - about 300 volts/cm torr. For a Maxwellian distribution of electron energies

$$D/W = 1/38.92 \times \eta/E \quad (\text{Cochran \& Forester}) \quad 2.16$$

where  $\eta$  is the electron temperature, i.e. the ratio of the mean kinetic energy of the electrons to their thermal energy. From the data of Schlumbolm (1965) for methane

$$\eta = 200 \text{ for } E/P = 300 \text{ volts/cm torr}$$

and so

$$D/W = 2 \times 10^{-5} \text{ cm}$$

If this value of  $D/W$  is taken as the mean value for the avalanche region, which has a length of the order of the wire diameter, then

$$\bar{\epsilon}_a \approx 5 \cdot 10^{-3} / \sqrt{N'} \text{ mm} \quad 2.17$$

where  $N'$  is the mean number of electrons in the avalanche. As far as

the positive ions in the avalanche region are concerned, their diffusion coefficient is about  $5 \times 10^{-2} \text{ cm}^2/\text{sec}$ . and since it is customary to use the first few microseconds of the anode pulse, the diffusion of their centre of charge in this time will be

$$\epsilon_a^+ \approx 10^{-2} / \sqrt{N''} \text{ mm} \quad 2.18$$

where  $N''$  is the number of positive ions drifting. However, since the position has actually been measured continuously during the positive ion drift, the observed FWHM in position, due to the positive ions, will be smaller than this.

In a proportional counter  $N < N' < N'' \approx 10^4$  to  $10^7$  and so the only really significant factor is the electron diffusion in the non-avalanche region. For a proportional counter, if the possibility of ultra-violet spreading of the discharge is ignored, the position resolution along the anode wire should be given by equation 2.13

$$\text{i.e. } R = \epsilon_{\text{drift}}^- = 4 \sqrt{\rho \log_e 2 \cdot \int \frac{D^-(r)}{W^-} dr} / \sqrt{N}$$

which has a value in this case of  $0.75/\sqrt{N}$  mm for primary ionization formed close to the counter window. For high energy particles which pass through the counter at right angles to the anode, the contributions from each element of the track of the ionization must be summed. This gives a resolution limitation smaller than  $0.75/\sqrt{N}$  mm.

This theory can be applied to multiwire counters of the design to be described in Chapter VI to give the same order of resolution limitation.

b) The Spark Chamber.

The analysis of spark chamber resolution is similar. In this case, the multiplication of primary electrons, under the influence of an electric field, continues until the space charge field of the slowly moving positive ions negates the applied field. Further development of the discharge is due to the creation of more avalanches along the axis of the initial ones by ultra-violet photons emitted in recombination processes in the space charge limited avalanches. There are a number of factors which broaden the discharge, namely, the diffusion of the primary ionization during the time between the ionization being formed and the chamber being triggered; the diffusion of the ions during the avalanche; and the broadening of the avalanche due to the positive ion space charge, as described by Llewellyn-Jones (1966). However, it can be shown that, due to the large number of ions in the avalanche, the error in the mean position of the spark from the avalanche effects are small compared with the diffusion during the triggering time. For a chamber filled with neon at atmospheric pressure with a 1cm gap and a clearing field of 50 volts/cm, the diffusion coefficient of the electrons in the gas, calculated from the data of Healey & Reed (1941), is about  $6 \times 10^{+3} \text{ cm}^2/\text{sec}$ . For a typical trigger delay time of  $3 \times 10^{-7} \text{ sec}$ . this diffusion results in an error in the mean position of the N initial electrons of  $1.4/\sqrt{N} \text{ mm FWHM}$ . The positive ions can be ignored due to their small diffusion coefficient. Thus for minimum ionizing particles where N is about 50 ion pairs/cm in neon, the error in the mean of the distribution is about  $1.4/\sqrt{50} \text{ mm}$ , i.e. 0.2mm FWHM, and this should

be the position resolution of the chamber.

Conclusion.

These rather approximate calculations serve to give some idea of the basic physical resolutions of the detectors. It is of interest to note that the intrinsic resolution of the proportional counter is of the same order as that of the spark chamber, but is poorer than that of the semiconductor detector.

The theory for the resolution of a cylindrical proportional counter will be considered again later, when the resolution predictions for different mixtures of argon and methane are compared with the experimental results.

Chapter III.PRINCIPLE AND DESIGN OF SOME PROPORTIONAL  
COUNTER SYSTEMS.Introduction

The technique of charge division on a resistive electrode was chosen for the proportional counters to be described in this thesis.

When an ionizing particle enters a proportional counter, a charge pulse is induced on an electrode, which is usually the anode of the counter, mainly by the positive ions from the avalanche moving in the electric field; if this electrode is resistive and effectively earthed at both ends the charge will leak off as a current in both directions.

For example, consider a particle producing ionization in a cylindrical proportional counter at a distance X from one end and Y from the other. Then the pulse induced on the anode wire will cause a current

$$I_x \propto \frac{1}{R_x} \quad 3.1$$

to flow in the X direction and

$$I_y \propto \frac{1}{R_y} \quad 3.2$$

in the Y direction

where  $R_x$  and  $R_y$  are the resistances to earth in the two directions.

$$I_x + I_y \propto \left( \frac{R_x R_y}{R_x + R_y} \right)^{-1} \quad 3.3$$

$$\text{and so} \quad \frac{I_x}{I_x + I_y} = \frac{R_y}{R_x + R_y} = \frac{y}{L} \quad 3.4$$

where  $L$  is the length of the anode of uniform resistance.

If these currents are integrated by low impedance charge sensitive

preamplifiers connected to the ends of the wire, where they behave as virtual earths, and are filtered and further amplified, then a measure of the position of a counter avalanche is given by the ratio of the output from one end of the wire to the total output.

This can be extended to position detection in two dimensions, if a separate electrode is provided for each dimension.

However, as a consequence of using this method of analysis, there are certain limitations to the linearity and position resolution.

A proportional counter with a resistive electrode effectively grounded at both ends can be considered to be a diffusive transmission line with its two ends connected to earth. Then the theory developed for the similar case of a semiconductor counter by Owen & Awcock (1967) and Kalbitzer & Melzer (1967) can be applied to find the limitations to linearity and resolution. These authors have shown that, for such a detector, the rise time of the pulses appearing on the preamplifiers at each end of the resistive electrode depends on the position of the ionization released in the counter. It can be appreciated, therefore, that for a fixed amplifier time constant there may be a variation of the total output signal with position and a non-linearity in the position signal. The magnitude of this effect depends on the distributed resistance (R) and capacitance (C) of the detector and on the amplifier time constants. According to Doehring, Kalbitzer & Melzer (1968) the variations and non-linearities are less than 1% if, for equal integrating and differentiating time constants,  $\tau_A$  in the amplifier

$$\frac{RC}{\pi^2} \leq 0.19 \tau_A$$

where  $RC$  is the time constant of the detector; and the results of Owen & Awcock (1967) suggest that these effects are negligible if

$$\tau_A \geq 2RC \quad 3.6$$

The equivalent noise generator of a diffusive transmission line detector grounded at both ends was shown by Owen & Awcock to be a resistance in parallel with a capacitor. The resistance  $R_d$  is equal to the resistance of the signal electrode and the capacitance  $C_d$  is the detector capacity divided by 3, if the amplifier time constant is longer than that of the detector. According to Owen & Awcock, the resulting noise from the detector is then just the Johnson noise from the signal electrode, which can be expressed in terms of mean square number of electrons at a preamplifier input as

$$n_d^2 = \frac{4kT}{e^2} \left( \frac{\tau_A}{R_d} \right) \quad 3.7$$

The noise from the input stage in each of the preamplifiers can be considered to be generated by a resistance  $R_s$  in series with the input to the preamplifier. For a field effect transistor

$$R_s \approx \frac{1}{g_m}$$

where  $g_m$  is the transconductance of the f.e.t. An analysis of the output noise in terms of the mean square number of electron charges at the input gives

$$n_A^2 = \frac{4kT}{e^2} \left[ \frac{R_s}{\tau_A} (C_f + C_d)^2 + \frac{\tau_A}{R_d} \left( \frac{R_s}{R_d} \right) \right] \quad 3.8$$

where  $C_f$  is the feed back capacity of the charge sensitive preamplifier.

Since the position measurement is obtained from division of the

signal from one end of the electrode by the total signal, the noise in both these quantities will play a part in limiting the resolution. The noise from one end is the sum of the Johnson noise and the preamplifier noise expressed as

$$N^2 = n_d^2 + n_A^2 \quad 3.9$$

In the case of the noise in the total output signal, the Johnson noise entering the two preamplifiers is correlated and so averaged out in the summing process, leaving only the total preamplifier noise .

$$\text{i.e. } N_t^2 = n_A^2 + n_A^2 \quad 3.10$$

It should be possible to minimise the electronic noise by the choice of an optimum amplifier time constant  $\tau_A$  for the particular values of  $R_d$  and  $C_d$  in use. However, in the system to be described, the time constants were not optimised for low noise but were fixed at 2 microseconds to satisfy the pulse shape requirements of the ratio circuitry.

For a typical counter of length between 10cm and 100cm (electrode resistance of 1 kilohm to 10 kilohm), preamplifiers of series noise resistance about 200 ohms, and main amplifiers of 2 microseconds time constant, the Johnson noise predominates and is of the order of  $10^4$  rms electrons. Therefore, in order to achieve a resolution of better than 0.5% of the detector's length, the detector signal must be equivalent to about  $10^7$  to  $10^8$  electrons. Under these conditions the proportional counter is probably operating in a region of limited proportionality and certain difficulties, which will be discussed later, are introduced.

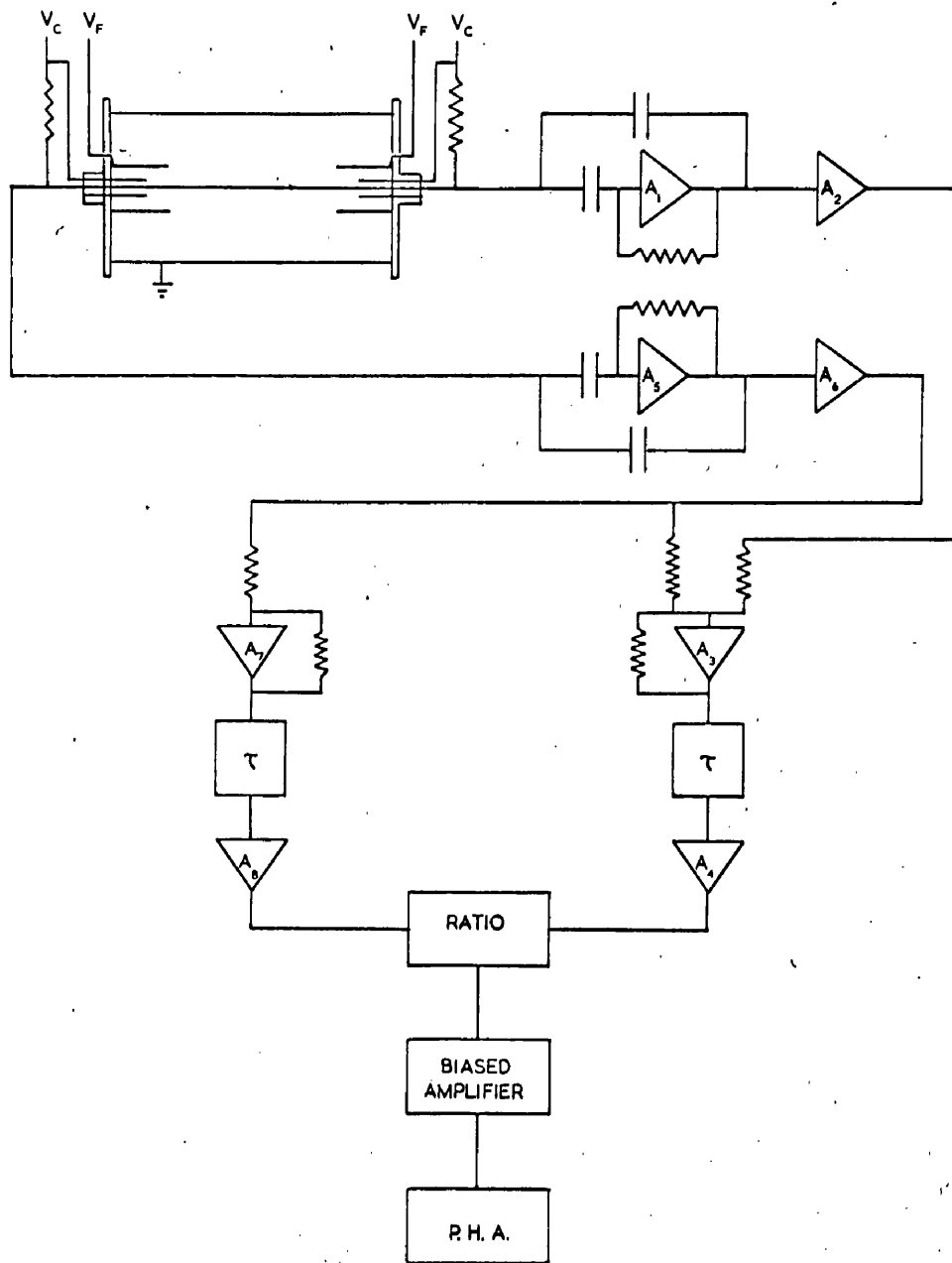
Electronic System for Position Analysis.

Before the development of and the measurements on the proportional counter systems are fully described in later chapters, an outline of the design of counters adopted and of the electronic circuitry required is now given.

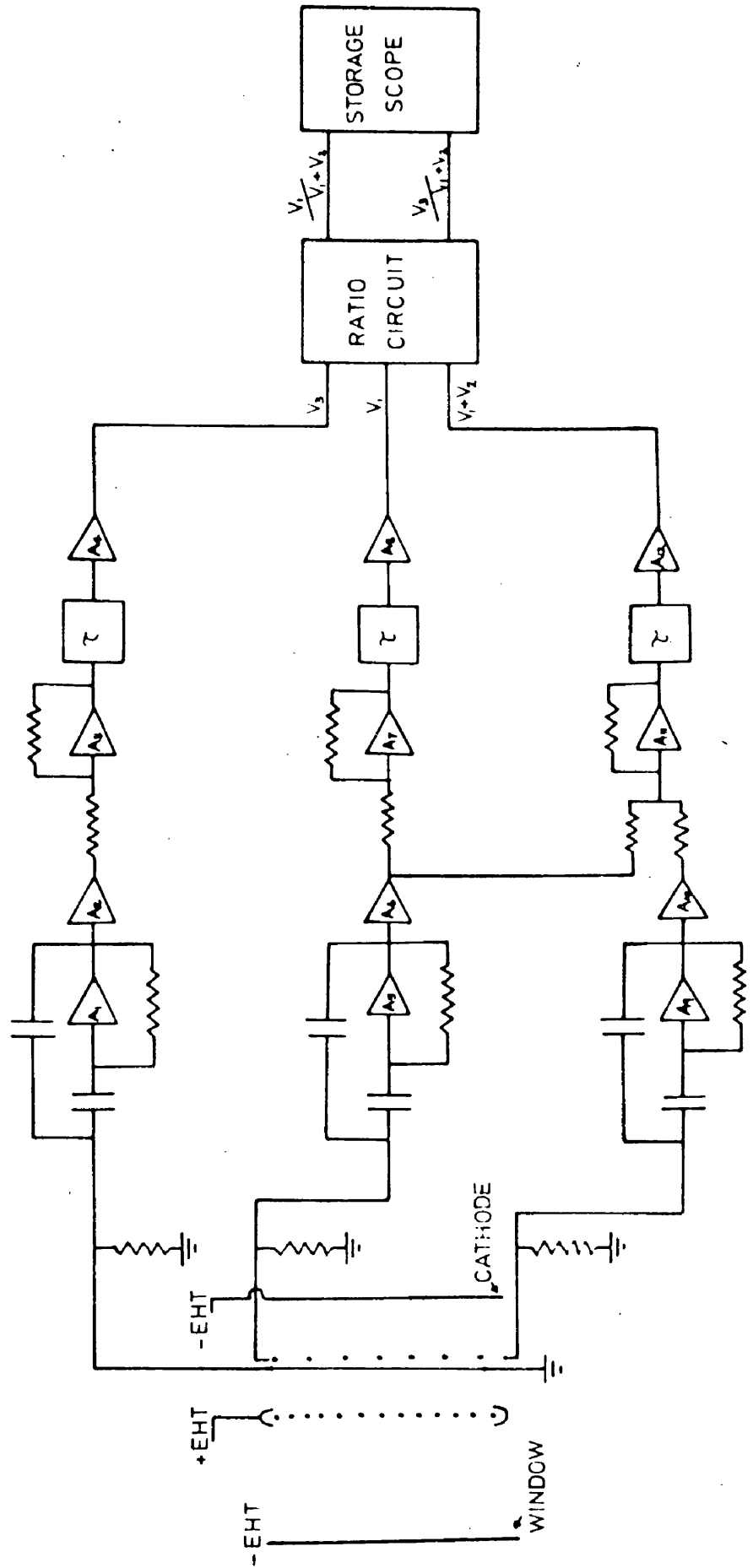
A block diagram of the one dimensional system is shown in Fig.3-1. Each counter used in this case is of the standard cylindrical type, fitted with high resistance anode wire which is held at positive potential and acts as the signal electrode. To each end of this anode is connected directly a charge sensitive (field effect transistor) preamplifier which acts as a virtual earth and integrates the total charge arriving at each end. The output signals from these are amplified with 2 microsecond equal integrating and differentiating time constants. The total signal is obtained by summing the output of both preamplifiers on an operational amplifier which is part of the input stage of one of the main amplifiers. The signals from the main amplifiers are then fed to a ratio circuit, and the ratio obtained is stored in a multichannel pulse height analyser. In order that accurate measurements of small changes in the position signal from the ratio circuit can be made, a biased amplifier is used between the ratio circuit and the pulse height analyser. This circuit biases off the lower part of a pulse and allows the peak region to be measured at higher gain than otherwise.

The two dimensional system shown in Fig.3-2 is very similar to that for one dimension. A multiwire anode counter is used, but the

BLOCK DIAGRAM OF THE ONE DIMENSIONAL COUNTER SYSTEM.



BLOCK DIAGRAM FOR 2 DIMENSIONAL COUNTER SYSTEM



signal in this case is induced on wires lying between the anode and the cathode. As described in Chapter VI there are two sets of induction planes of resistive wire, and the wires in one are perpendicular to but insulated from the wires in the other. This allows position detection in both dimensions. The anode is held at a positive potential and the cathode negative, and the induction wires are at ground potential. It is assumed that the total charge signal on the two planes will be in a constant ratio close to 1, and so, only one total signal output is required for the two dimensions. Then one plane of wires has a preamplifier at each end, while the other has a preamplifier at one end only and is earthed at the opposite end. The main amplifiers are the same as for the one dimensional case and the ratio circuit was extended to allow both signals to be processed simultaneously. Fig.3-2 shows the storage of the output on a cathode ray storage oscilloscope, although a bidimensional multichannel analyser was also used for measurements.

The input stages of the preamplifiers had to be modified before they were suitable for these applications; since it was necessary to have higher effective input capacities than in standard preamplifiers, in order to obtain a large ratio change from one end of a counter to the other. The coupling capacitors were included in the feed back loops of the amplifiers, so that the anode wire at high voltage could be connected directly to the charge sensitive inputs of the preamplifiers; and the feedback capacitors were increased from 1 picofarad to 20 picofarads to give effective input capacities of  $5 \times 10^4$  picofarads.

The sensitivities of the amplifiers then become 0.02 volts per  $10^7$  electron charges at their inputs.

If the position resolution of the system is to be better than 0.5% of the total length, it is clear that the system used for taking the ratio must give this accuracy, i.e. the variation of ratio output for a change in input pulse height at constant ratio, or for a change in count rate must be smaller than this value. This is a fairly difficult requirement which at the time of designing and building the one dimensional detector system was not met by any commercially available units. Thus a circuit had to be designed and built specially for this counter system.

#### The Ratio Circuit.

A ratio circuit can be designed in several ways; perhaps the simplest system is to digitise the outputs from the counter and then carry out the division by computer (Debenham et al (1969)) but this tends to be rather expensive in that it monopolises a small computer during the time when the counter system is in operation.

Some circuits use logarithmic techniques which have the advantage that they can accept a large dynamic range of pulse heights, and in many cases can analyse the input in less than 1 microsecond. One method (Bennet (1962)) is to utilise the exponential decay time of RC networks, but this is probably inferior to the more standard design of Strauss & Brenner (1965) in which division is accomplished by taking the logarithm of the input signals, subtracting and taking the antilogarithm of the difference. An accuracy of division of about 0.25%

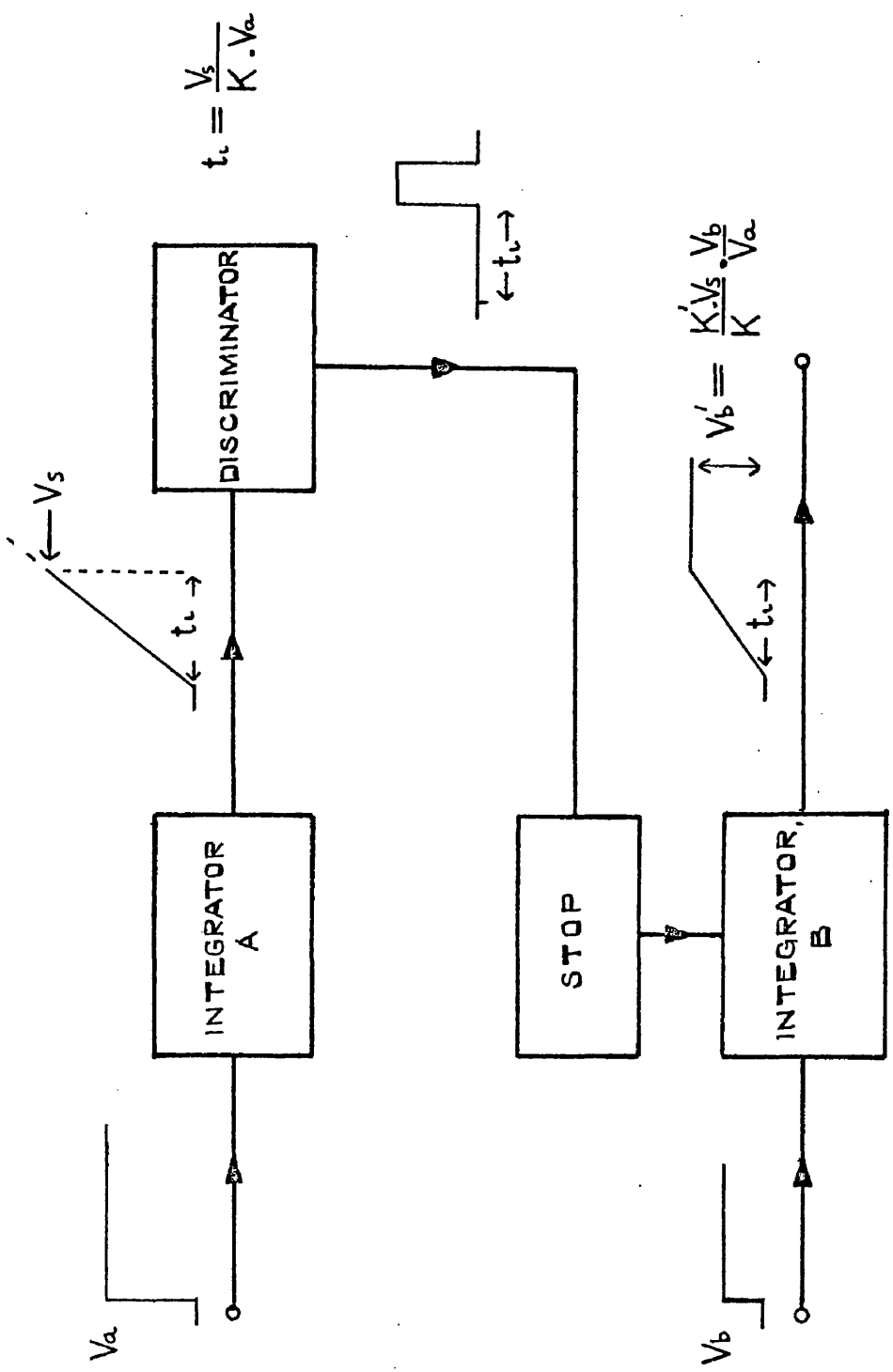
is obtained from this latter circuit, but the relative complexity of the solid state log. and antilog. function generators needed to obtain such accuracy did not seem desirable to the author.

If a high dynamic range of input signal is not required (and this is the case for the counter system described here), there is a simpler type of circuit which relies for its operation on the relationship between input and output voltage and time in an integrating circuit. Several designs of ratio circuit based on this principle have been reported, e.g. by Tsukuda (1964) and by Kuhlmann & Schimmer (1966) but they have tended to show excessive dispersion of their output, i.e. a variation of the ratio output of several percent, either for variation of the input at constant ratio over its dynamic range or for variation of the repetition rate of the input pulses over its possible range.

It seemed, however, that the accuracies of such systems could be improved by the use of better circuitry, dc coupled to avoid count rate effects. Therefore, a new ratio circuit, using the voltage-time relationships of integrating circuits was designed and built to provide the accuracy required for the proportional counter system.

The basic operation of such a ratio circuit is shown in Fig.3-3. Suppose it is required to find the ratio  $V_b/V_a$  of two voltage steps  $V_a$  and  $V_b$ . Then if these steps are applied simultaneously to the inputs of two integrating circuits, the output voltages are given after a time by

PRINCIPLE OF OPERATION OF THE RATIO CIRCUIT.



$$V_a' = K.V_a.t \quad 3.11$$

$$V_b' = K'.V_b.t \quad 3.12$$

where K and K' are constants of the integrators. If the output from integrator A is used to trigger a discriminator at a level  $V_s$  and the discriminator signal stops the integration of  $V_b$ , then, from equations 3.11 and 12 the integration time  $t_i$  is

$$t_i = \frac{V_s}{K.V_a} \quad 3.13$$

and

$$V_b' = \frac{K'.V_s}{K} \times \frac{V_b}{V_a} \quad 3.14$$

i.e. the output of integrator B is proportional to the ratio of  $V_b$  to  $V_a$ .

However, the amplified proportional counter pulses are not voltage steps and only remain at their peak voltage level for a short time. In practice, therefore, these pulses have to be stretched and maintained at their peak amplitude while the integration is carried out. Further circuitry is required - to reset the system after a ratio has been measured; to perform functions such as the shaping of the output; and to restrict the operation to a range of input pulses for which the system is linear and accurate.

The full block diagram of the author's ratio circuit which incorporates pulse stretcher circuits and a single channel pulse height analyser to control its operation is shown in Fig.3-4 and will now be discussed.

Positive pulses (from the main amplifier) enter the system



through gates which are normally open, and are then delayed by 1 microsecond before they appear at the stretcher inputs in order to cut down the effect of certain switching transients in these circuits. If the denominator ( $V_1 + V_2$ ) pulse exceeds a fixed level set on the pulse height analyser, the lower level discriminator output sets the flip-flop 1 which opens the stretcher gates and allows stretching of the pulses to commence. The resulting negative stretched pulses are only allowed to proceed through the gates to the integrators if  $V_1 + V_2$  lies within a definite window range of the pulse height analyser. These stretcher-integrator gates are controlled by the window output of the pulse height analyser through flip-flops IIA and IIB, and integration is initiated by the same window signal through flip-flop III. The  $V_1 + V_2$  integrated output triggers a discriminator at a fixed threshold voltage, and the output of the discriminator performs a number of functions. Firstly, it resets the flip-flops I and II and so, by resetting the stretchers and closing the stretcher-integrator gates, stops the integration. After a 3 microsecond delay it resets flip-flop III which controls the integration, thus giving a 3 microsecond long flat top to the integrator output. The direct signal from the discriminator is also used to control the output gate so that only the last 3 microseconds of the  $V_1$  integrated pulse appears as the ratio output. There may be a slight delay in this discriminator firing which leads to dispersion in the circuit; but this is compensated for by a variable delay in the setting of the flip-flop IIB and so in the starting of the numerator integration.

However, with this system, it is possible that pulses which lie above the analyser window could be stretched but would not be integrated. In this case, the stretcher would not be reset, since there would be no discriminator signal. This was overcome by using the upper level discriminator output of the analyser to reset flip-flop I in such a situation.

The input gates in front of the stretchers and pulse height analyser are to prevent other pulses entering the system while the previous ones are still being processed, and they are normally open. They are controlled through flip-flop III, being closed by the window pulse from the pulse height analyser and reopened at the end of the output pulse by the delayed discriminator signal. In order to prevent the processing of chopped pulses caused by the input gates opening when pulses are present on the input, the denominator ( $V_1 + V_2$ ) pulses operate a veto discriminator as they appear at the input gates. The output from this discriminator is present for the time duration of the  $V_1 + V_2$  pulse and is added to the main discriminator output in such a way as to inhibit the resetting of flip-flop III. This prevents the opening of the ratio circuit until the input pulses are no longer present.

#### Important Points in the Circuitry.

The main causes of dispersion and non-linearity in a ratio circuit of this type are non-linearities in the stretchers and the integrators; the distortions of pulse heights by the addition of pedestals and transients from gate circuits; delays in stopping the

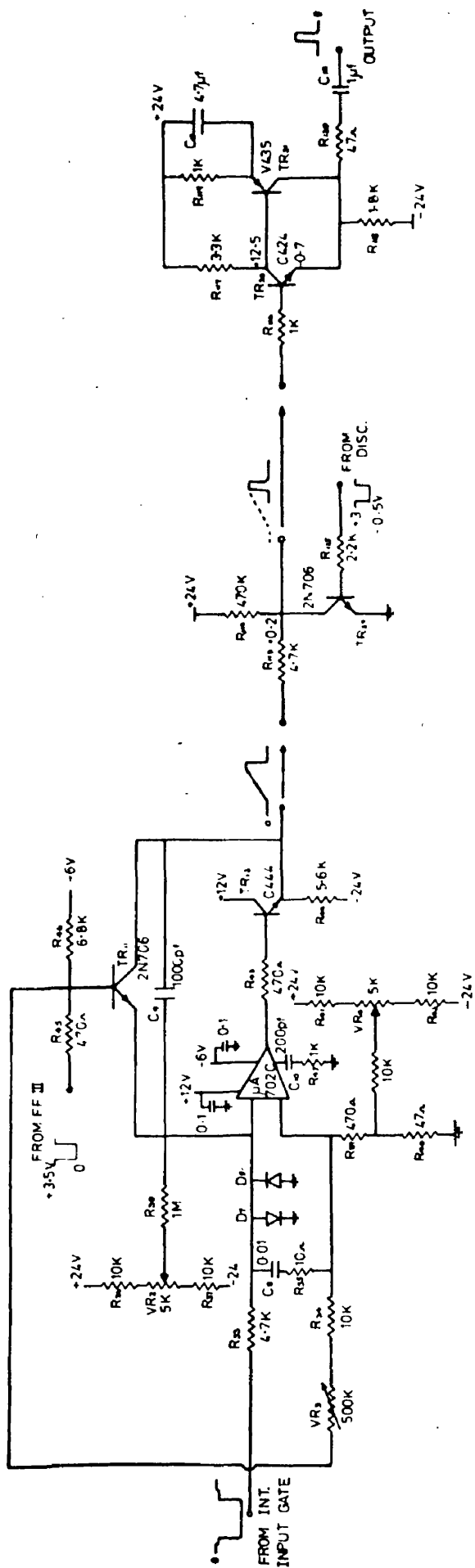
integration; and variation in the relative discrimination level ( $V_s$ ) with count rate. These effects have been reduced to an acceptable level in the present circuitry as shown in Fig.3-5 to 3-8. Integrated circuits have been used wherever possible, because of their reliability, small size, and low cost; and dc coupling has been adopted between all the analogue stages to avoid the large variation of output pulse height with count rate, which is inherent in many designs. Each circuit will not be described in detail, but the salient features which led to the attainment of the necessary accuracy are discussed below.

Each stretcher circuit effectively charges a capacitor through a diode to the peak voltage of the input pulse, and allows the capacitor to hold this voltage for a required time. In order to avoid non-linearities associated with the voltage drop across the charging diode and the pedestal introduced by the stretcher gate, the condenser charging is performed within the feed back loop of a high gain operational amplifier (SGS  $\mu$ A 702c integrated amplifier). The drop in amplitude of the stretched pulse with time is maintained at an acceptable level by the use of a high input impedance field effect transistor source follower output circuit across the storage capacitor. A second feed back loop, which only becomes operational when the charging diode has cut off, is provided to prevent saturation and possible damage to the integrated circuit when a stretched pulse is being held and no input is present.

The gate between the stretcher and integrator uses a current switching technique to reduce switching transients which, if present,



RATIO CIRCUIT

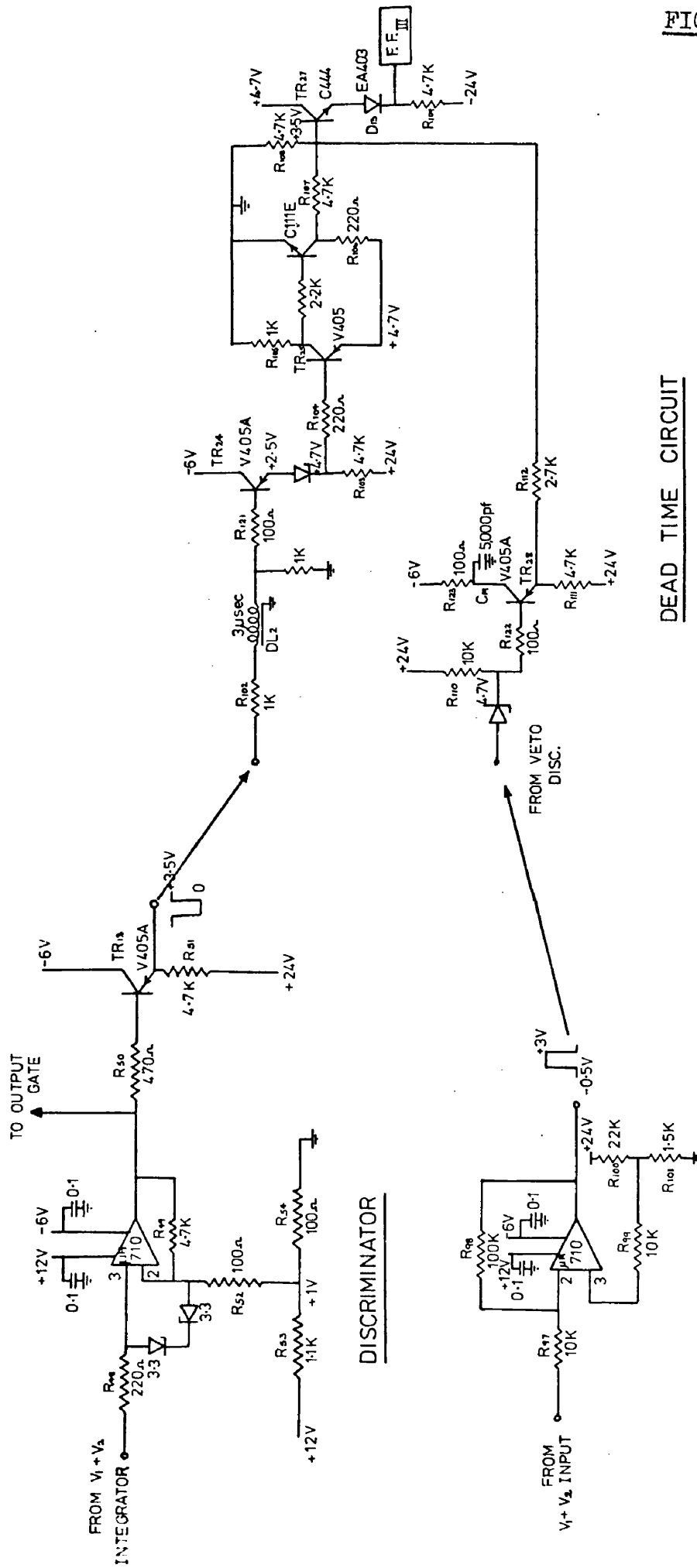


INTEGRATOR

OUTPUT GATE

OUTPUT CIRCUIT

RATIO CIRCUIT

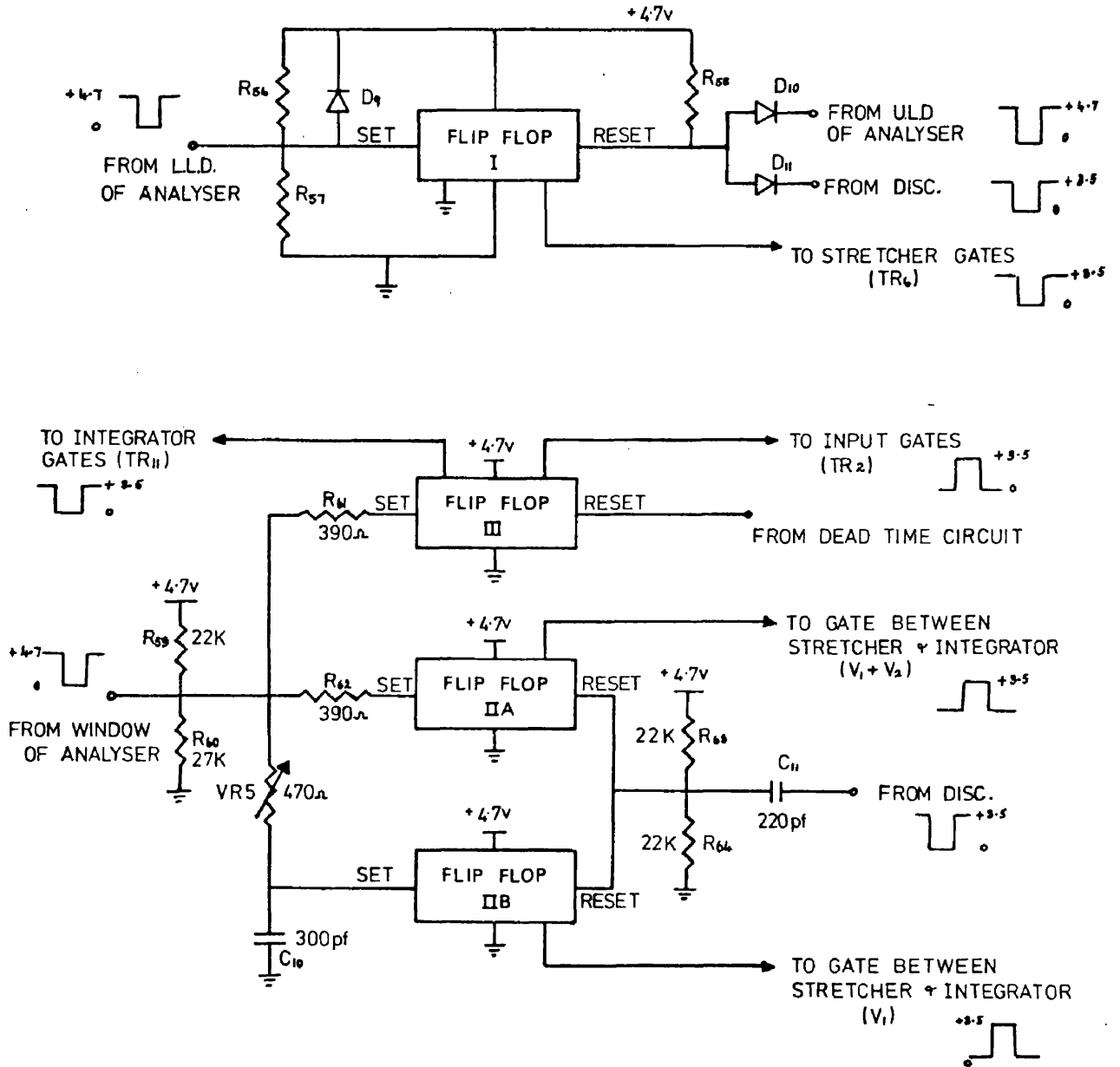


DEAD TIME CIRCUIT

VETO DISCRIMINATOR

RATIO CIRCUIT

LOGIC CIRCUITRY



FLIP FLOPS - ST828A (ELECTROSIL)

DIODES EA 403

would be integrated to cause an error, and when closed attenuates the negative stretched pulse to less than 1% of its input amplitude. There is an offset (about 40 mV) across the gate when it is closed, but the only effect of this is to cause a slight slope on the top of the output ratio pulse.

High linearity of integration is achieved by the use of an operational integrator circuit built around a  $\mu$ A 702C integrated amplifier. However, the accuracy is limited by a pedestal appearing on the beginning of the output ramp, caused by the gate across the integrator capacitor opening. Although this effect can be made small by a suitable choice of gate transistor, with a low emitter base capacity (2N706), a rather crude form of compensation has to be used to eliminate it. This consists of feeding a small part of the integrator gate driving signal to the input of the operational amplifier opposite that to which the integrating capacitor is connected.

Because of the difficulties which can be caused by pedestals from input gates being added to the pulses to be stretched, these gates, in this design, are normally open and the pedestals which appear when they close occur at a time after the peak pulse height has been measured and stretched.

The logic circuitry which is controlled by a single channel pulse height analyser modified to give window, lower level discriminator and upper level discriminator signals, and by a Schmitt trigger discriminator circuit using a SGS  $\mu$ A 710 integrated amplifier, is fairly standard. However, as mentioned before, there is a time delay of 40 nanoseconds

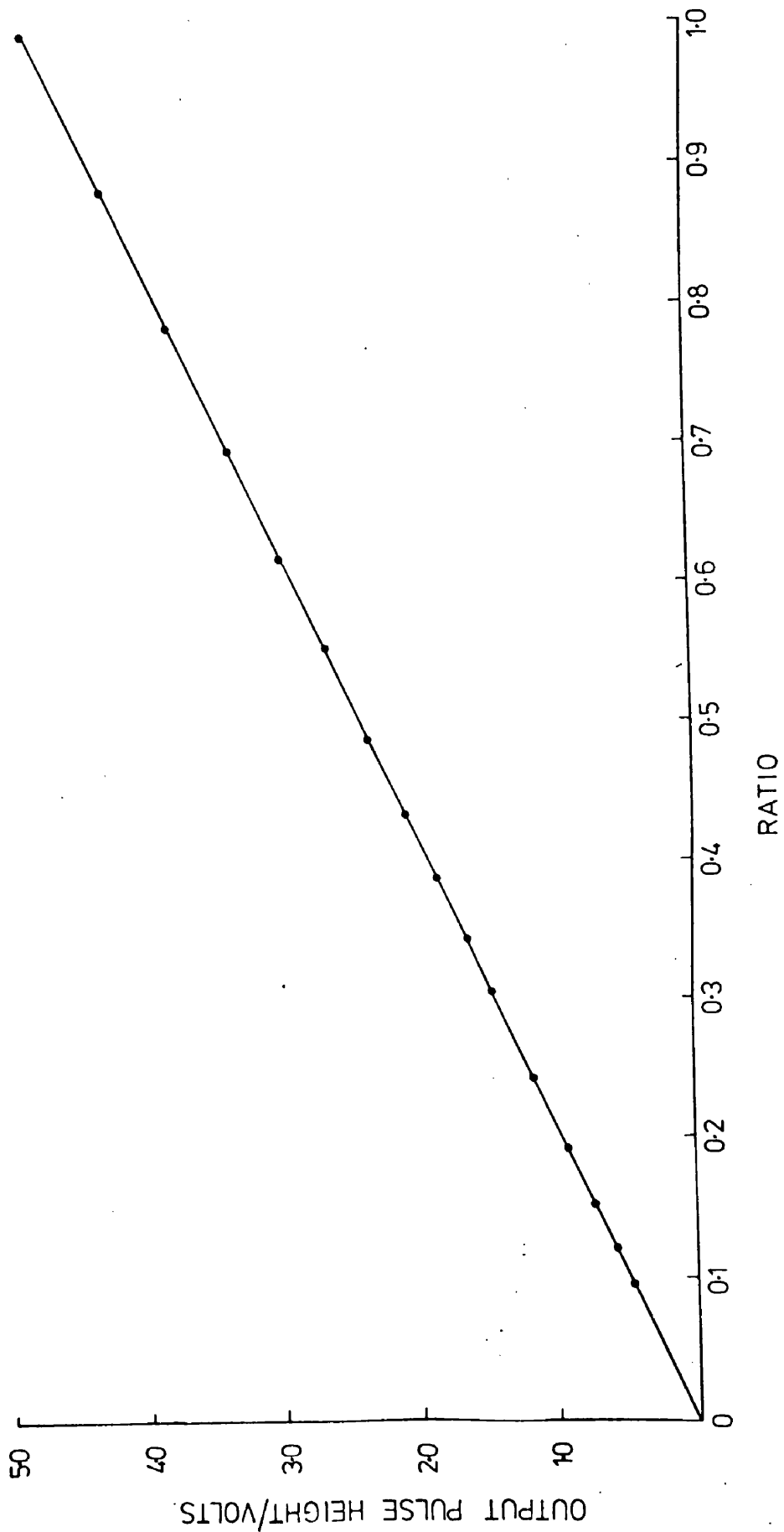
between the denominator ramp reaching the trigger level of the discriminator and the integration being stopped. This is enough to cause considerable variation of the output ratio pulse height as the input pulse heights are varied, at constant ratio, unless the start of the numerator integration is delayed by the same time. The necessary delay is provided by a variable RC network at the input to flip-flop IIB.

#### Performance of the Ratio Circuit.

The ratio circuit described accepts positive pulses of 2 to 5 volts in height, and up to 12 microseconds long, with a minimum rise time of 1.5 microseconds over a ratio range of 0.1 to 1, to give positive 3 microsecond long output pulses of 0.5 to 5 volts. Both the dynamic range and the rise time are limited by the stretcher circuits which become non-linear above a 5 volt input due to saturation effects; are non-linear below 0.2 volts input since the charging diode then cuts off before the feed back loop has time to compensate for the gate pedestal; and are unstable for faster rise times. The non-linearities of the stretcher circuits have been checked to be less than 0.2% of full scale over the 0.2 to 5 volt range and the decay in amplitude of the stretched pulses is less than 0.1% per microsecond.

The linearity of the ratio circuit, as measured on a multi-channel analyser and with an accurately calibrated attenuator to provide the ratio input from a pulse generator, is shown in Fig.3-9. The integral non-linearity is less than 0.2% of the full scale output.

LINEARITY OF THE RATIO CIRCUIT.



The dispersion of the circuit on varying the input over the 2 to 5 volt range at constant ratio is less than 0.25% of the full scale output, values at typical ratios being

<u>ratio</u>	<u>dispersion</u>
1	0.04%
0.5	negligible
0.25	0.2%
0.1	0.2%

The analysis time of the circuit, depending on the input pulse height, varies from about 10 to 20 microseconds and so a count rate of about  $5 \times 10^4$  per second is attainable. The change in output over this frequency range is always less than 0.2% of the full scale output.

An extension of this circuitry for the two dimensional counter system, where two ratios with a common denominator pulse are taken, was straightforward, since all that was required was another numerator side of the circuit, which was then controlled by the existing denominator and logic.

Since this circuit was built, several other designs of ratio circuit have been reported.

That of Doehring et al (1969), using the properties of a logarithmic function generator, and of Hodby (1970) using an analogue multiplier in the feed back loop of an operational amplifier, achieve a dispersion of 1% over a larger dynamic range than that of the author's circuit. Petin (1969) uses a rather complicated analogue to digital coding technique to give a dispersion of 0.4% over a dynamic

range of 100:1. However, it does not seem that these would be any more suitable for the author's counter systems.

Chapter IV.PROPORTIONAL COUNTERS FOR POSITION SENSITIVITY  
IN ONE DIMENSION.

In Chapter II it was stated that the intrinsic limitation to position resolution in a gas proportional counter is due to the diffusion of the primary charge carriers, combined with the possible spreading of the discharge by ultra-violet effects. It was hoped that it would be possible to justify this statement by resolution measurements. Unfortunately, the other limiting factors such as the electronic noise in the system, which is particularly important with this resistive method of position location, the interaction of the radiation with the detecting medium and the lack of collimation of the incident radiation tend to be present in most cases, and often mask the intrinsic counter effects. However, it can be shown that for the case of the avalanches resulting from single electrons (where  $N = 1$  in equation 2.13) in a counter of suitable length, operated at high gain, it should be possible to separate resolutions of the order of the diffusion limitations from the other effects.

Two counters were built, one 10cm long and the other 100cm long. The shorter of these was intended for -

- a) the measurement of the position resolution of single electron avalanches to allow comparison with the diffusion theory.
- b) the measurement of alpha particle and x-ray resolution for which diffusion effects should be small.

The 100cm counter was intended to demonstrate the potential of this method of position detection for possible use in scattering experiments or in the focal plane of a magnetic spectrometer.

#### The Design of the One Dimensional Counters.

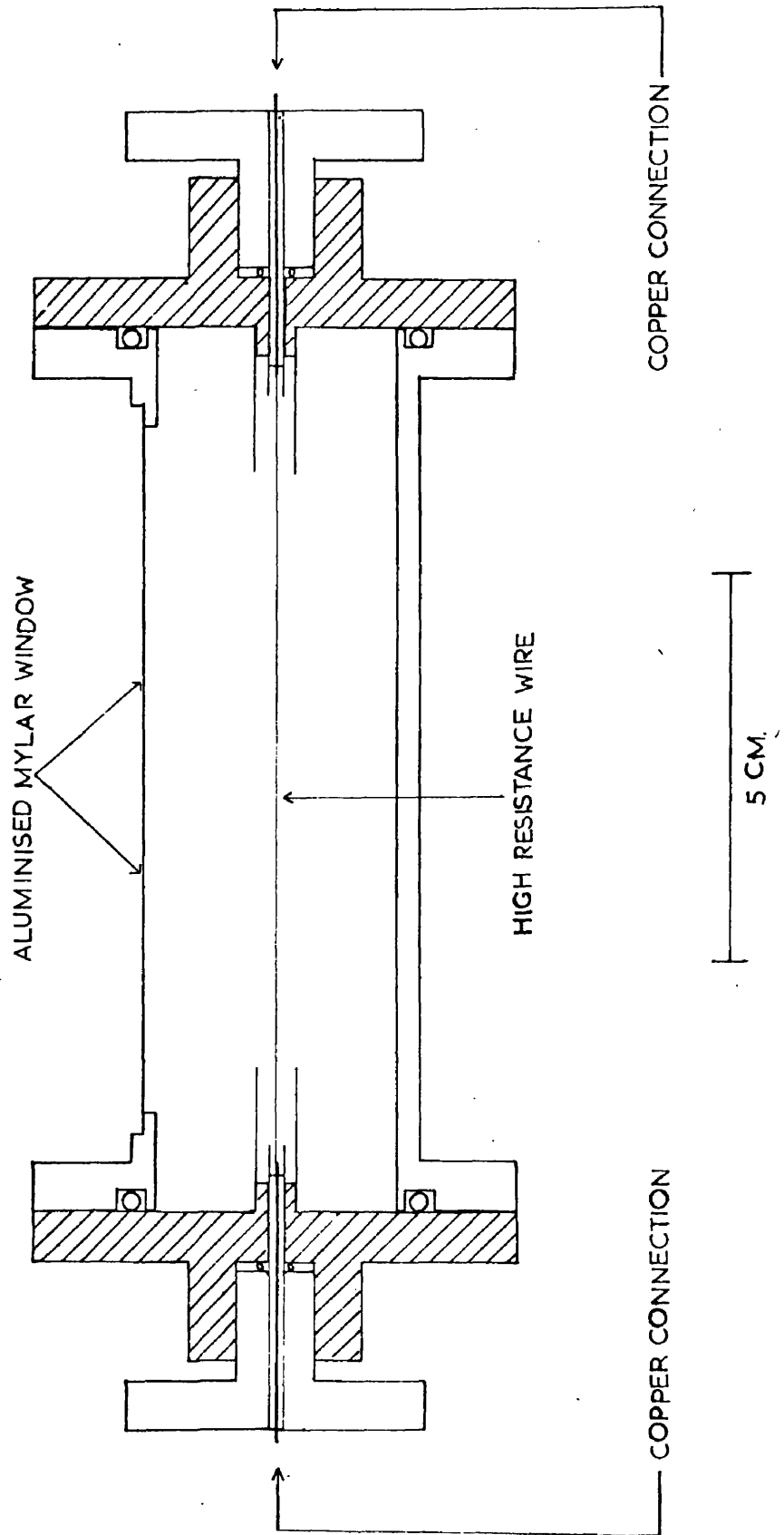
The proportional counters for sensitivity to position in one dimension are of standard cylindrical geometry as shown in Fig.4-1.

Both counters are constructed of cylindrical brass tubes of 3cm diameter with a window slit of width 1cm machined along 7.5cm and 97.5cm of their length respectively. Aluminised mylar windows with the internal aluminium coating making electrical contact with the brass are mounted over the slits, and inlet and outlet pipes are provided at both ends of the counters to allow filling gas to be flowed through them. The end pieces of the counters, attached to flanges in the brass tubes, are of perspex and there are O-ring gas seals between the parts to maintain gas tightness. Nickel field tubes of length 2cm and diameter 5mm are mounted on the perspex ends. The guard tubes of thick walled brass of 2mm diameter, are mounted on brass plugs which screw into the perspex end pieces against O-ring seals.

10 $\mu$ m diameter stainless steel wire was chosen for the counter anodes because of its high resistance (85 ohms per cm), availability and relative ease of handling; although, because of the fineness of the wire, the normal method of mounting a proportional counter anode - that of attaching it to a spring at one end of the counter and fixing it at the other - could not be easily managed. The wire ends are

COUNTER FOR POSITION SENSITIVITY

IN ONE DIMENSION.



crimped inside copper capillary tubing of 1mm outside diameter and 0.3mm inside diameter, which gives a good electrical connection to the resistance wire. This capillary (with the wire attached), insulated from the guard tubes with rubber sleeving, is held in place at the outside of the brass plugs with epoxy cement.

A liner is fitted to the barrel of the short counter only and initially an aluminium one was used; but this was changed to copper for reasons which will be mentioned later.

Copper boxes are provided at the ends of the counters for the purpose of shielding the connections to the power supplies and to the preamplifiers which are very sensitive to electrical interference.

In order to reduce electromagnetic interference induced in the loop which is formed by the anode wire and the preamplifiers, the signal from one end is brought along the bottom of the counter barrel by means of coaxial cable to the other end. This minimises the area of the loop. Both preamplifiers are connected to the same end box. The signal in the coaxial cable is guarded by having the outside braiding at the anode wire potential.

The counters' circuit is shown in the block diagram of Fig.3-1, the anode positive voltage being provided by a variable 6KV power pack, and the field tube voltage from a potentiometer connected to the same power supply.

For the 10cm counter the total anode electrode resistance is 700 ohms with a capacity of about 10 picofarads including the capacity of the coaxial cable; and so using a preamplifier which has  $C_f = 20$

picofarads and whose field effect transistors has  $R_s$  about 200 ohms, the noise in the system for equal differentiating and integrating time constants of 2 microseconds can be calculated from equations 3.9 and 3.10. The equivalent noise on the position signal is then

$$N = 5 \times 10^4 \text{ rms electrons} \quad 4.1$$

and on the total signal

$$N_t = 3.25 \times 10^4 \text{ rms electrons.} \quad 4.2$$

The resulting position resolution depends on both these quantities but mainly on the noise on the position signal. For counter pulses equivalent to  $5 \times 10^7$  electrons at the preamplifier inputs, the diffusion limitation for single electron avalanches in methane should be a factor of two above the noise limitation.

Similarly, in the 100cm long counter where the resistance is 8.8 kilohms and the capacitance less than 100 picofarads, the equivalent noise level on the position signal is calculated to be

$$N = 1.22 \times 10^4 \text{ rms electrons} \quad 4.3$$

and on the total signal

$$N_t = 2.6 \times 10^3 \text{ rms electrons} \quad 4.4$$

In this case it is the Johnson noise from the anode which predominates.

#### The Short Counter System.

With the 10cm long counter connected as in the block diagram Fig.3-1, the electronic system was checked with simulated proportional counter pulses, of rise time 100 nanoseconds and fall time of 100 microseconds, from a mercury relay pulse generator. These pulses were

injected at either end of the counter through a 20 picofarad capacitor and allowed a calibration of the gain of the system and a measurement of the noise level to be made. In the work to be described, the amplifier gains were usually such that the pulse heights from the counter were equivalent to about  $5 \times 10^7$  electrons at the preamplifier inputs.

According to Hanna, Kirkwood & Pontecorvo (1949), a counter used to give an output of  $10^7$  to  $10^8$  electrons is no longer operating in the proportional region of amplification, the criterion for this being that the product of the number of primary electrons and the gas gain should be less than  $3 \times 10^6$  if the ionization is over a small region of the counter. As it may be that the Geiger threshold is being approached, the work of Rose & Korff (1941) suggests that it is probably not justified to assume that ultra-violet effects are not present. As will be discussed in the next chapter, these may take the form of the photo-emission of secondary electrons at the cathode or in the gas.

In order to check the operation of the 10cm counter at such a gain, the pulse shapes from the preamplifiers due to single electron avalanches in 90% argon 10% methane mixture, flowing through the counter, were observed. (The avalanches resulted from photoelectrons released from the counter window by a focussed beam of light, as will be mentioned later). It was found that the leading edges of these pulses were ragged, having a staircase-like appearance with a time between steps of about 0.3 microseconds. Since this corresponds to the time taken for an electron drifting at about  $5 \times 10^6$  cm/seconds to cross

the 1.5cm distance between the anode and cathode, it seems that the stepped leading edges were due to photoelectrons being released from the aluminium liner of the cathode by the ultra-violet photons from the discharge. The replacement of the aluminium liner with a copper one, passivised by the formation of a thin copper oxide layer, as recommended by Curran & Craggs (1949), to give it a low photo-sensitivity, reduced the observed effect but did not eliminate it. However, if the percentage of quenching methane in the argon was increased to about 30% the ragged leading edges of the preamplifier pulses disappeared.

A loss of energy proportionality of the counter for pulse heights of about  $5 \times 10^7$  electrons was demonstrated with the 5.5 MeV alpha particles and the 14-22 keV x-rays of americium 241; as the pulse height from the alpha particles was less than twice that from the x-rays.

#### The Measurement of Position Resolution for Single Electron Avalanches.

As was stated earlier, the measurement of this quantity provides a method of checking one of the fundamental limits to the resolution of the counter.

The 10cm counter was fitted with a 40  $\mu\text{m}$  thick mylar window, lightly aluminised on the internal side to give about 5% optical transmission. Photoelectrons were released from this aluminium surface by light focussed on the mylar through a narrow slit of less than 0.3mm width placed against the window. In order to achieve a reasonable count rate of a few hundred counts per minute, a 6 volt, 55 watt, quartz

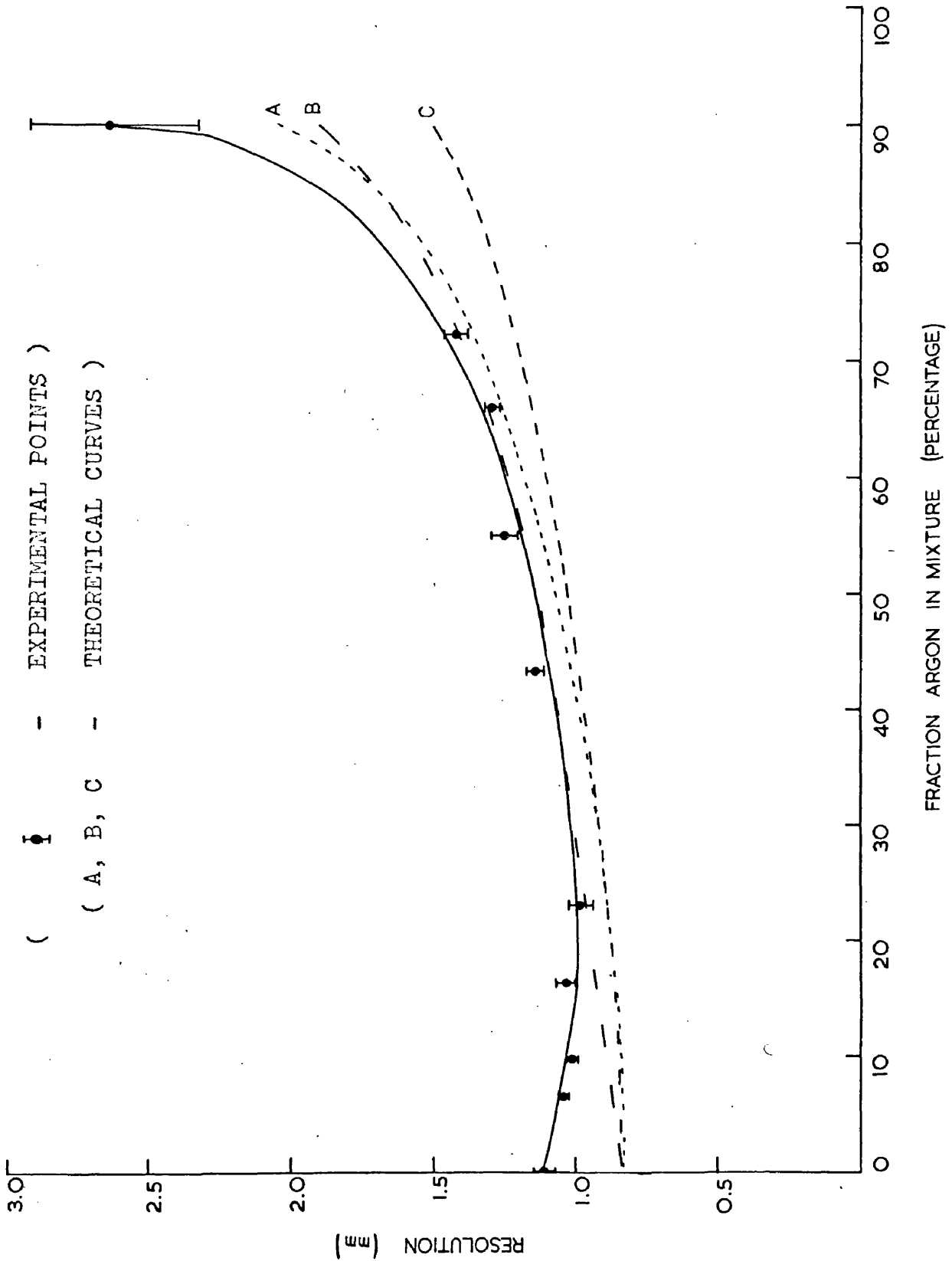
iodine lamp, enclosed in an aluminium casing with a condenser lens mounted on a draw tube for focussing, was used and the lamp was powered by a 50 c/s ac from a transformer. Since the overall count rate was low (not greater than 500 per minute), there was little possibility of pile up of pulses from the counter, even if all the photoelectrons were released at a time corresponding to the peak voltage being applied to the lamp. Care was taken with the selection of the aluminised mylar used, so that there were no pin holes or scratches in the aluminium coating from which photoelectrons might be preferentially emitted.

After position calibration of the system with the light source, the resolution was measured for a number of different mixtures of argon and methane flowing through the counter at about 50 cc per minute. The gases used were Air Products 90% argon/10% methane mixture and Air Products methane (98% pure), the mixing being carried out after the flow of each was regulated in a mercury manometer flow meter. The voltage applied to the counter ranged from 1740 volts for 90% argon/10% methane, to 3230 volts for methane alone.

The overall resolution figures varied from 1.1mm FWHM for no argon in the mixture to a minimum of 0.98mm for 23% argon/77% methane and then to a maximum of 2.6mm for 90% argon/10% methane. The experimental values of the resolutions are shown in Fig.4-2 and are discussed in Chapter V, where they are compared with the theoretical predictions for resolution limitation due to diffusion.

A possible source of error in these measurements was the setting of the EHT voltage so that the pulses analysed were from the

POSITION RESOLUTION FOR SINGLE ELECTRON AVALANCHES IN THE 10cm COUNTER.



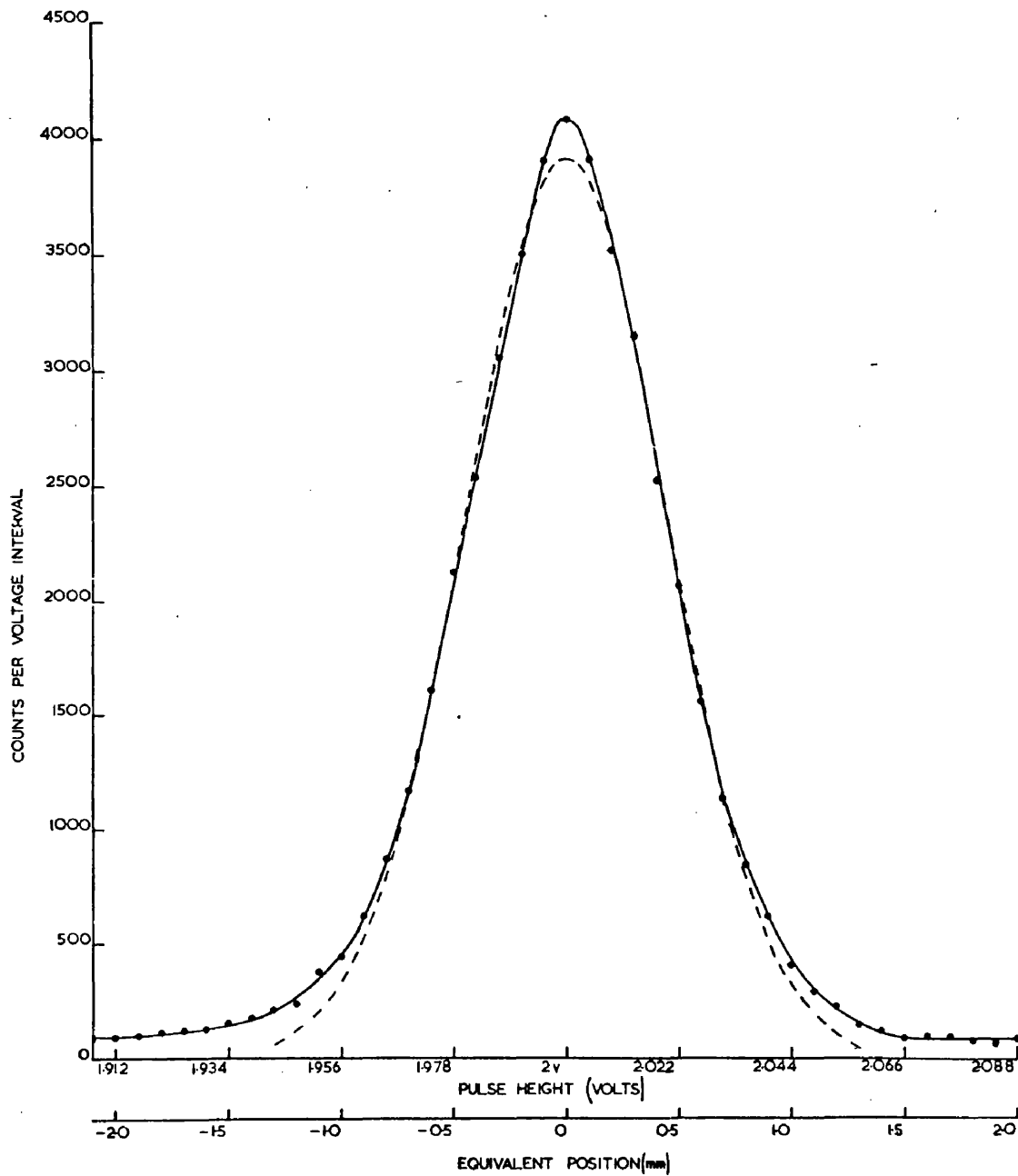
same part of the single electron pulse height spectrum in each case. This was checked and it was found that the resolution did not vary for changes of about  $\pm 2\%$  in this voltage. It seems fairly certain that the voltage could always be set within this limit in practice. A narrower slit (less than 0.1mm) was used, the count rate then being less than 100 per minute, to see if this improved the resolution. However, no such effect outwith the errors in the previous readings was observed. A typical position peak is shown in Fig.4-3.

The range of pulse heights processed by the ratio circuit was measured with the mercury relay pulse generator to be  $2.56 \times 10^7$  to  $6.4 \times 10^7$  electrons, with a noise level of approximately  $5.4 \times 10^4$  rms electrons. The average effect of this noise, found by continuously varying the pulse generator output over the input range, was equivalent to a resolution limitation of 0.33mm.

The significance of the above results is discussed in the following chapter; the resolution for the single electron avalanches does not appear to be limited by either electronic noise or collimation, and the resolution of 1.1mm for methane is reasonably close to the figure of 0.75mm calculated in Chapter II.

However, according to the diffusion theory, it would be expected that the intrinsic resolution for alpha particles would be better than this, since  $N'$  (the number of primary electrons) of equation 2.14 is then large. The following measurements were carried out to see if this was so.

A TYPICAL POSITION PEAK FOR SINGLE ELECTRON AVALANCHES  
(DASHED CURVE - BEST GAUSSIAN FIT TO THIS PEAK)



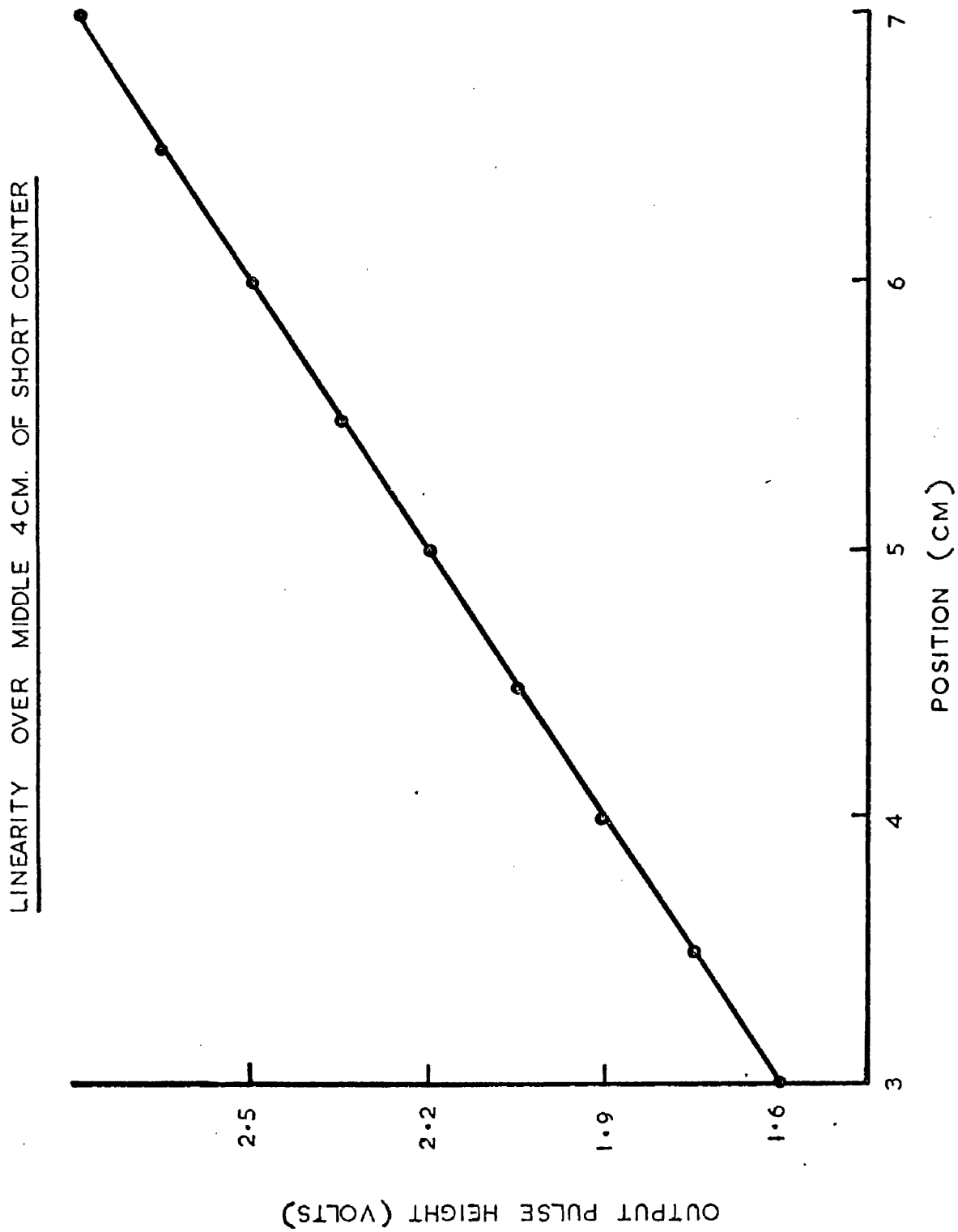
The Measurement of Position Resolution  
for Alpha Particles.

A collimated beam of 5.5 MeV alpha particles was obtained from a 1mm wide strip of americium 241 of strength 20  $\mu\text{Ci}$ , mounted on a lead backing, and placed 1cm behind two 3mm thick aluminium plates which formed a variable slit. The alpha particles were allowed to enter the counter through a 5  $\mu\text{m}$  thick aluminised mylar window. If allowance was made for the thickness of the source covering, the 1cm of air between the source and the slit, and the mylar thickness, the range of the alpha particles inside the counter was calculated to be about 8mm.

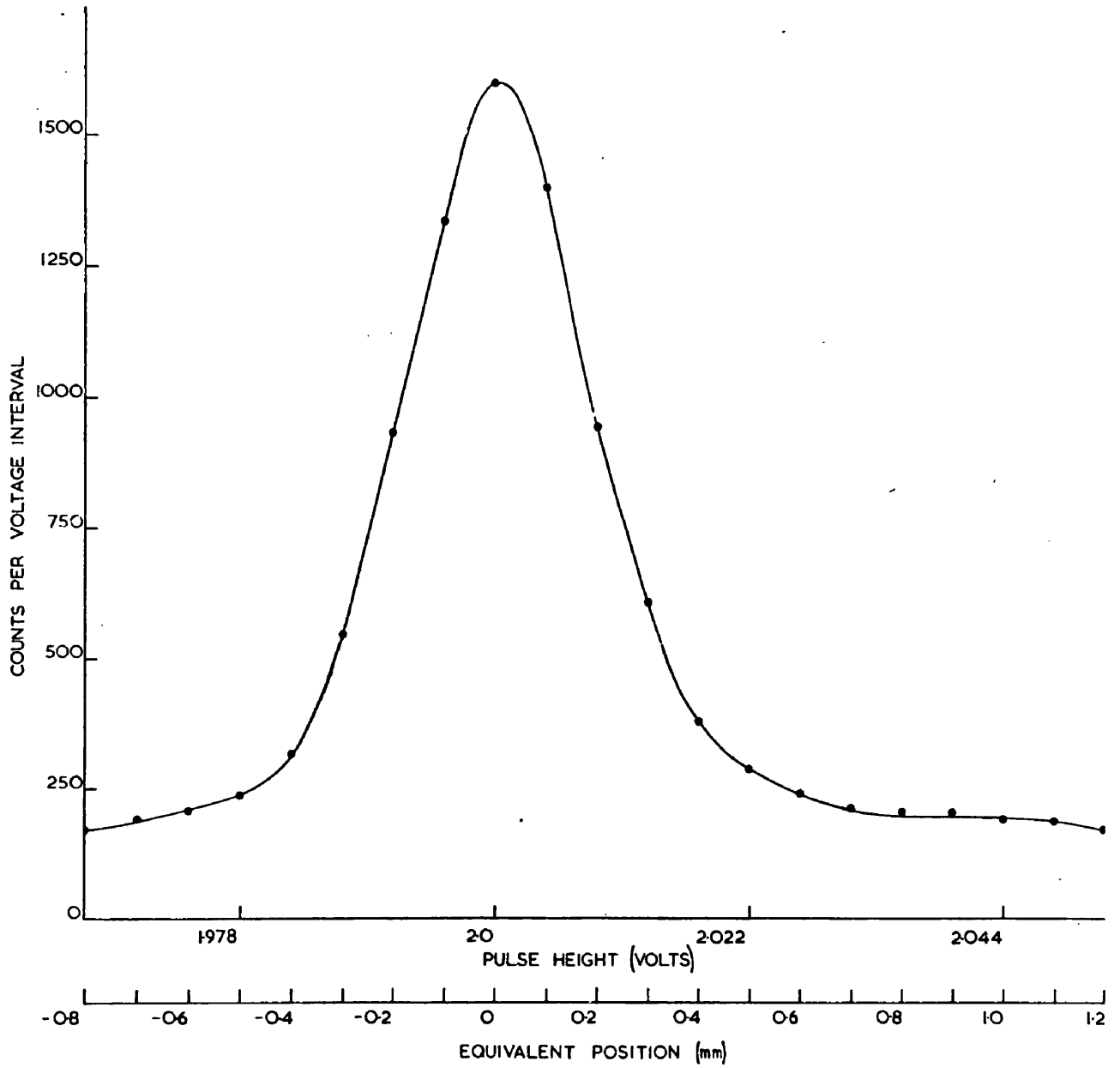
With a flow of methane through the counter and the source mounted on a travelling microscope stand, the linearity of the counter across its middle 4cm was measured to give the result of Fig.4-4. It was found that the resolution was dependent on counter voltage for a constant setting of amplifier gain and ratio circuit window width, which only accepted pulses in the range equivalent to  $2.56 \times 10^7$  to  $6.4 \times 10^7$  electrons at the preamplifier inputs. The best resolution figure attained of about 0.42mm was above the noise limitation of 0.33mm. The position peak for this resolution is shown in Fig.4-5. The same value for this alpha particle resolution was found for 90% argon/10% methane gas, and agreed fairly well with the measurement on an autoradiograph of the collimated source. This was made with a photographic plate placed at a distance of one half of the alpha particle range from the slit, and suggested that the effective collimation was 0.4 to 0.5mm.

The fact that there was an improvement in resolution with

FIG. 4-4

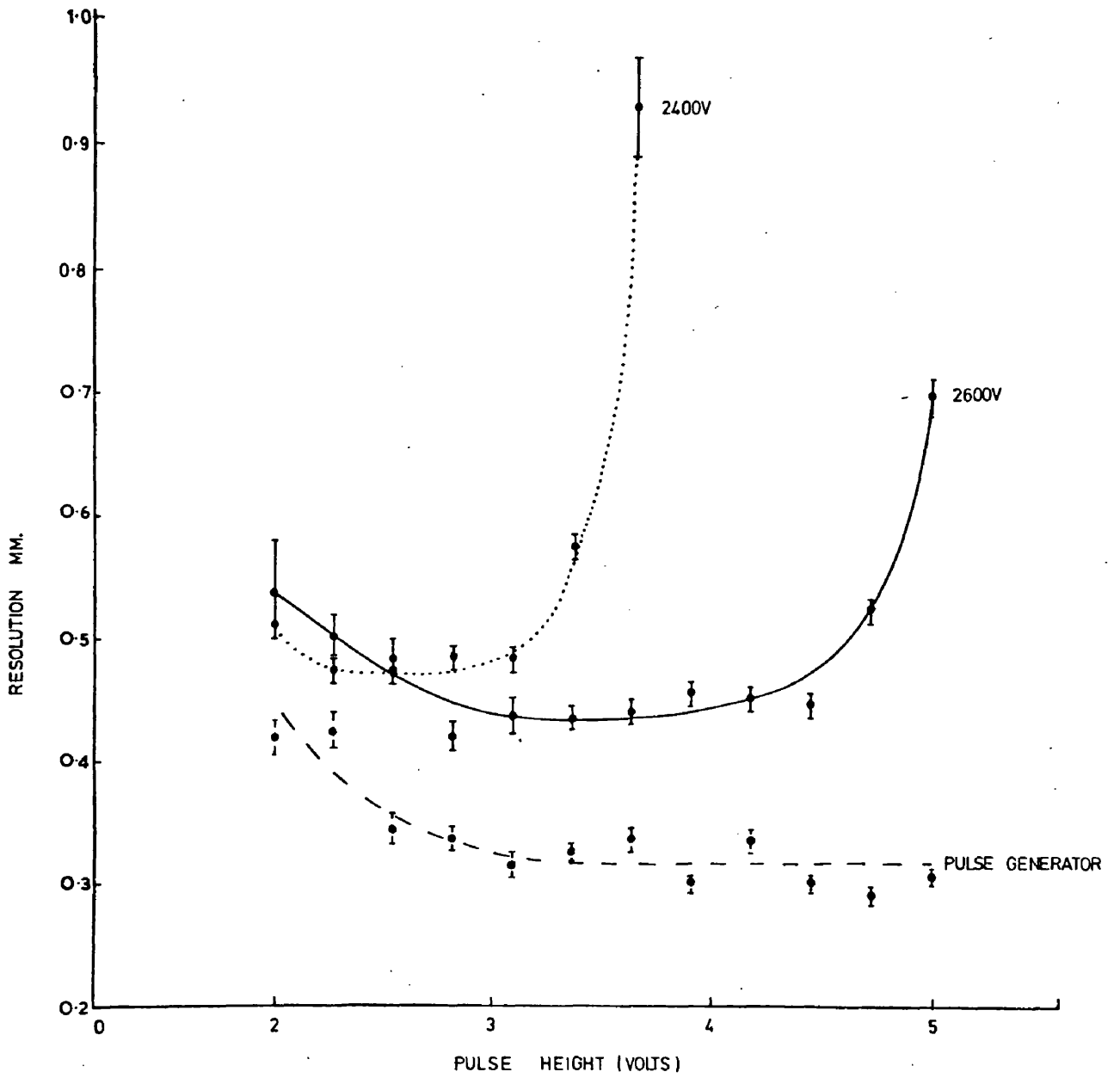


TYPICAL POSITION PEAK FOR ALPHA PARTICLES IN THE 10cm COUNTER.



increasing counter voltage suggests that the position resolution for large pulses is not so good as for small ones, perhaps because the larger pulses may result from particles which move at an angle to the perpendicular to the counter wire. With their ionization spread over a greater length of counter, these particles may give pulses which are not so strongly limited by the space charge in the avalanche as are the pulses from particles perpendicular to the wire. Fig. 4-6 shows the variation of alpha particle resolution with pulse height for two fixed counter voltages, the dotted curve being the corresponding limitation to the resolution of pulse generator pulses due to noise. This was carried out using a two dimensional multichannel pulse height analyser, with the total pulse height on one bank of channels and the position signal on the other. As can be seen, the resolution curves are always above that of the noise, due to the width of the source, and they decrease with increasing pulse height to a minimum and then increase again. It can be shown that the decrease at the beginning is just that of the noise effect becoming less important. However, the resolution of the large pulses is indeed poor. It should be mentioned that the noise curve is not really the shape which would be expected - that of the noise limitation being inversely proportional to the pulse height. The approach to a constant limitation at large values of pulse height is thought to have been due to the introduction of interference to the signal from the ratio circuit. This interference occurred on long cables which were used between the circuitry and the pulse height analyser.

VARIATION OF ALPHA PARTICLE RESOLUTION  
WITH PULSE HEIGHT.



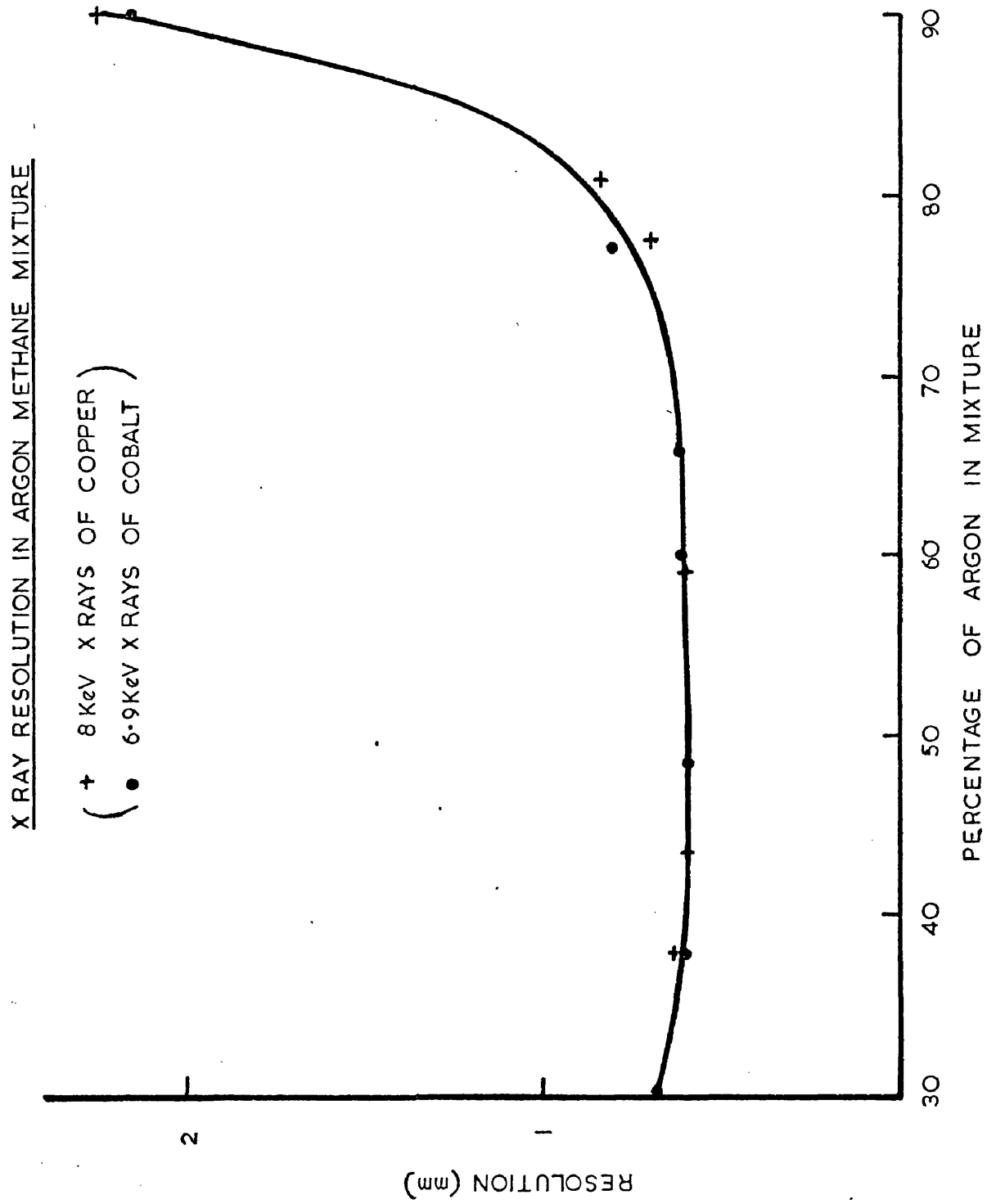
The Measurement of X-ray Position Resolution.

A beam of x-rays from a high intensity dc powered x-ray tube, fitted with a focussing 100  $\mu\text{m}$  broad filament assembly, was collimated by a fine round edged slit before entering the 10cm counter. The width of the beam at the equivalent distance in air of the back wall of the counter was checked photographically to be less than 0.15mm.

With a cobalt anode in the tube giving x-rays of 6.9 keV, the position resolution was measured at a count rate of about 100/sec. for a number of different percentages of methane in argon, the counter output pulses being in the range of  $3.45 \times 10^7$  to  $8.6 \times 10^7$  electrons. The variation of the resolution with mixture is shown in Fig.4-7 where it can be seen to deteriorate from about 0.6mm for 50% methane to about 2mm for 10% methane present. The best resolution of 0.6mm was considerably greater than the average noise limitation (approximately 0.25mm), but a careful check showed that this was not the result either of poor collimation of the beam or lining up of the counter with the beam.

The x-rays are absorbed in the gas (mainly in the argon, since the absorption coefficient of argon is about 30 times that of methane at this energy) by the photoelectric effect, and for energies of this order the photoelectrons are mainly emitted at right angles to the incident beam. Therefore, the resolution could be expected to be limited by the range of the photoelectrons which ionize the gas. A calculation of the resolution limitation due to this effect is complicated, but a typical value for the cobalt x-rays probably lies

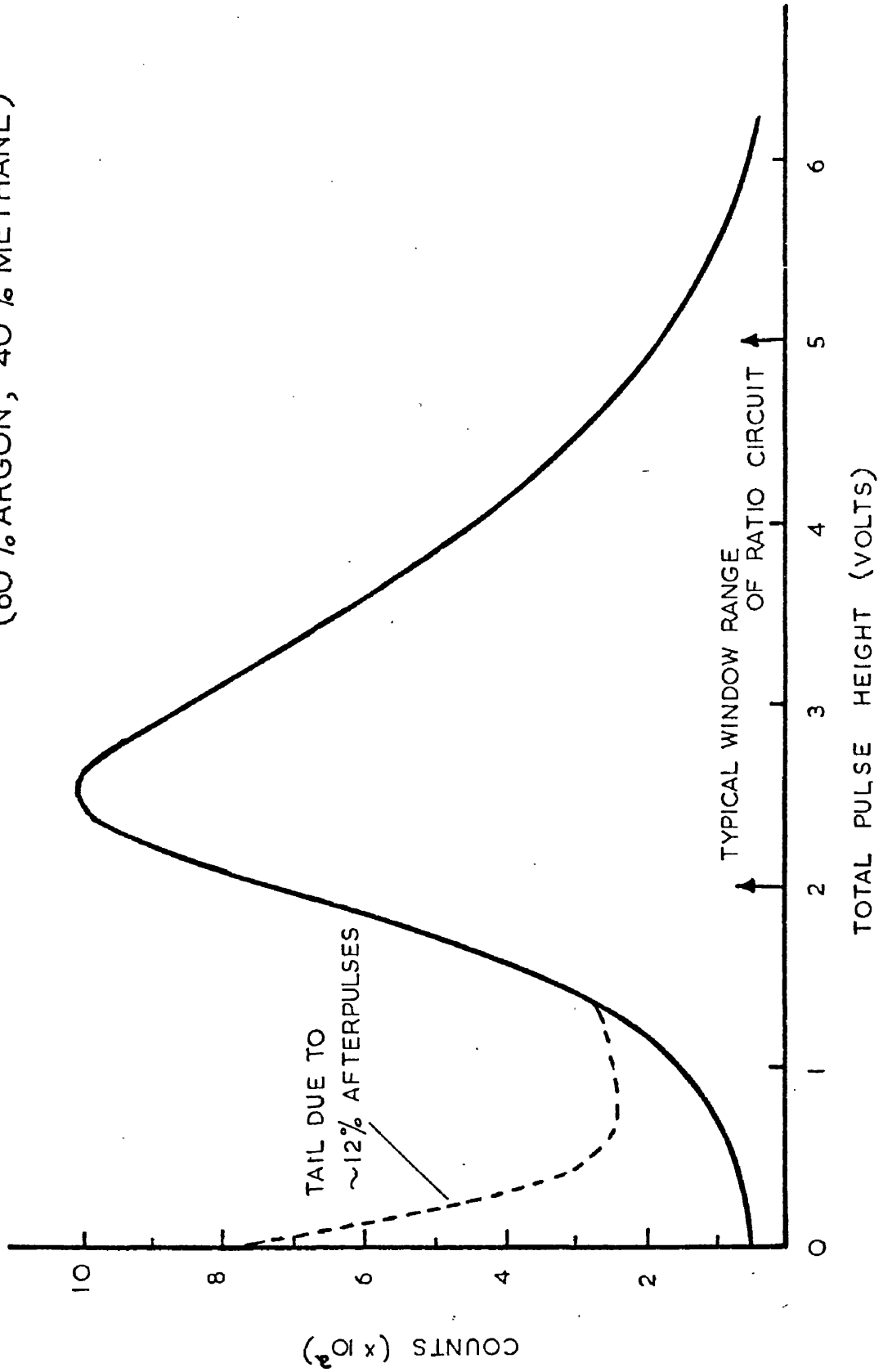
FIG. 4-7



between 0.2 and 0.4mm. However, since the ratio of the range of the  $K_{\alpha}$  x-rays of copper (8keV) to those of cobalt (6.9keV) in argon/methane mixture is  $3/2$ , it could be expected that the position resolution for the x-rays would be in the same ratio. The resolutions for the x-rays of copper (from a copper anode in the x-ray tube) were measured and are also shown in Fig.4-7. It can be seen that there is no significant difference between the two energies of x-rays. This suggests that there may be some other limiting factor present. Also the worsening of the resolution when low concentrations of methane are used is indicative of another effect - perhaps the spreading of the discharge by ultra-violet photons. This latter idea is borne out by the fact that if the counter gain is reduced by a factor of 4, with a corresponding increase in amplifier gain and noise level, the resolution in 90% argon/10% methane actually improves from 2mm to 1mm; a reduction of a factor of 2 in counter gain for a resolution value of 0.6mm did not seem to show any improvement, although in this case the noise is of more importance and could easily mask any other small change in the resolution. The possibility of ultra-violet effects will be discussed further in the next chapter.

While these measurements were being made it was noticed that the x-ray spectrum had a low energy tail which was due to afterpulses which followed the main pulses within 2 milliseconds. Fig.4-8 shows an example of the output pulse height spectrum, the dotted tail being the effect of the afterpulses. An estimate of the number of these pulses was made by allowing the total pulse signal from the counter to

PULSE HEIGHT SPECTRUM FOR 6.9 KeV X-RAYS.  
(60% ARGON, 40% METHANE)



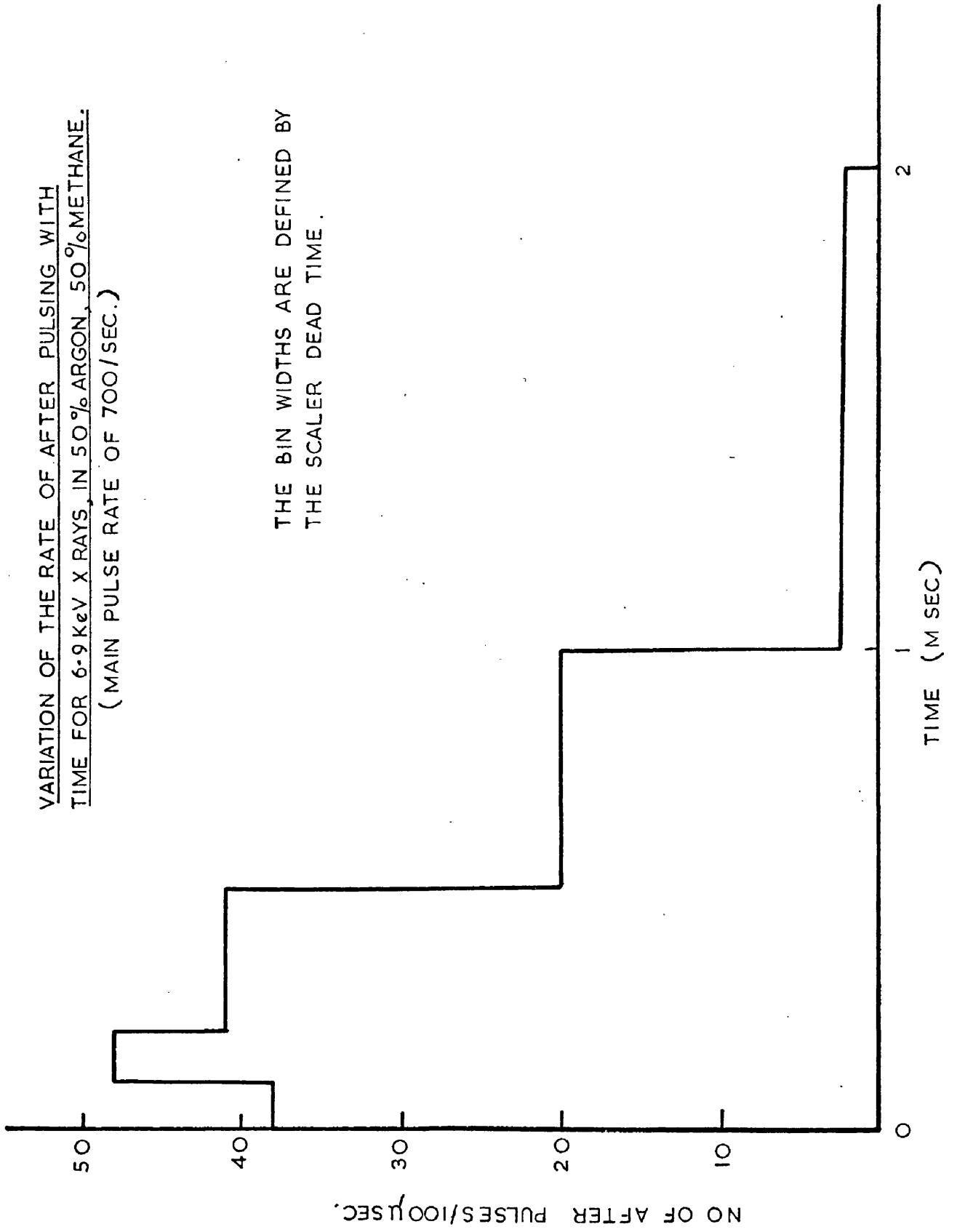
trigger a discriminator (set at a trigger level just above the noise) and then counting the output of the discriminator in two scalers, one of which had a selected insensitive time after each count accepted. The difference in these two scalers, after correction for normal statistical effects, gave the required figure. It was found in this way that while the fraction of afterpulses could be as high as 50% of the number of main pulses for the 6.9keV x-rays in certain mixtures of argon and methane, the single electron avalanches showed only a 1 or 2% effect. This suggested that the cause of the effect was probably electron capture by some impurities in the gas in the drift region of the counter, with the subsequent release of the trapped electrons in the high field region around the anode (see Wilkinson (1950)). The impurities seemed to be present in the methane gas used, and replacement with research grade methane (99.95% pure) allowed the level of the afterpulsing to be reduced to less than 2% for the x-rays. A typical time distribution of these pulses with respect to the main pulses is shown in Fig.4-9, the majority of the afterpulses lying within the first millisecond.

The presence of the afterpulses is really only of importance in position measurement if they have a pulse height such that they can be analysed along with the main pulses and so contribute to the position resolution. In the case of alpha particles where the number of afterpulses could be expected to be fairly large - since the number of primary electrons which may be captured is high - their pulse height will be down at the level of the noise and they can, therefore,

FIG. 4-9

VARIATION OF THE RATE OF AFTER PULSING WITH  
TIME FOR 6.9 KeV X RAYS, IN 50% ARGON, 50% METHANE.  
(MAIN PULSE RATE OF 700/SEC.)

THE BIN WIDTHS ARE DEFINED BY  
THE SCALER DEAD TIME.



be ignored. For the pulses resulting from single electron avalanches, the opposite is true - here the pulse caused by the capture of an electron in the drift region will not really appear as an afterpulse but rather as a delayed main pulse. However, the chances of the one electron being captured are low and so it seems unlikely that this effect need be considered with regard to the resolution measurements for the single electron avalanches. In the case of the x-rays of about 6 to 8 keV used here, the loss of proportionality which accompanies high counter gain has the effect of bringing the pulse height of the afterpulses close to that of the x-rays. It was measured, however, that even for the case of the 50% afterpulsing there were less than 5% extra ratio circuit output pulses. It is unlikely, therefore, that this would alter the position resolution of the x-rays, and certainly a check, with a gas filling which gave only a few percent afterpulses, showed no improvement in position resolution.

#### General Measurements on the System.

As was mentioned in Chapter I, one of the advantages of a proportional counter over a spark chamber should be in the count rate capability of the device. With the 10cm counter system, a rate of output of position information of  $2 \times 10^4$  counts per second was recorded over 1cm of counter, i.e. about 20 times that of a spark chamber. However, measurements have suggested that for the cobalt x-rays incident on a very short length of counter (about 0.15mm), the resolution was twice as poor at  $5 \times 10^3$  counts per second as at 100

counts per second. The worsening of the position resolution at the higher count rate was probably due to errors in the measured position, as a result of the pulses from the main amplifiers being superimposed on small undershoots from the previous ones, and not to any basic counter effect.

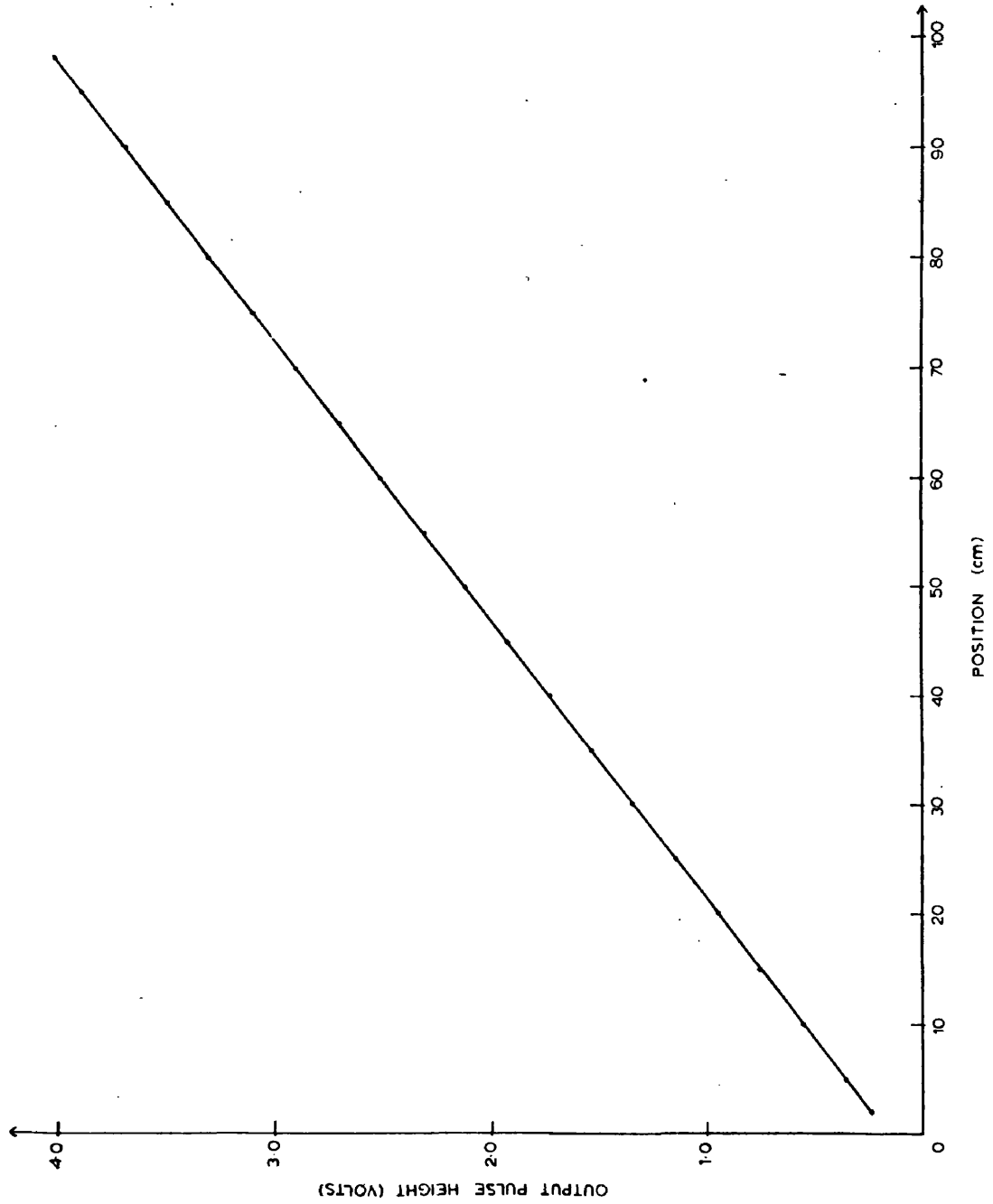
As far as the efficiency of the electronic system is concerned - i.e. the proportion of counter pulses analysed by the ratio circuit - this is limited by the relation between the input range of the ratio circuit and the pulse height spread from the counter, and also by the possible loss due to the 20 microseconds dead time of the ratio circuit. For the x-rays used above, the efficiency at low count rate was about 75%.

#### The Demonstration of the One Metre Long Counter.

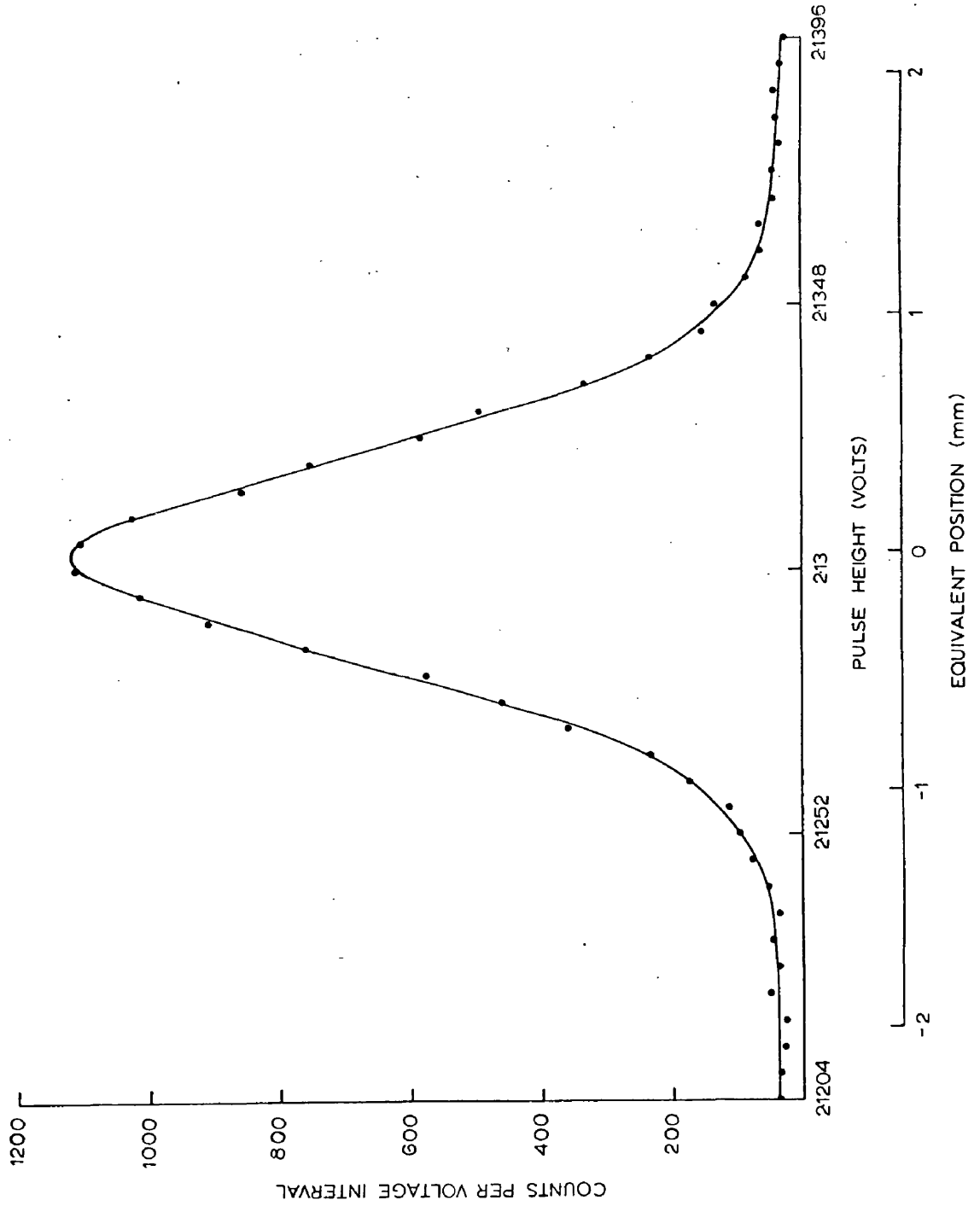
The last of the work carried out on the one dimensional system was the demonstration of the 100cm long counter, which was set up in the same way as the short counter. The linearity of this counter was measured using the collimated americium alpha source, and as can be seen from Fig.4-10, any non-linearity is less than 0.2% of the full scale output. The resolution of the alpha source, measured in methane, and in 90% argon/10% methane mixture, was 1.2mm at one end improving to 0.9mm at the other, for counter pulses in the range  $3.45 \times 10^7$  to  $8.6 \times 10^7$  electrons. It appears that in this case the limitation to resolution was a combination of the electronic noise from the system, the dispersion of the ratio circuit, and the collimation of the source. A typical position peak is shown in Fig.4-11.

FIG. 4-10

LINEARITY OF THE 100 cm COUNTER.



TYPICAL POSITION PEAK FOR ALPHA PARTICLES IN THE 100cm COUNTER.



Chapter V.THE PERFORMANCE OF THE ONE DIMENSIONAL  
COUNTER SYSTEM.

The limitation to the resolution of a gas proportional counter owing to the diffusion of the primary electrons in the gas was shown in Chapter II (equation 2.13) to be of the form

$$R = 4\sqrt{e \log e^2 \int \frac{D}{W} dr} / \sqrt{N} = 4\sqrt{e \log e^2 \left(\frac{D}{W}\right)_{\text{mean}} e} / \sqrt{N} \quad 5.1$$

A typical value of about  $0.75/\sqrt{N}$  mm was calculated for methane and, in order to allow a comparison between the experimental resolution of the single electron avalanches (where  $N = 1$ ) and the diffusion limitation to be made, it is necessary to evaluate  $D/W$  for different mixtures of argon and methane.

No experimental data is available for  $D/W$  in argon/methane mixtures. Vorobev et al (1962) have calculated values of a closely related quantity, the electron temperature, for small fractions of methane in argon, from their measurements of electron drift velocity in the mixture and from data on the mean free path of electrons in argon of Townsend & Bailey. However, their method is not applicable to more than about 5% of methane in the mixture.

Values of  $D/W$  in a gas mixture can be calculated in the following way.

The Diffusion of Electrons in Argon/Methane Mixture.

For the electrons in a gas it has been shown by Townsend (e.g. 1947) that if a Maxwellian distribution of energy is assumed

$$D = \frac{1}{3} \frac{\lambda}{P} u \quad 5.2$$

$$W = 0.815 \left( \frac{e}{m} \right) \left( \frac{E}{P} \right) \left( \frac{\lambda}{u} \right) \quad 5.3$$

$$W^2 = 0.407 f u^2 \quad 5.4$$

$$\frac{1}{2} m u^2 = \frac{3}{2} kT \cdot \eta \quad 5.5$$

where  $D$  is the diffusion coefficient of the electrons in the gas at pressure  $P$ , temperature  $T$ , under the influence of an electric field of  $E$  volts per cm.  $W$  is the drift velocity of the electrons in the gas.  $f$  is the fractional energy lost by an electron in a collision with a gas molecule.

$\lambda$  is the electron mean free path at 1mm pressure.

$u$  is the rms agitation velocity of the electrons

and  $\eta$  is the electron temperature.

Since the electrons in a gas mixture undergo collisions with the molecules of both constituents of the mixture, the number of collisions per cm will be the sum of the number of collisions per cm with each constituent, and in a similar way the energy lost per cm will be the sum of the energies lost per cm to each constituent, i.e.

$$\frac{1}{\lambda_m} = \frac{F}{\lambda_{CH_4}} + \frac{(1-F)}{\lambda_A} \quad 5.6$$

$$\text{and } \frac{f_m}{\lambda_m} = F \frac{f_{CH_4}}{\lambda_{CH_4}} + (1-F) \frac{f_A}{\lambda_A} \quad 5.7$$

where  $F$  is the fraction of methane in the mixture.

This last equation can be reduced to

$$\frac{f_m}{\lambda_m} = F \frac{f_{CH_4}}{\lambda_{CH_4}} \quad 5.8$$

since it has been shown by Cottrell & Walker (1965) that  $f_{\text{methane}}/f_{\text{argon}} \approx 10^4$ , while  $\lambda_{\text{methane}} \approx \frac{\lambda_{\text{argon}}}{10}$ .

The quantity which can be calculated for the electrons in the mixture is actually  $(\eta/E)$  where from the equations 5.2 and 5.3 above

$$\frac{D}{W} = \frac{1}{38.92} \frac{\eta}{E} \quad 5.9$$

Two procedures, using different experimentally measured quantities, for calculating  $(\eta/E)$  will be outlined.

The first of these is similar to a method used by English & Hanna (1953) for argon/carbon dioxide mixtures. This allows values of the mean free path  $\lambda$  and the energy lost per collision  $f$  for electrons in argon/methane mixture to be calculated, by means of equations 5.6 and 5.8, from the same quantities in argon and methane separately. The values of  $\lambda$  and  $f$  in the mixture are found for a particular value of electron temperature ( $\eta$ ) and, from equations 5.3 and 5.4, they give the electron drift velocity ( $W$ ) and electric field per unit pressure consistent with this electron temperature. Thus the ratio  $(\eta/E)$  in the mixture is found. The free path and the energy lost per collision in methane are obtained from the measurements of Cochran & Forester (1962); and the free path in argon from the measurements of Townsend & Bailey, which are listed in Healey & Reed (1941).

The second method is rather more simple and was devised by

the author. It uses experimental values of the electron drift velocity in argon/methane mixtures to allow the required quantity  $(\eta/E)$  in the mixture to be calculated from the available experimental data on pure methane.

From equation 5.8

$$\frac{f_m}{\lambda_m} = F \frac{f_{CH_4}}{\lambda_{CH_4}}$$

and from equations 5.3 and 5.4 it follows that

$$\frac{f}{\lambda} \propto \frac{W \cdot E/p}{u^3} \quad 5.10$$

and so equation 5.8 becomes

$$\frac{W_m (E/p)_m}{u_m^3} = \frac{F \cdot W_{CH_4} (E/p)_{CH_4}}{u_m^3} \quad 5.11$$

where  $u_m$  is defined for a particular  $(E/P)$  in the mixture.  $W_{CH_4}$  and  $(E/P)_{CH_4}$  are the equivalent values, in methane alone, of the drift velocity and electric field which are consistent with this value of  $u_m$ .

At any  $(E/P)_m$  of interest,  $W_m \cdot E/P_m$  is obtained from the data of English & Hanna, and so  $W_{CH_4} \cdot (E/P)_{CH_4}$  is found from 5.11. Then the electron drift velocity measurements either of English & Hanna or Cottrell & Walker are used to allow  $(E/P)_{CH_4}$  to be evaluated. The value of electron temperature  $(\eta)$  at this value of  $(E/P)_{CH_4}$  is obtained from the data of Cochran & Forester.  $(\eta/E)$  in the mixture is then found.

Since  $(E/P)$  is a function of position in a cylindrical counter it should be the mean value of  $(\eta/E)$  in the mixture over the distance drifted by the electrons which is used for calculating the diffusion limitation. Unfortunately, the lack of available data on the drift velocity of electrons in methane at  $(E/P)$  values above 3 volts per cm per torr renders this impossible, and so values at fields corresponding to the middle of the drift distance of the counter are used. When  $(\eta/E)$  is known,  $D/W$  is obtained from equation 5.9 and the value of the resolution limitation for single electron avalanches is found from equation 5.1 with  $N = 1$ .

#### Comparison of the Experimental Results with Theory.

Before the calculated figures can be directly compared with the experimental results for the resolution of single electron avalanches, it is necessary to make two corrections. Firstly, the mean electronic noise measured in the system (about 0.33mm) has to be added quadratically to the theoretical figures, and then allowance has to be made for the finite width of the focussed image on the aluminised mylar. This was carried out by summing a number of Gaussian distributions of FWHM predicted by the theory over the width of the working slit (0.3mm), the calculation being performed on an IBM 360/44 computer.

The variation of resolution for single electron avalanches with gas mixture is shown in Fig.4-2, the black curve representing a fit to the experimental points. The errors shown are a measure of the uncertainty of the full widths of the position peaks. Three theoretical curves are shown :

Curve (A) from the first method of calculating  $D/W$  and curves (B) and (C) from the second method. (B) uses the drift velocity in methane of Cottrell & Walker and (C) that of English & Hanna. It can be seen that the agreement between the theoretical curves is imperfect, giving some idea of the uncertainty of the data from the literature. The observed resolution, however, appears to be larger than that predicted by the electron diffusion theory. At low concentration of argon the difference between the experimental and theoretical values increases with decreasing percentage of argon, and no explanation for this is offered; while at high argon concentrations, e.g. 90% argon/10% methane, it was found that the resolution measurement was considerably poorer than expected. Also this latter position peak had a background tail on it which was not present on the others. These observations, together with the fact that at high concentrations of argon, the leading edges of the preamplifier pulses were ragged, as was mentioned before, could be consistent with the possibility that the resolution here was not just limited by electron diffusion but was being worsened by the spreading of the discharge by ultra-violet photons.

Ultra-violet photons have been observed to be liberated from the avalanches in a proportional counter by a number of workers, e.g. Rose & Korff (1941) and Campion (1968). A possible result is to increase the effective gas multiplication by the release of photoelectrons either at the cathode or in the filling gas of the counter. The importance of this effect, and where the photoelectrons are released, depends on a number of factors, such as the gain of the counter, the

constituents of the filling gas, and the material of the cathode; and in the limiting case of the Geiger counter, it can lead to the spread of the discharge along the counter length. In the case of the 10cm counter, which may be operating fairly close to the Geiger threshold, it is thought that there may be a spreading of the discharge taking place for all the concentrations of methane used. This could be due to photoelectrons released in the methane quenching gas, and also, for low concentrations of quenching gas, to photoelectrons released from the cathode, as indicated by the ragged leading edges to the preamplifier pulses.

The x-ray resolution measured is consistent with this reasoning. The values for copper and cobalt x-rays were essentially the same and did not appear to be limited by the collimation of the x-ray beam, by the electronic noise or by the distance travelled by the photoelectrons. The resolution varied with gas mixture in a similar way to that for single electron avalanches, in that it improved from about 2mm for 90% argon/10% methane, to 0.6mm for 50% argon/50% methane. These values possibly give a measure of the ultra-violet spreading of the discharge (plus electronic noise), without the electron diffusion effects being significant, although at a lower value of relative counter gain than for the single electron case.

It is of interest to note that in the short counter the alpha particle resolution, which was limited to 0.42mm by lack of collimation, did not show a variation with gas mixture. This suggests that, at the lower relative counter gain used, the spreading of the discharge,

although possibly still present, was not so significant in its effect on resolution.

As mentioned earlier, typical position peaks for the system are shown in Figs. 4-3, 4-5. If electron diffusion was the only limiting factor to position resolution, it would be expected from equation 2.3 that the resolution peak for single electron avalanches would be Gaussian in shape. However, the finite width of the masking slit, the possible presence of ultra-violet spreading of the discharge, and the electronic noise in the system could be expected to alter this. Fig. 4-3 shows such a peak and its deviation from a computer fitted Gaussian curve.

#### Electronic Performance of the Counter System.

Both counters were limited in their resolution by electronic noise, the measured limitation in the short counter being equivalent to approximately  $5.4 \times 10^4$  rms electrons and in the long counter to about  $1.5 \times 10^4$  rms electrons. These figures are in fairly good agreement with the values predicted theoretically, as expressed in 4.1 to 4.4.

The distributed RC time constant of the long counter system is approximately  $5.7 \times 10^{-8}$  secs, i.e.  $\approx \frac{1}{30} \tau_A$ ; and so the non-linearity of the position measurements should be very small. As mentioned before, this non-linearity was less than 0.2%, which is about the same as that of the ratio circuit itself.

#### Conclusion.

The measurements carried out on the one dimensional counters

have suggested that the spread of the discharge by ultra-violet effects may be an important limitation to such a design of proportional counter system. It must be realised, however, that this is probably just a consequence of the high counter gain which is necessary to overcome the electronic noise in the system, and need not be a limitation if a different method of obtaining position information is used. In general, with a counter of this type, the position resolution will improve with increasing counter gain (since the signal to noise ratio improves) until this other limitation is encountered. However, the optimum value of resolution found will depend on many factors, such as the length of the counter, the resistance of the collecting electrode and the pressure and constituents of the gas filling.

These counters have been shown to be capable of resolution of about 0.5mm in 10cm and 1mm in 100cm and so are an improvement on the other designs of gas proportional or Geiger counters which were in existence when the work was undertaken, e.g. the proportional counter of Kuhlmann et al (1966) with a resolution of 1.2mm in 30cm, and the Geiger counter of McDicken (1967) with 2cm resolution in 70cm. Their resolution is also better than that of most semiconductor, resistive electrode type, position sensitive detectors, which are usually limited in resolution to 1% of their length, e.g. Melzer et al (1968) achieved 0.57mm resolution in 5.3cm.

Chapter VI.A PROPORTIONAL COUNTER FOR POSITION SENSITIVITY  
IN TWO DIMENSIONS.Introduction.

As was discussed in the first chapter, there were few detectors available in 1967 which could provide two dimensional position information of high resolution over an area of several hundred square centimeters for x-rays and charged particles and still retain a high count rate capability and a simple readout system. The author's work on proportional counters for position sensitivity in one dimension has shown the potential of these devices with respect to resolution, count rate and ease of readout; and it seems that if such a system were extended to be sensitive over a given area, and to give position information in two dimensions, it could be very useful for nuclear scattering experiments or for the image formation of x-ray distributions.

The building of a proportional counter to be sensitive over an area requires an anode which is extended in space but which still maintains a high electric field close to it. The simplest method of achieving this is to have a plane of parallel anode wires between two parallel cathode planes, as reported by Rossi & Staub (1949). Each anode wire acts as an individual counter; and so a counter array to give position information in one dimension is available. Such a system has been introduced by Charpak et al (1968).

There are several ways of obtaining two dimensional position information from such a proportional counter, and most of these use

two planes of wires arranged so that the wires in one plane are at right angles to the wires in the other. Each wire plane can then provide information in one dimension. The simplest case, which is really only of use for charged particles which pass through such a detector, is to have two separate counters at right angles to each other. This arrangement has been used recently by Amato & Petrucci (1968) for the study of profiles of high energy particle beams. For radiation which is absorbed in the counter, the position co-ordinate in one dimension can be obtained from a multiwire anode and in the other from the cathode if it is also fabricated as a wire plane. It is important to note that while the position information as read out on the anode wires is limited by their spacing - since each wire behaves as a separate counter - the effect of the cathode wire spacing on the position resolution is considerably smaller. This is because the cathode signal, which is due mainly to the movement of the positive ions from the avalanche close to the anode, is induced on a number of the cathode wires. It is the mean position of the charge induced on the cathode which must be measured. It should be possible to observe the same effect on a grid placed between the anode and the cathode; and, in fact, position information in both dimensions should be obtainable in this way, with only a small dependence on the grid wire spacing, if two grids at right angles to each other are used. This method may have advantages over those which require the anode to give information in one of the dimensions; since an anode structure such as a fine mesh, which itself is unsuitable for giving position

information, may be used to reduce the limitation to resolution which results from finite anode wire spacing.

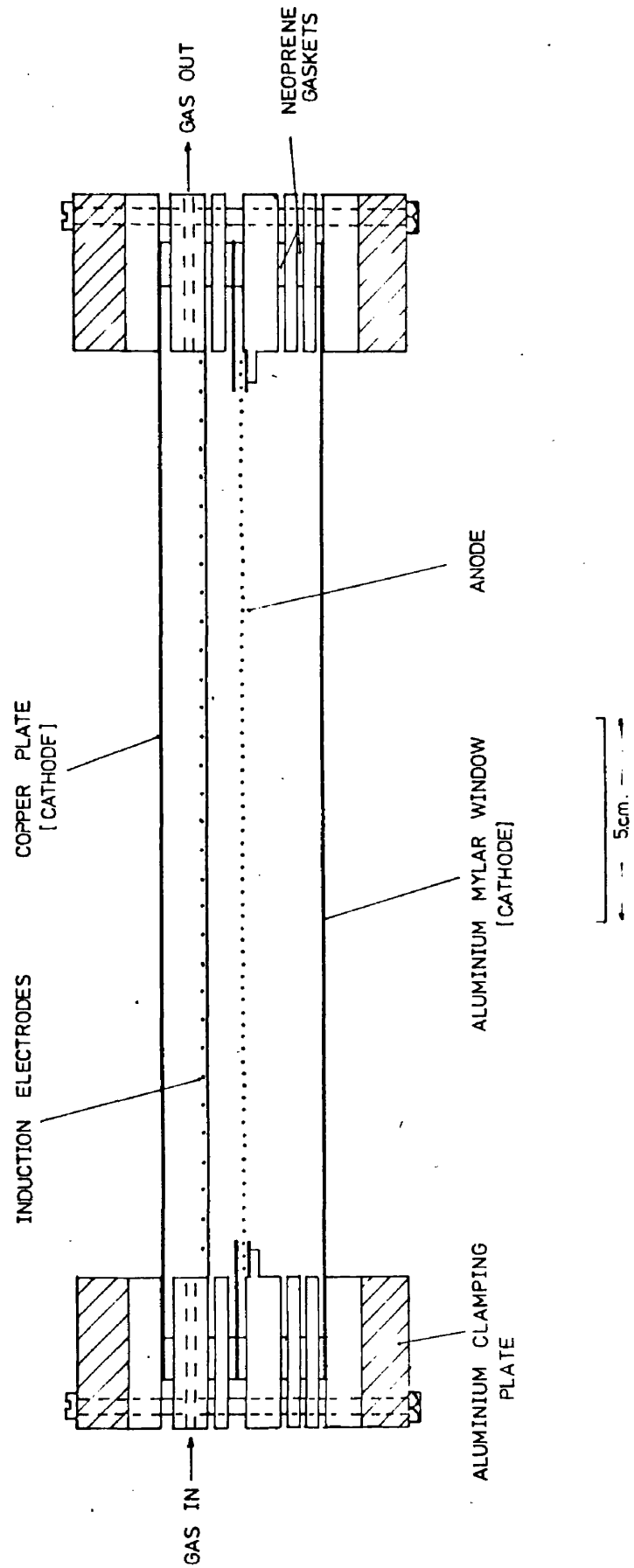
This new method of obtaining the signal from electrodes placed between the anode and cathode of a proportional counter is used in the detector to be described in this chapter. The electrodes are two grids of resistive wire at right angles to each other; and the wires in each are in series so that the mean position of the charge induced on either grid, by the movement of the positive ions in the avalanche away from the anode, can be determined by the method of charge division on a resistive electrode.

It had been hoped that an anode of very fine construction could have been used in a counter of this type, and some tests were carried out with nickel micromesh supplied by E.M.I. This mesh was of 10  $\mu\text{m}$  web and 58  $\mu\text{m}$  aperture but it appeared that a much larger aperture to web ratio was required if the proportional counter avalanche was only to occur close to the anode. Although a mesh or grid of the required dimensions possibly could have been etched on a suitable material, it was decided just to use a plane of wires as the anode for the testing of the two dimensional counter.

#### The Two Dimensional Counter.

This counter, as shown in Fig.6-1, consists of a plane of anode wires held 1.9cm from two cathode plates with two planes of induction electrodes mounted close together and positioned symmetrically between the anode and one of the cathodes. The anode is of 25  $\mu\text{m}$  diameter tungsten wire with a spacing between adjacent parallel elements.

TWO DIMENSIONAL POSITION SENSITIVE COUNTER.

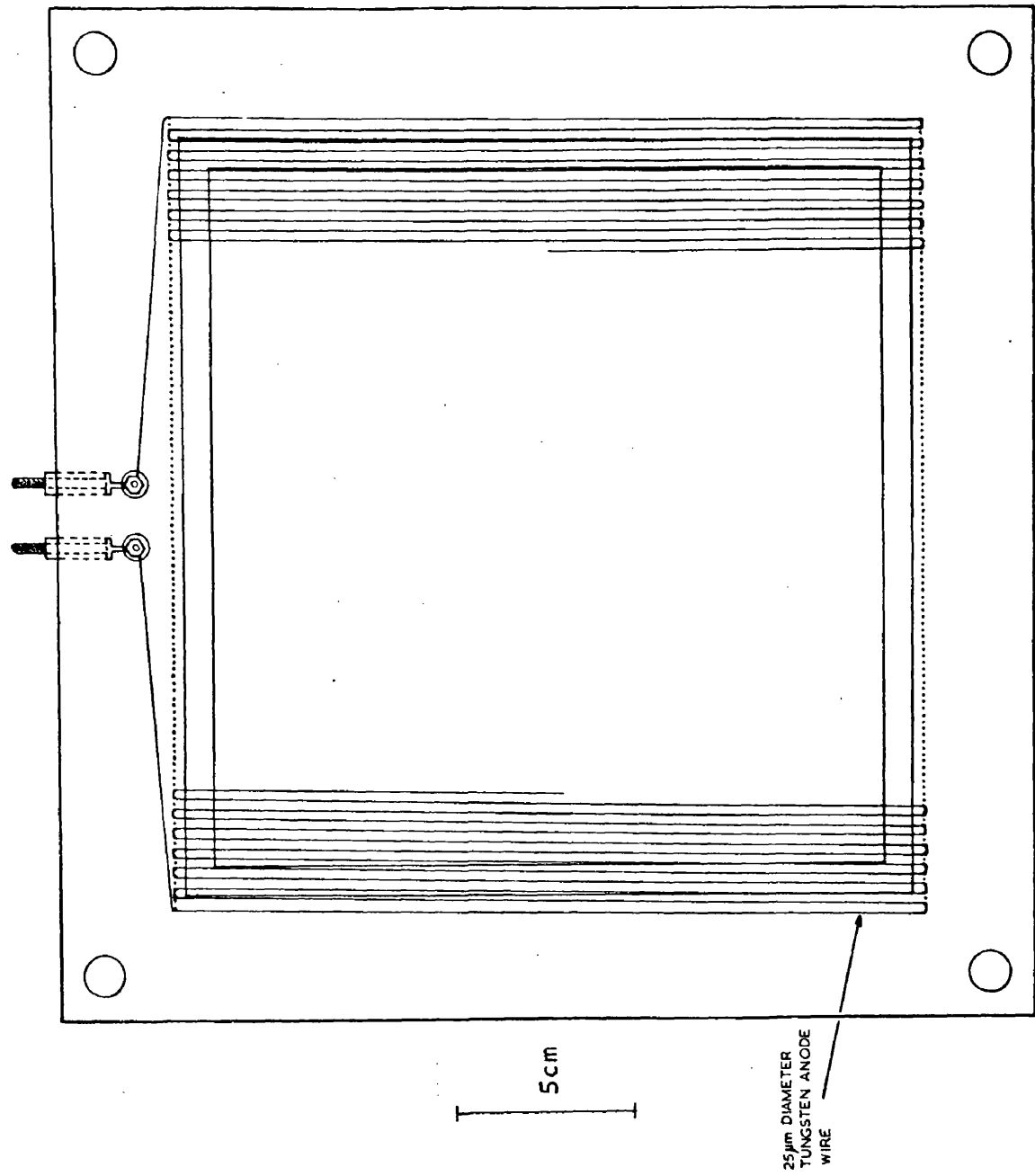


of 3mm, while the stainless steel induction wires of 25  $\mu\text{m}$  diameter have a spacing of 7mm between adjacent elements.

The anode, induction electrode, and spacer frames are perspex of 23cm square inside and these, together with the other electrodes, are separated with neoprene gaskets to maintain gas tightness. The whole assembly is clamped with 1.5cm thick aluminium frames for rigidity. The counter is operated with a gas flow and provision is made for the entry and exit of the gas by means of polythene tubing. The perspex frame on which the anode is mounted is shown in Fig.6-2. 1mm holes drilled at 2mm intervals along two opposite top faces of the frame allow nylon pegs of 1mm diameter to be inserted into the frame, and by choice of the position of the pegs a continuous anode wire can be wound, so that the separation between adjacent sections can be 1,3,5,7, etc. mms. The 25  $\mu\text{m}$  diameter tungsten wire was chosen for the anode, as this was found to be the smallest diameter of wire which could be continuously wound around the pegs with relative ease. (An anode frame was later wired with 10  $\mu\text{m}$  tungsten wire, but this proved to be a difficult operation). The wire spacing of 3mm was adopted as this was experimentally found to be the minimum which would allow a high counter gain without excessive sparking. Considerable care was taken in the wiring of the anode frame by hand to ensure that the wire tension was uniform and that all the wires lay in the same plane.

It had been found from preliminary testing that the anode wires close to the edges of the counter were liable to spark unless field control electrodes were provided around the edges on each side

PERSPEX ANODE FRAME FOR TWO DIMENSIONAL COUNTER.



of the anode wires. One of these is a copper frame of thickness 1.5mm mounted on a perspex rim inside the anode frame, so that the separation between the frame and the wires is 1.5mm; and the other is a 1.5mm thick aluminium frame separated from the anode by a 1.5mm thick neoprene gasket. Both field control electrodes, which penetrate the sensitive area of the counter by 5mm around each edge, are held at the anode potential.

The induction electrodes are mounted on a perspex frame in a similar way to the anode. The 25  $\mu\text{m}$  stainless steel wire was chosen in this case because of its relatively high resistance and the pegs in the frame were arranged to allow a spacing of 7mm. The resistance of each set of wires end to end is 10 kilohms, and one set is insulated from the other. This was achieved by raising the wires in one plane above the other by means of lengths of polythene tubing of 0.75mm diameter placed under one set of wires between the pegs and the edges of the perspex frame.

A number of different cathodes have been used in the counter. The front cathode, i.e. the one in the half of the counter which does not contain the induction planes, is 20  $\mu\text{m}$  thick aluminised mylar, while the rear cathode has been either 0.8mm thick copper sheet or 5  $\mu\text{m}$  thick aluminised mylar. This latter window, for the entry of alpha particles, was formed by fixing the mylar to a brass frame with epoxy cement and heating with an infra red lamp to remove the creases.

Aluminium sides can be attached to the counter for screening purposes, and an aluminium screening box surrounds the high voltage

and preamplifier connections. Fig.6-3 shows the counter with the preamplifiers connected.

#### Block Diagram of the Electronics.

The block diagram of the electronic arrangement has already been described in Chapter III, but before the electrostatics of the system are discussed, it is important to point out again how the position information is obtained. The resistive wires in each induction grid are in series and so the ratio of the signal taken from one end of the grid by a charge sensitive preamplifier to the total signal will be a measure of position. This is used for one dimension. However, in order to simplify the division circuit, the position in the other dimension is obtained by dividing the signal from one end of this electrode, with the other end earthed, by the total signal on the first induction electrode.

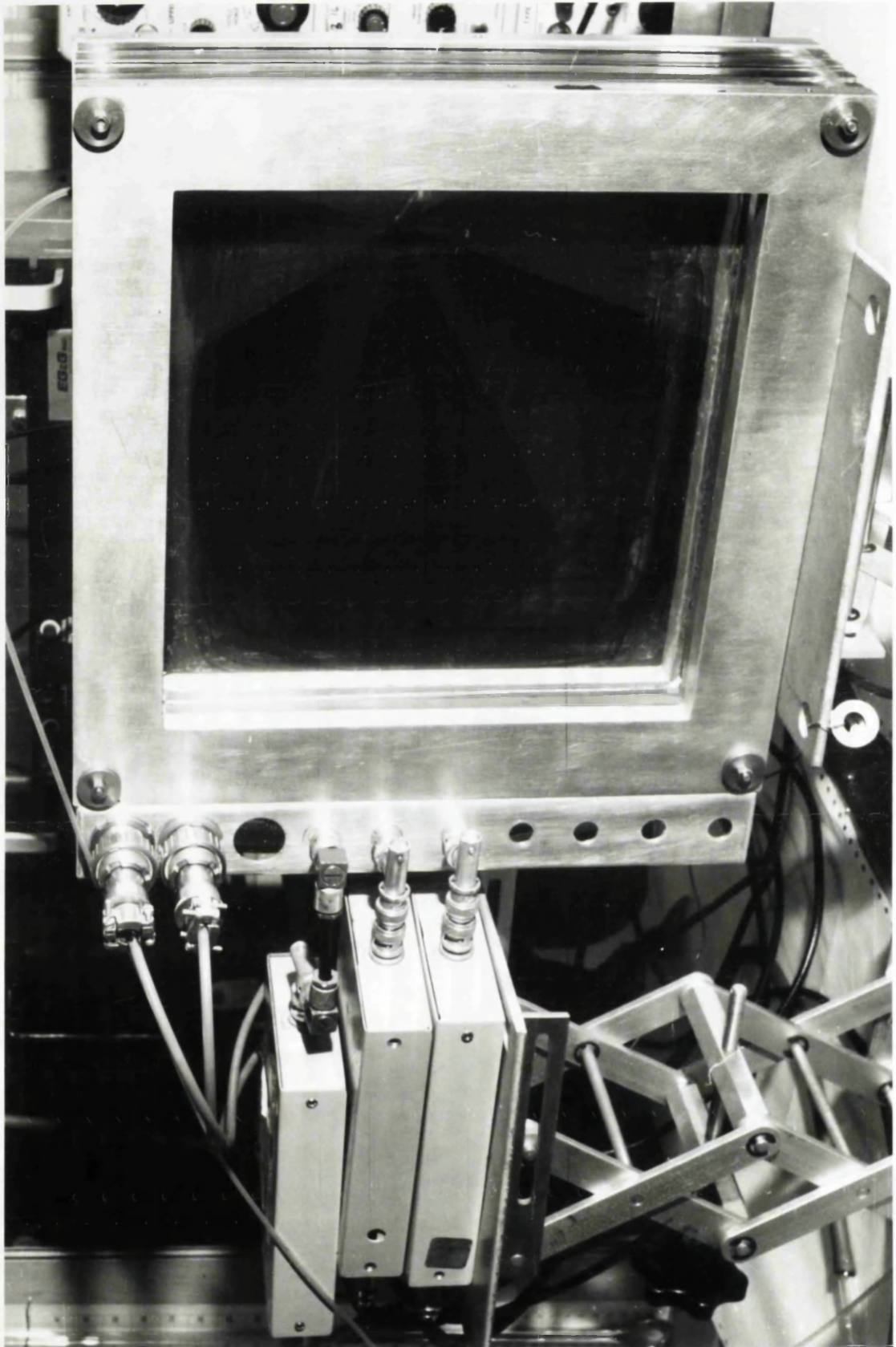
#### Electrostatics of the System.

It has been shown by Morse & Feshbach (1953) that the potential distribution around an assembly of parallel wires of unit line charge and spacing 'a', lying in the x,y plane is given by

$$\psi = - \log_e 4 \left[ \sin^2 \left( \frac{\pi x}{a} \right) + \sinh^2 \left( \frac{\pi z}{a} \right) \right] \quad 6.1$$

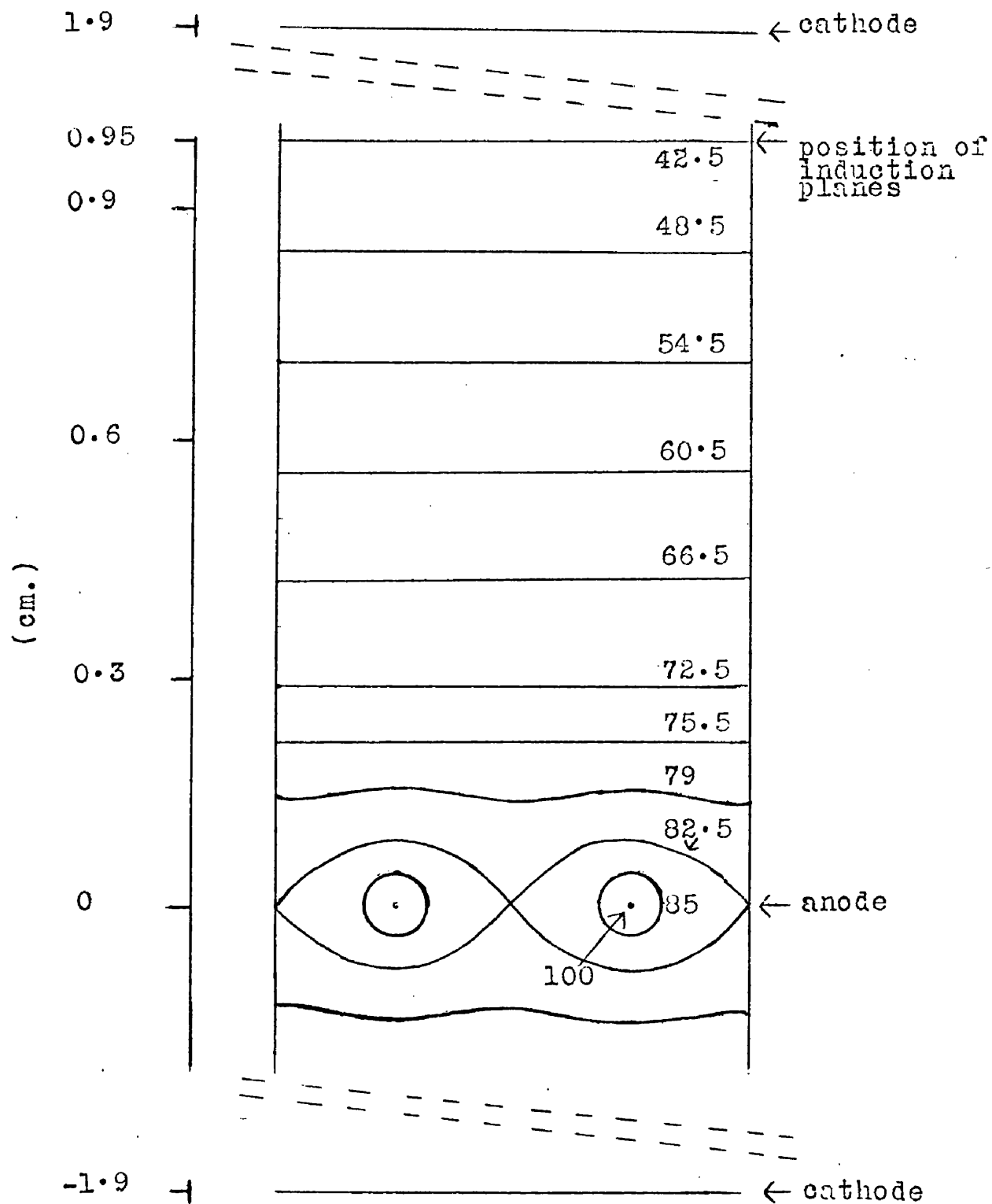
where the (x,z) co-ordinate system is centred on one of the wires and z is the vertical distance from the x,y plane. Some of the equipotentials in the two dimensional counter, calculated from equation 6.1 for 100 volts applied between the anode and cathode, are shown in Fig.6-4. The presence

FIG. 6 - 3



EQUIPOTENTIALS OF THE ANODE IN THE TWO DIMENSIONAL COUNTER.

(100V APPLIED BETWEEN THE ANODE AND CATHODE)



of the induction planes was assumed to leave the equipotentials undistorted.

For small distances  $r$  from a wire where  $r^2 = x^2 + z^2$

$$\psi \approx -\log \frac{4\pi^2}{a^2} r^2 \quad \text{for} \quad r < \frac{1}{10} a \quad 6.2$$

so that the electric field is

$$E \propto \frac{1}{r} \quad 6.3$$

which is similar in form to the electric field from a single wire in cylindrical geometry: while at large distance, i.e.  $z > a$

$$\psi \approx \frac{2\pi |z|}{a} \quad 6.4$$

$$\text{i.e. } E \approx \frac{2\pi}{a} \quad 6.5$$

and so the electric field is constant.

Therefore, the use of an array of parallel wires as a counter anode does result in an electric field which is high close to the wire, and has a constant value beyond a distance of the wire spacing from the anode plane. It is expected that in a proportional counter most of the multiplication will take place close to the anode wires, and so, each wire will essentially behave as a separate counter.

In general, in a gas proportional counter, a signal of opposite polarity to that induced on the anode appears on the other electrodes; the relative distributions of the charge between these electrodes depends on the ratios of their capacities with respect to the positive ions. Unfortunately, the case of the two crossed parallel wire grids placed on an equipotential in a counter is difficult to analyse; the nearest approach is that of Bunemann et al (1949) who considered the

effect of a single grid in an ion chamber.

Because of the complexity of the situation the experimental findings, mainly, are considered.

For the measurement of position information there are two factors which are relevant in connection with the induction wire spacing -

- a) The mean position of the charge induced by the avalanche at the anode will depend to some extent on the position of the avalanche with respect to the wires, i.e. on whether the avalanche occurs opposite an induction wire or between two such wires.
- b) The size of the signal induced on an induction electrode will depend on whether the avalanche occurs opposite a wire of the induction plane or opposite the space between two wires. This variation of amplitude of the mean signal value will be periodic with the grid spacing.

In the case of two grids at right angles where one lies slightly behind the other, the situation is rather more complicated as a result of the shielding effect of one grid on the other. However, periodic variations in amplitude and periodic non-linearities in position will occur in both dimensions. For the particular experimental arrangement used - that of taking the total signal from one dimension only - it is clear that the apparent position recorded by the detector in the dimension in which both position and total signals are taken, will only be affected by the errors introduced by (a) above. However, in the other dimension, where only a position signal is taken, the variation

in amplitude of (b) will also cause position errors. The fact that the anode wires will also limit the resolution in one dimension will lead to a rather complicated total effect.

#### The Electronic Noise in the System.

The capacity of one of the induction grids, placed between the anode and the cathode, can be calculated from the potential distribution of equation 6.1 to be 45 picofarads. It is assumed that this is not altered significantly by the presence of a second grid. Then for  $C = 45$  picofarads and the resistance of each induction electrode of 10 kilohms the equivalent noise at the input of a position preamplifier is -

$$N = 1.16 \times 10^4 \text{ rms electrons} \quad 6.6$$

and the equivalent noise on the total signal is -

$$N_t = 2.26 \times 10^3 \text{ rms electrons} \quad 6.7$$

as calculated from equations 3.9 and 3.10.

The Johnson noise appearing on the position signal will be the main limitation to the resolution.

#### The Operation of the Counter.

For almost all the experimental work with this system, the counter, with a flow of 90% argon/10% methane through it, was connected as in Fig.3-2. In some cases, however, the storage device used was a pulse height analyser and not an oscilloscope. The induction wires were held at zero potential and positive and negative voltage was applied to the anode and cathode respectively. In all cases the main

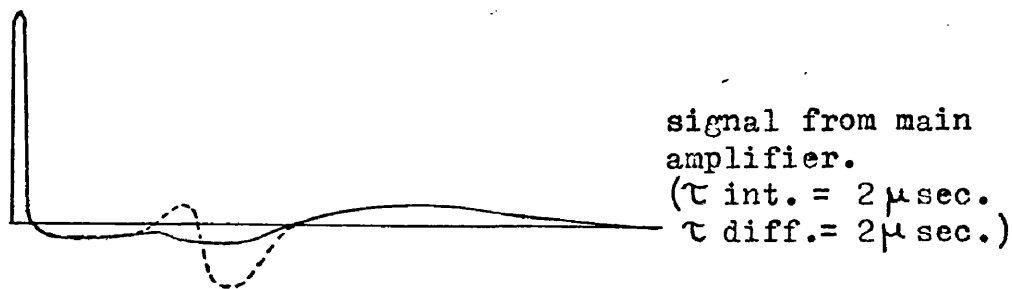
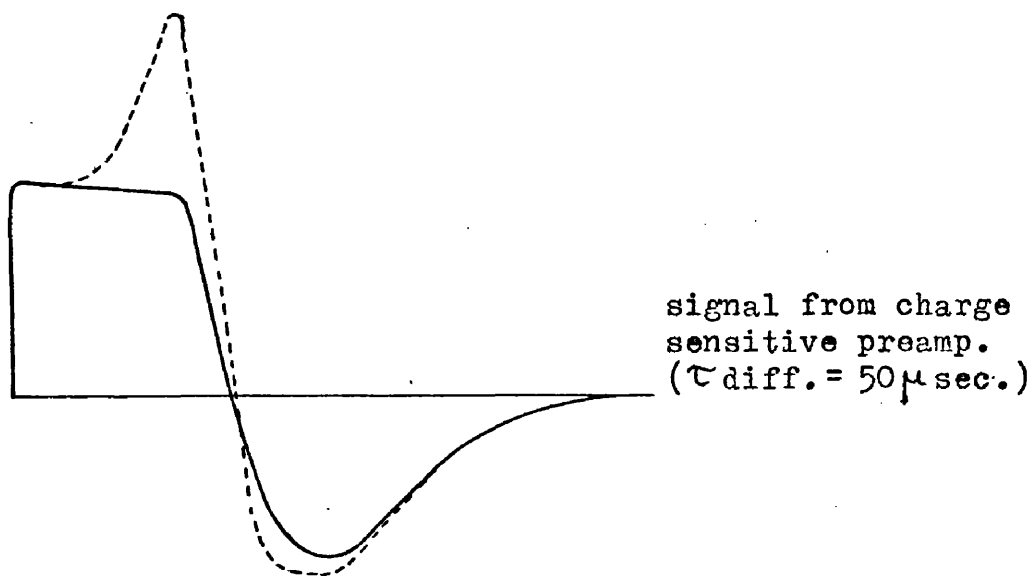
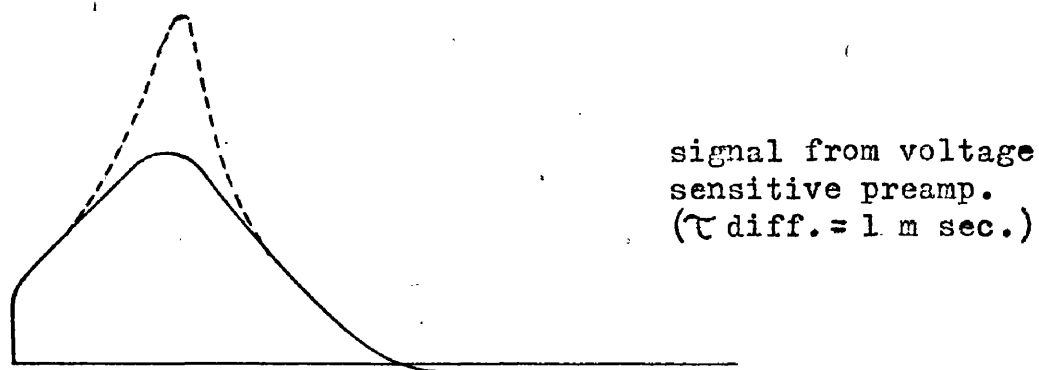
amplifiers used had equal integration and differentiation time constants of 2 microseconds.

It was found that in order to achieve an output pulse height equivalent to  $10^7$  electrons at the preamplifier input with 5.5 MeV alpha particles, the induction planes had to be held closer in potential to the anode than the equipotential diagram of Fig.6-4 would suggest. Otherwise, sparking took place between the induction wires and the anode field control electrode, apparently across the insulation; and the ratio of anode to cathode voltage had to be smaller than 1:1 to eliminate it. The calculated ratio value from Fig.6-4 is 1.33:1. It later became apparent that this affected the gain of the counter, which was about 10% lower if the counter avalanche took place opposite an induction wire than if it occurred between two such wires.

With amplifiers, of calibrated gain and equal 2 microseconds differentiating and integrating time constants, on the anode and each induction electrode, it was measured that 37% of the total charge pulse, complementary to that on the anode, appeared on the induction electrode closest to the anode, and 28% appeared on the second induction grid. Presumably the other 35% was induced on the cathode.

The pulses from the induction planes were of opposite polarity to the anode pulses, and were unlike the normal proportional counter type pulses in that they returned to zero or close to zero after the transit time of the positive ions. In Fig.6-5 the shapes of the pulses from the 5.5 MeV alpha particles of americium 241 are shown for signals equivalent to  $10^7$  electrons at the preamplifier inputs. The

PULSE SHAPES FROM THE INDUCTION WIRES FOR ALPHA PARTICLES  
IN 90% ARGON 10% METHANE MIXTURE.



0                      200                      400                      600

$\mu$  sec.

Dashed curve - source opposite induction wire.  
 Solid curve - source opposite space between two wires.

high tension voltage was  $\pm 3300$  volts on the anode and cathode respectively. These shapes were measured initially at the output of a voltage sensitive preamplifier of 1 millisecond differentiating time constant; then at the output of a charge sensitive preamplifier of 50 microseconds differentiating time constant; and, lastly, at the output of one of the main amplifiers of equal 2 microsecond integrating and differentiating time constants, connected to a charge sensitive preamplifier.

The fast pulse rise time of 400 nanoseconds corresponded to the positive ions leaving the very high field region close to the anode. This fast rise was followed by a slowly rising portion, as can be seen with the voltage amplifier of long time constant, and this is due to the ions drifting for about 150 microseconds from the anode to the induction wires. If the ions passed close to an induction wire, a larger signal than otherwise was induced after 150 microseconds as a result of the cylindrical geometry of the wire. The pulse fell again in about 200 microseconds as the ions moved from the induction wires to the cathode. It can be seen that the pulse rise at 150 microseconds, when the source was opposite an induction wire, appeared on both the preamplifier and main amplifier outputs. The pulse shapes from the two sets of wires were very similar.

For all positions of the source the main amplifier output had a 5% overshoot above the axis between 100 and 600 microseconds. It is clear that this could limit the accuracy of pulse division at high count rate since pile up of a pulse on the tail of the one before it could

take place. However, it was found experimentally that this overshoot was reduced to a negligible size if double differentiation instead of single differentiation was used in the main amplifier.

#### Total Pulse Height Information from the Counter.

As has been mentioned before, there is usually a loss in proportionality of the pulse height with the energy deposited in the counter gas, if a proportional counter is operated to give an output pulse height of greater than  $3 \times 10^6$  ion pairs. The exact gas gain of the two dimensional counter was not known because of the effect of the amplifier time constant on the pulse shape, but a pulse, equivalent to about  $10^7$  electrons, was required at the preamplifier input to achieve a high signal to noise ratio. Fig.6-6 shows the variation of the pulse height with voltage applied to the counter for the alpha particles and x-rays from americium 241. It should be noted that the full 5.5 MeV of the alpha particles was not deposited in the counter because of an air space of about 1cm in the collimator and the thickness of the mylar counter window. The effective alpha particle energy was probably less than 1 MeV.

The loss of energy linearity towards the operating pulse height of  $10^7$  electrons at the input can be clearly seen.

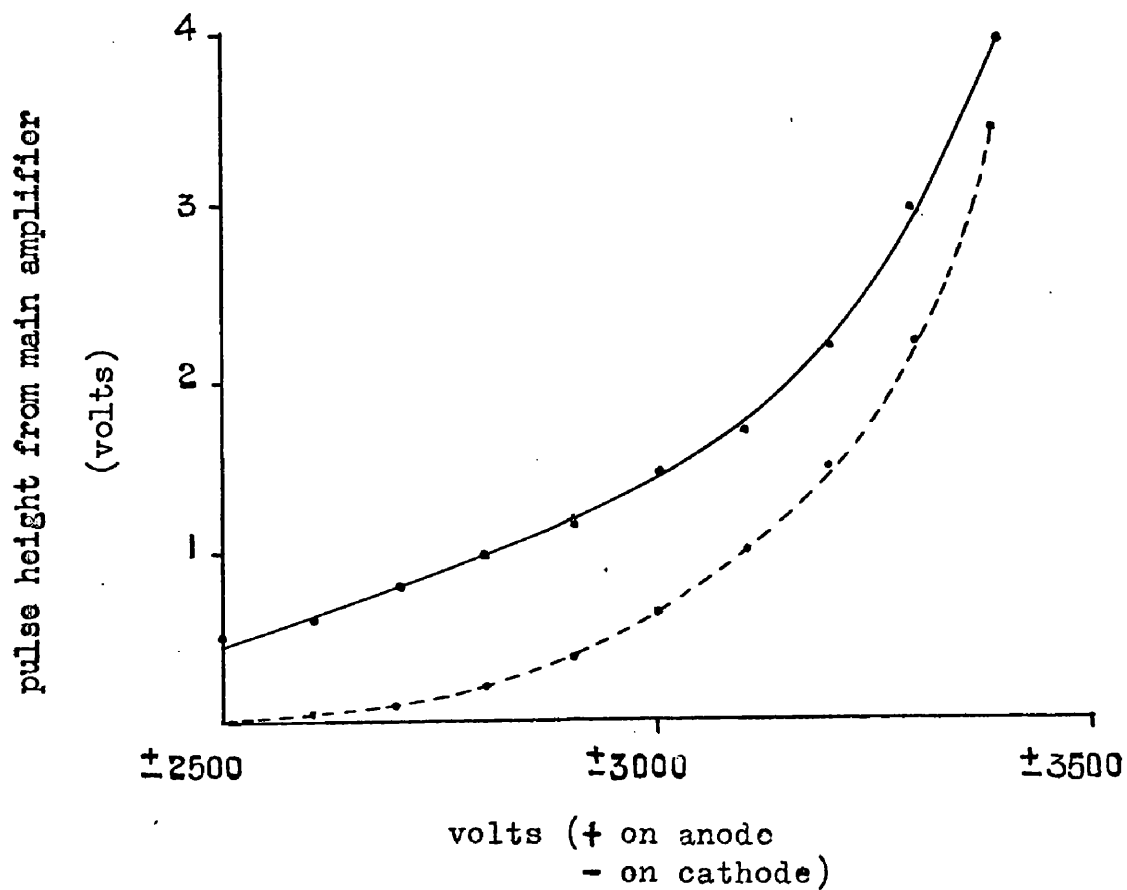
#### Measurement of Position in Two Dimensions.

A series of measurements of the linearity and the resolution of this counter were carried out with two collimated alpha particle sources. For the 5.5 MeV alpha particles the counter was operated at

VARIATION OF PULSE HEIGHT FROM THE COUNTER WITH VOLTAGE.

Solid curve - 5.5 MeV alpha particles from Am<sup>241</sup>

Dashed curve - ~ 20 keV x-rays from Am<sup>241</sup>



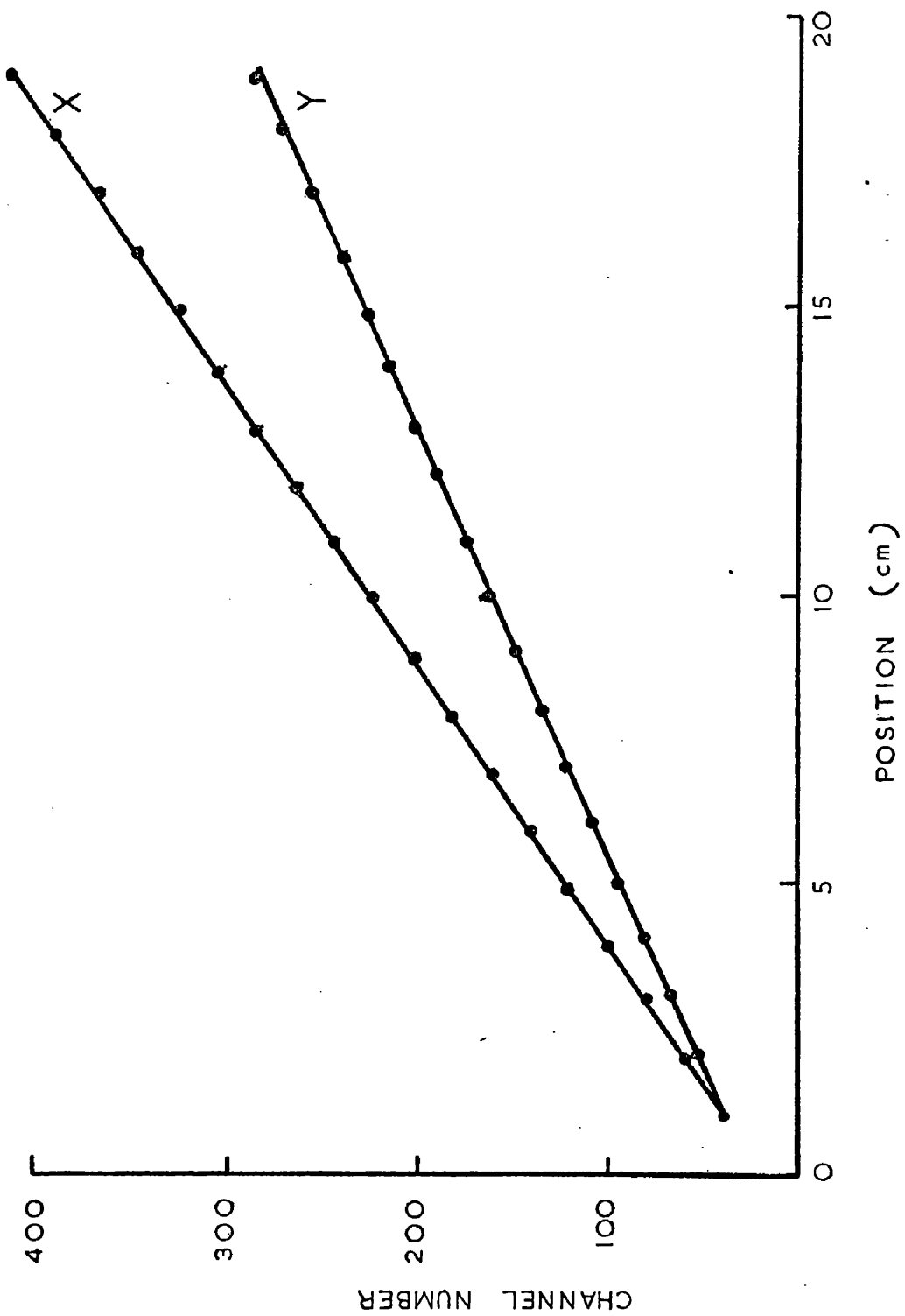
1 volt from main amplifier  $\equiv$  signal of  $3.5 \times 10^6$  electrons  
at preamplifier input

$\pm 3300$  volts to give pulses equivalent of the order of  $10^7$  electrons at the preamplifier inputs.

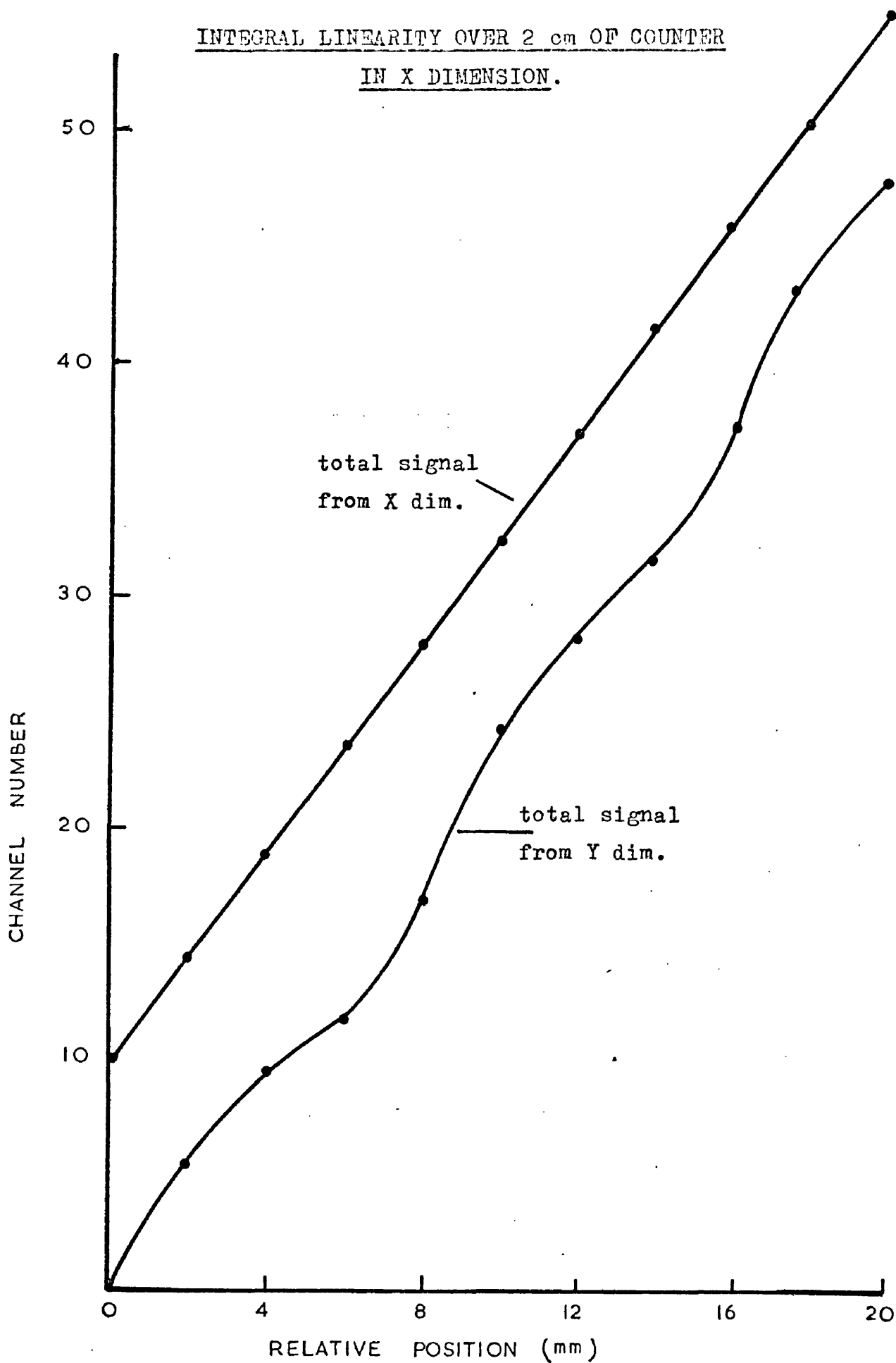
The linearities of the counter in the two dimensions for a collimated line alpha particle source, with the total signal taken from the dimension parallel to the direction of the anode wires (X dimension), are shown in Fig.6-7. It can be seen that there is a non-linearity towards the high end of about 1% of full scale in both dimensions. However, this was probably due to an end effect in the detector. For the induction electrodes R is 10 kilohms and C is about 45 picofarads and  $RC = 4.5 \times 10^{-7}$  seconds. This is less than the amplifier time constant of 2 microseconds, so that non-linearities of 1% magnitude would not be expected from the behaviour of the electrodes as diffusive transmission lines.

Fig.6-8 is the detailed linearity over a short length of counter in the X dimension under the two conditions of operation of the detector, i.e. firstly, with the numerator and denominator signal taken from the same induction plane, and then the numerator taken from the X plane and the denominator from the Y plane. It can be seen that while within the accuracy of the measurements the case of both signals from the same electrode shows no non-linearity effect, there is a non-linearity in the other case at the period of the induction wire spacing. The position of the alpha source was displaced up to  $\pm 0.7$ mm from its true position. Similar results were found in the Y dimension, and it is interesting to note that within the accuracy of measurement, the wire spacing of the anode did not cause any position error of greater

LINEARITY OF BIDIMENSIONAL COUNTER  
 (TOTAL SIGNAL PULSE OFF X DIMENSION)



INTEGRAL LINEARITY OVER 2 cm OF COUNTER  
IN X DIMENSION.



than  $\pm 0.3\text{mm}$ . This was probably due to the diffusion of the primary electrons smoothing out the effect of the finite anode wire spacing.

In the dimension in which the total signal was not taken there was a variation in the apparent position (as measured by the ratio signal) with position in the other dimension: with a collimated point alpha particle source this shift, of amplitude of the order of  $1\text{mm}$ , was observed to be periodic with the induction wire spacing in the other dimension. This effect was not observed if both position and total signal were taken from the same wire.

The non-linearities which occur when the position and total signals are taken from different induction planes are probably caused by the small variations of the signal amplitude induced on the induction electrodes, as discussed earlier.

The integral methods of measuring the linearity which were used in the preceding investigation are not very sensitive to small changes. This is partly due to the errors in measurement of the peak of a position distribution which may be of  $1.25\text{mm}$  FWHM. However, if a collimated point alpha particle source is scanned at a steady rate over a part of the counter, the number of counts per unit distance or the differential linearity is recorded and this gives more accurate information.

An americium  $^{241}\text{Am}$  alpha particle source, collimated to  $1.25\text{mm}$  was mounted on an X,Y pen recorder which was driven with a triangular wave form of 5 seconds period. This allowed the source to be scanned over a length in the X dimension or in the Y dimension.

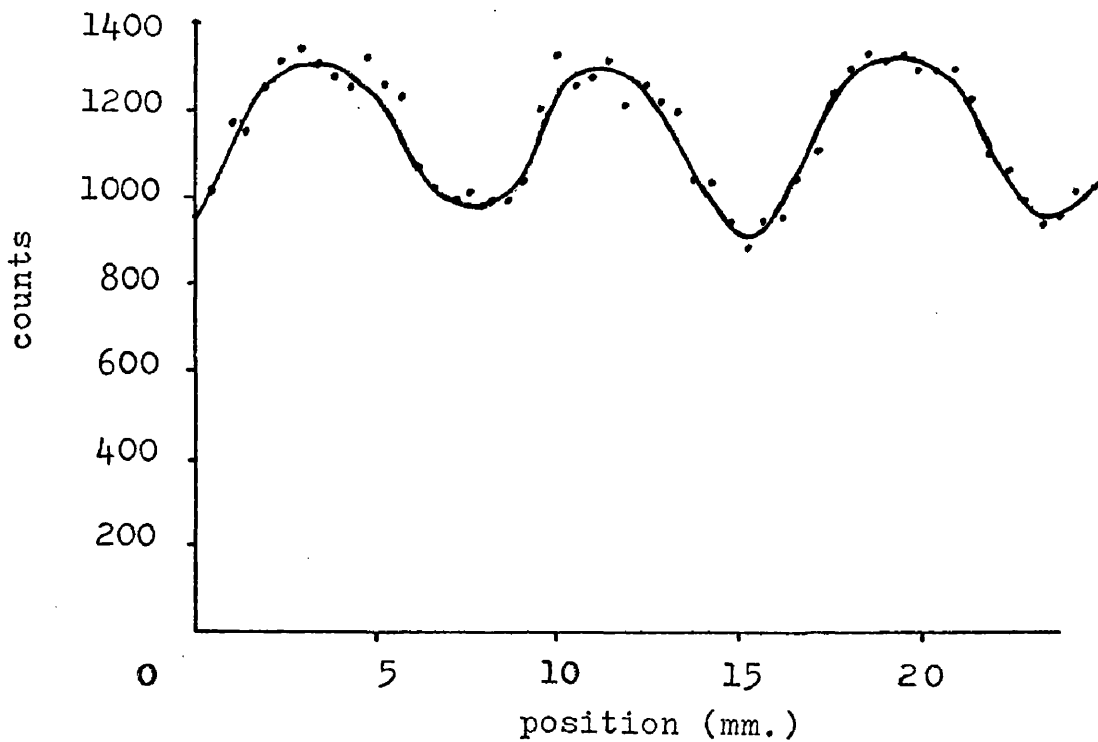
Typical X and Y differential linearities for the total signal taken from the X and Y dimensions respectively are shown in Figs. 6-9 and 10. Figs. 6-11 and 12 are the linearities for the total signal taken from the other dimension in each case. It should be mentioned that these curves were recorded monodimensionally and are not sections through a two dimensional pattern. Also, the zeros are arbitrary and are not the same for each curve.

In the X dimension, when both numerator and denominator are taken from the X dimension, there is a ripple in the differential linearity of about 12% amplitude at the period of the induction wires. This is approximately equivalent to a shift in position of  $\pm 0.2\text{mm}$  and is thought to be due to the error in position location caused by the finite spacing of the induction wires - effect (a) discussed in the section on electrostatics. When the total signal is taken from the Y dimension, the ripple in the X dimension is about 50% amplitude, which is equivalent to a shift in position of approximately  $\pm 0.6\text{mm}$ . In the Y dimension the curves are complicated by the finite spacing of the anode wires as this causes a periodicity.

In each of these cases a check was carried out to ensure that the variation of counter gain which was observed, apparently opposite the induction wires, did not alter the position count rate, as any variation in this rate would have tended to invalidate these linearities.

From these measurements it would appear that there were periodic inaccuracies, smaller than  $\pm 1\text{mm}$  in each dimension, in the location of charged particles.

DIFFERENTIAL LINEARITY IN X DIMENSION  
(TOTAL SIGNAL FROM X DIMENSION)



DIFFERENTIAL LINEARITY IN Y DIMENSION  
(TOTAL SIGNAL FROM Y DIMENSION)

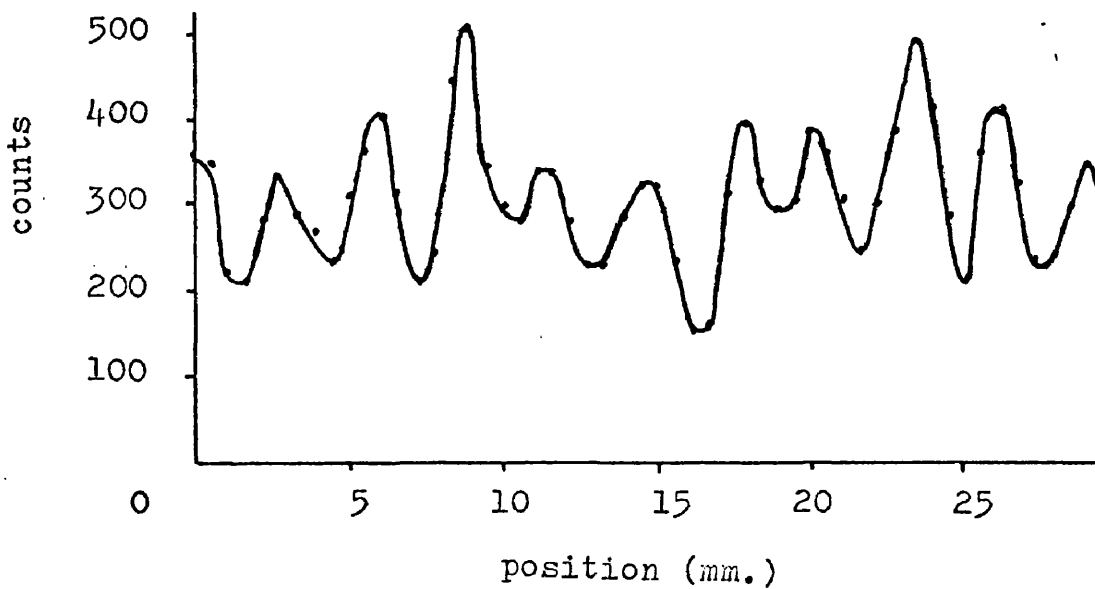


FIG. 6-11

DIFFERENTIAL LINEARITY IN X DIMENSION  
(TOTAL SIGNAL FROM Y DIMENSION)

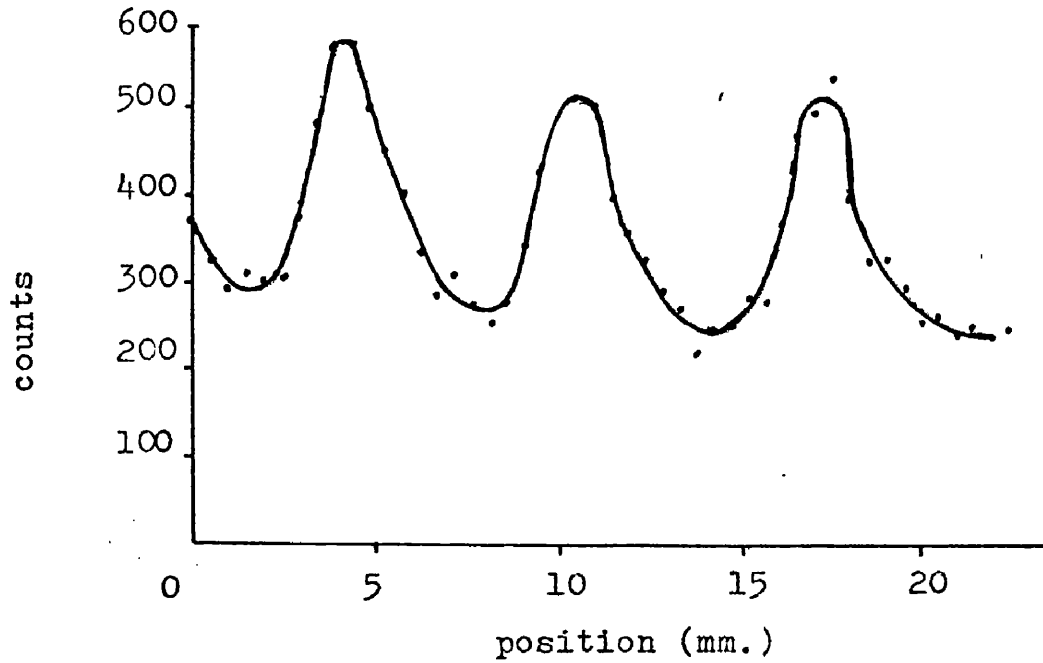
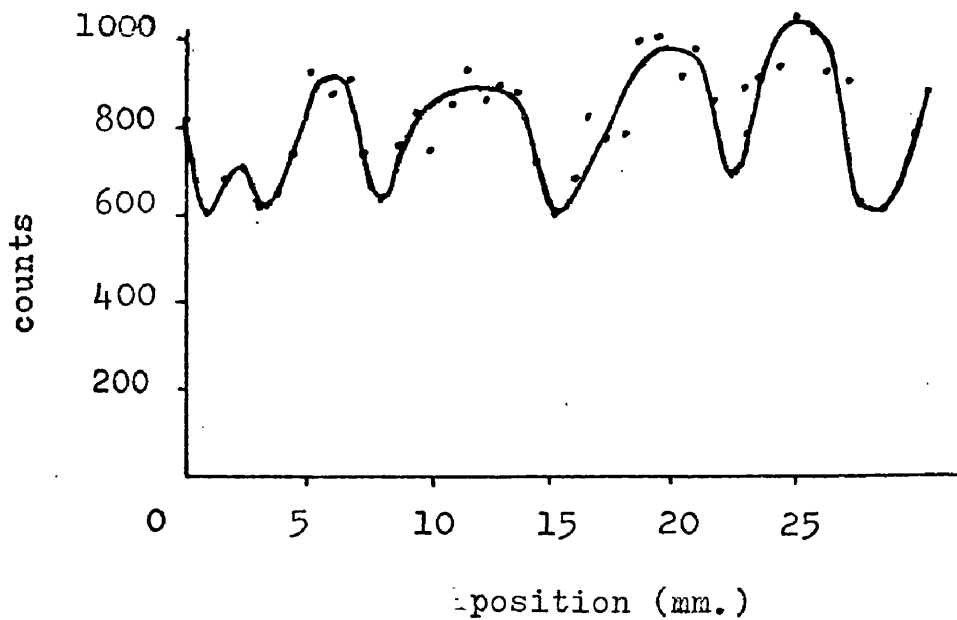


FIG. 6-12

DIFFERENTIAL LINEARITY IN Y DIMENSION  
(TOTAL SIGNAL FROM X DIMENSION)



The resolution limitation due to electronic noise was measured to be 0.75mm FWHM for pulses of  $10^7$  electrons from a mercury relay pulse generator. This is equivalent to a noise level of  $1.4 \times 10^4$  rms electrons on the position signal and is close to the value of  $1.16 \times 10^4$  predicted by the theory of Chapter III (see equation 6.6).

The mean position resolution for alpha particles in the dimension parallel to the anode was measured to be 1.25mm FWHM when the position and total signal were taken from this plane; the resolution limitation was thought to be a combination of the imperfect collimation of the alpha particle source and the electronic noise in the system. In the other dimension, where only a position signal was taken, the width of the peak depended on the position, but was on average about 1.4mm. If the Y dimension induction plane was used for the total signal pulse, similar results were obtained.

It is interesting to observe that the spacing of the anode wires in the Y dimension did not limit the resolution in that dimension as strongly as expected. This is probably a consequence of there being a large number of primary electrons to diffuse for each alpha particle detected; if there was only one such electron, the resolution in this dimension would be no better than the anode wire spacing.

#### Demonstration of the Counter as an X-ray Camera.

The image formation capabilities of a proportional counter such as this can be demonstrated either by recording the output information from the ratio circuit on a two dimensional multichannel analyser, or by

the display of the output on an oscilloscope with either storage facility or a photographic readout of its cathode ray tube screen. All these arrangements were used for the display of shadow images of a number of objects irradiated with x-rays of about 40 keV peak energy from a medical x-ray machine, or with x-rays of 14-22 keV from an americium 241 source. In the case of the oscilloscope output, the brightness of the beam was controlled by a signal of preselected length and delay from a pulse generator triggered by the X,Y position information signal, so that only the peak X,Y position was recorded and the zero spot and rise and fall lines were suppressed.

Some of the images obtained in this way are shown in Figs. 6-13 to 18 and will be discussed later. One of the difficulties encountered was the presence of areas and lines of high and low counter gain, which were apparently caused by certain of the anode wires lying out of the plane of the others, or by small non-uniformities in the peg spacing on the anode frame. This effect was reduced as far as possible by repositioning and waxing down to the edges of the perspex frame any wires which seemed out of place; but it was not eliminated.

Also, the x-ray position resolution seemed rather poor. In fact, the image of the edge of a lead sheet which was placed in front of the counter and exposed to the 40 keV x-rays took 5mm to fall to half height. Fig.6-19 shows a cross-section of this image stored on a multichannel analyser. The image of a 1mm slit in a lead sheet was also found to be broader than expected, at 7mm FWHM, as in Fig.6-20;

FIG. 6-13

IMAGE OF A HAND WITH 14 - 22 keV  
X-RAYS FROM AMERICIUM 241 AS  
DISPLAYED ON A STORAGE OSCILLOSCOPE.  
( DOSE OF 0.5 MICRORADS. )

FIG. 6-14

IMAGE OF A SPANNER WITH THE X-RAYS  
FROM AMERICIUM AS DISPLAYED ON A  
STORAGE OSCILLOSCOPE.  
DIAMETER OF SPANNER = 6cm  
( DOSE OF 2 MICRORADS )

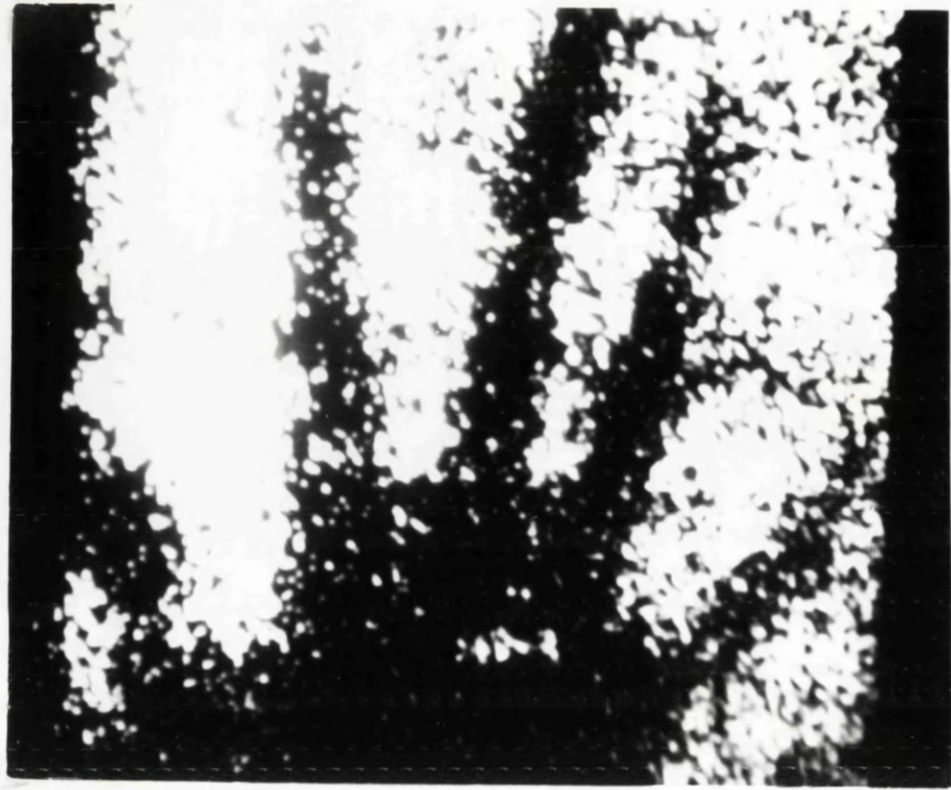


FIG. 6-15

IMAGE OF A CROSS SHAPED APERTURE  
IN A LEAD SHEET WITH THE AMERICIUM  
X-RAYS, AS DISPLAYED ON A STORAGE  
OSCILLOSCOPE (WITH UNEQUAL GAIN IN  
THE X & Y DIRECTION)  
LENGTH OF CROSS = 11cm. WIDTH OF  
ARM = 2cm.  
(DOSE OF 2 MICRORADS)

FIG. 6-16

IMAGE OF THE SAME CROSS AS RECORDED  
PHOTOGRAPHICALLY FROM A NORMAL  
OSCILLOSCOPE.  
(DOSE OF 4 MICRORADS)

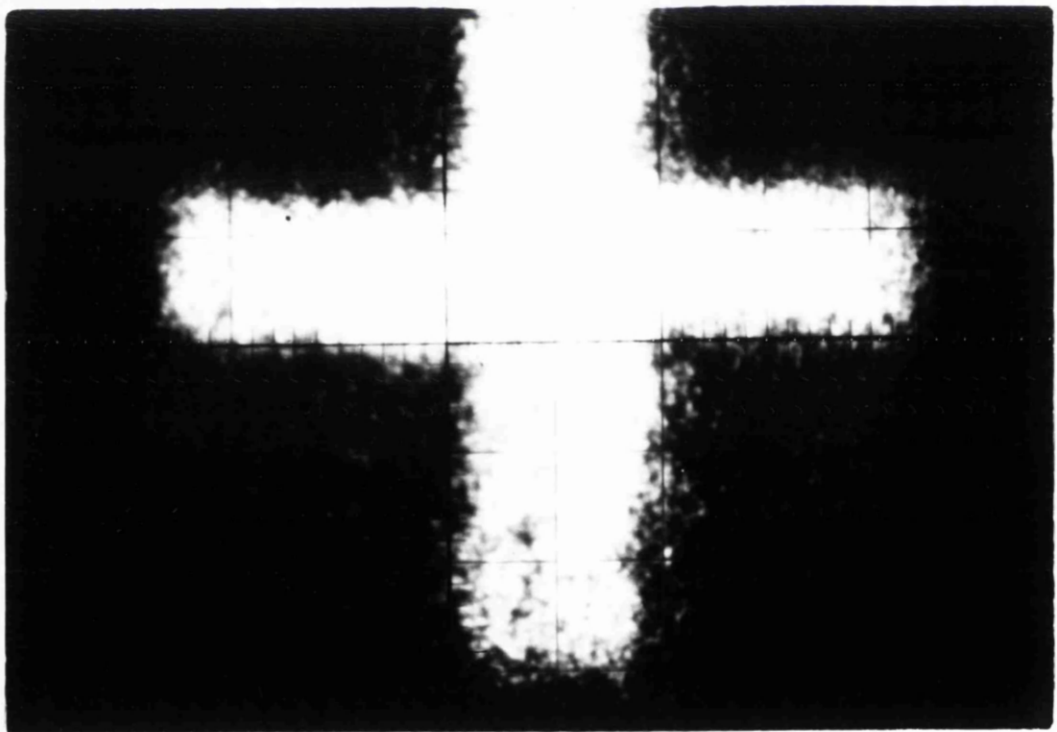
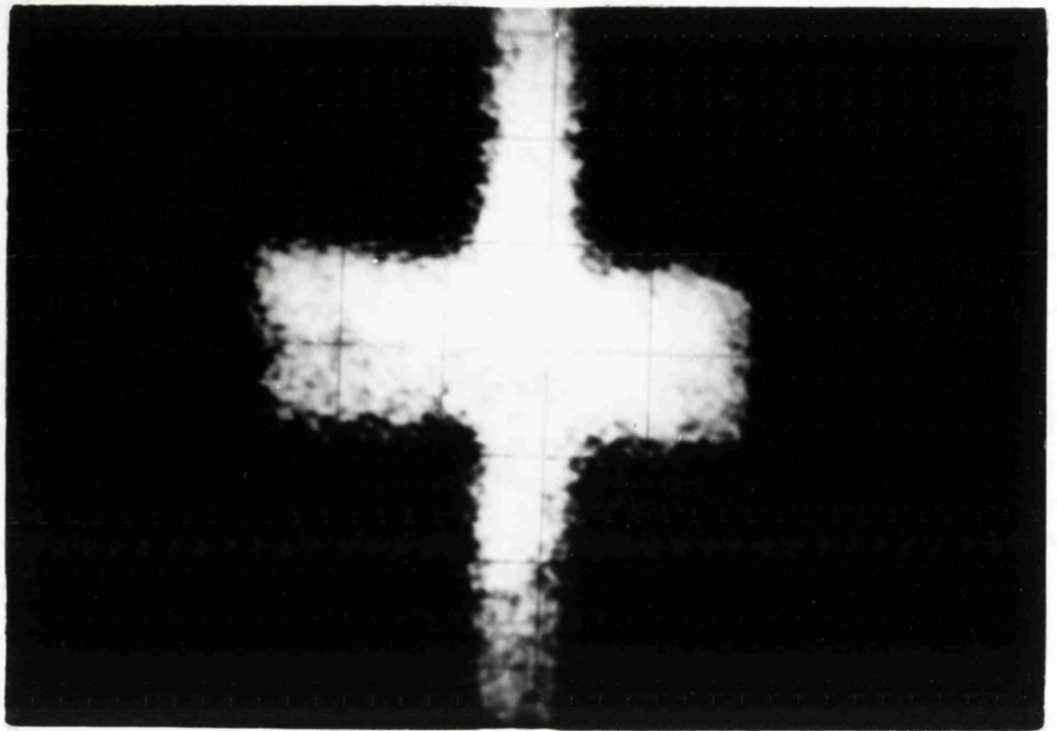
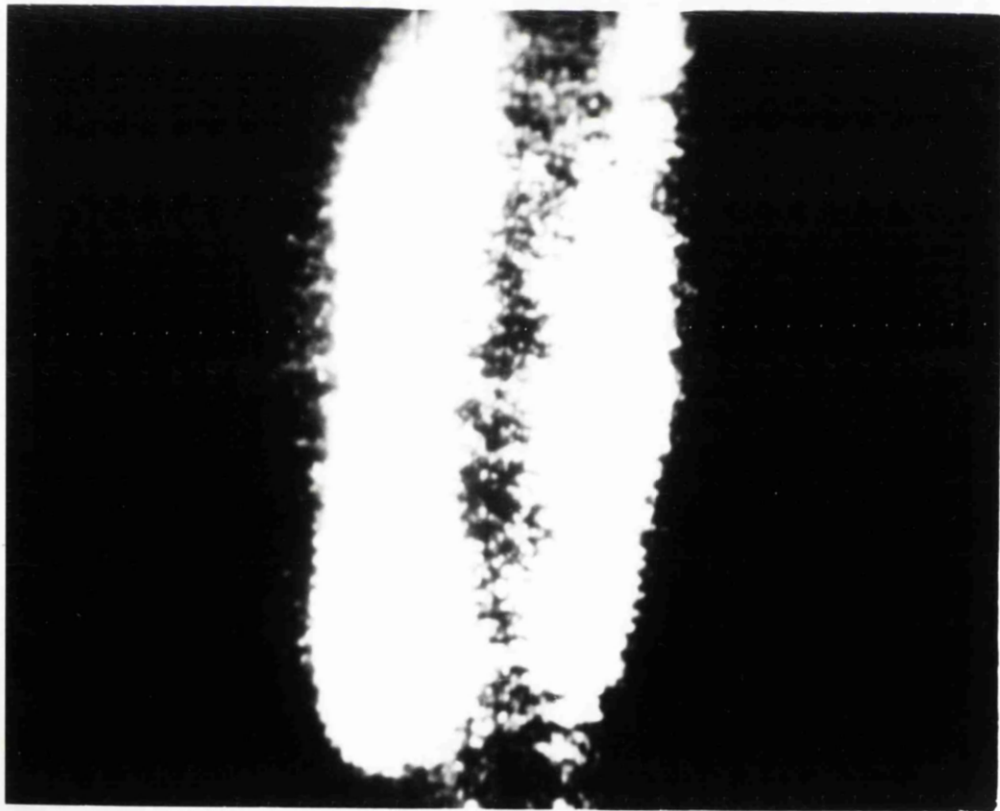
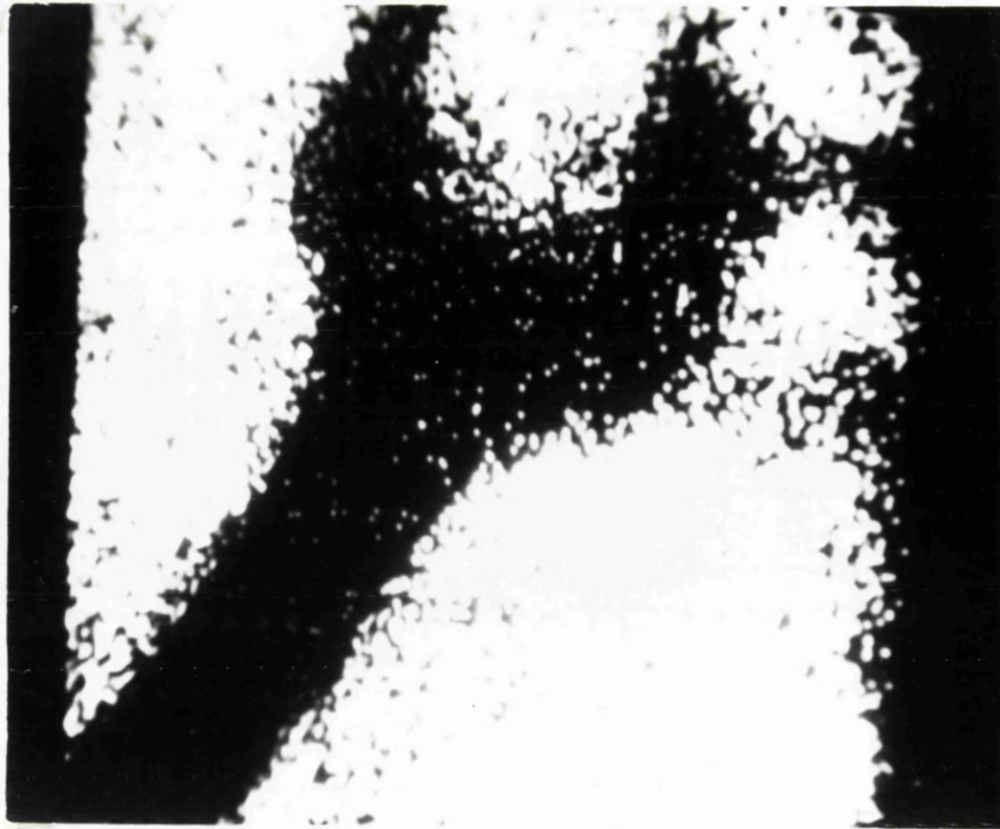


FIG. 6-17 . IMAGE OF A SPANNER WITH 40 keV  
PEAK X-RAYS FROM A MEDICAL X-RAY  
MACHINE AS DISPLAYED ON A STORAGE  
OSCILLOSCOPE.  
DIAMETER OF SPANNER HEAD = 8cm.  
(DOSE OF 1 MICRORAD)

FIG. 6-18 IMAGE OF A RAT WITH THE 40 keV  
PEAK X-RAYS AS DISPLAYED ON A  
STORAGE OSCILLOSCOPE.  
(DOSE OF 15 MICRORADS)



and yet the x-ray beam passing through the counter was checked photographically to be only 1mm wide. The noise limitation to the resolution was only about 1mm. Certainly the distance travelled by 40 keV photoelectrons in the argon/methane filling of the counter is about 1cm in a direction perpendicular to that of the incoming x-rays, but the poor resolution cannot be totally due to this, as it was possible to obtain a resolution of 3.3mm in the 10cm long one dimensional counter, set up in the same geometry and with the same x-ray beam. The above figures were obtained with the numerator and denominator signal taken from the same induction wires in a direction parallel to the anode wires; but there was very little difference if either the other induction wires were used for the denominator or if the resolution was measured in the other dimension.

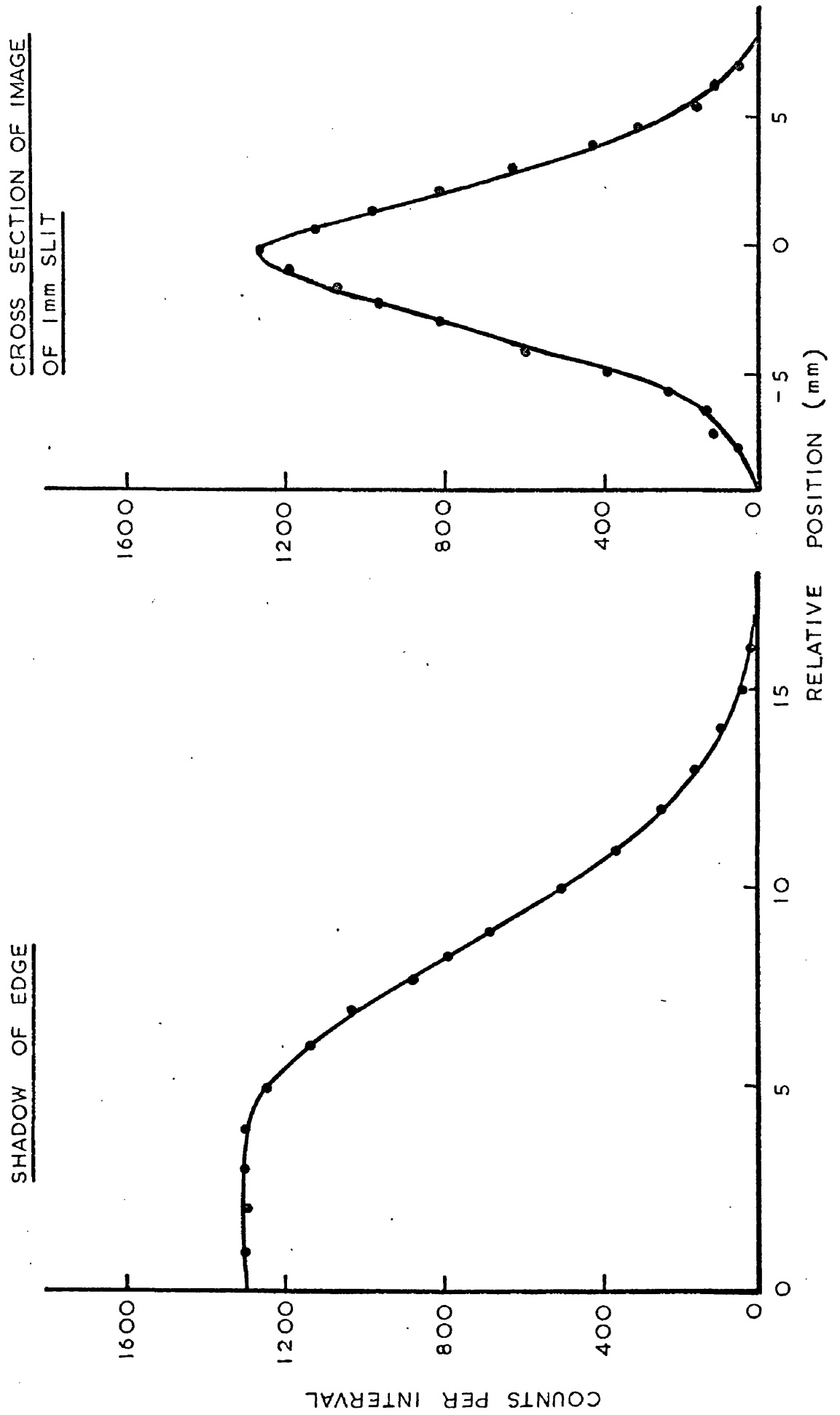
Also it seems unlikely that a limiting factor was ultra-violet broadening of the discharge, as an increase to 50% of methane quenching gas did not improve the resolution.

The reason for the poor x-ray resolution is not understood, but it is thought that the variation of the counter gain close to the induction wires may have had the effect of shifting the apparent mean position of the ionization released by the photoelectrons from the x-rays.

However, it has been decided to leave this problem to be investigated at a future date after a new counter has been built and the gain modulation effects are possibly no longer present.

Some of the images obtained and displayed on an oscilloscope are shown in Figs. 6-13 to 18 - those of a hand and a spanner exposed

POSITION RESOLUTION FOR X-RAYS. (40 keV. PEAK ENERGY.)



to the 14-22 keV x-rays from the americium source and of a cross, cut out from a lead sheet, exposed to these x-rays. The image of a different spanner taken with the 40 keV x-rays from a medical x-ray set is also shown, as is the image of a rat with the same x-rays. In the image of the rat, the dark area down the centre is thought to be the area of the animal's backbone and the thicker part of its ribs, which were not resolved.

The radiation dose which is shown for each figure was obtained from a calibration of the americium source and the x-ray machine against a standard ion chamber. The effect of the differing doses on the qualities of the images can be seen. For instance, the image of the hand with a 0.5 microrad dose shows considerable grain or quantum noise, while the crosses, with their 2 and 4 microrad doses do not show so much. The lower the dose, the less detail is perceptible; and it has been shown by Tol et al (1955) that the minimum fractional change in intensity observable between resolution elements can be expressed as

$$c = \frac{k}{\sqrt{N}} \quad 6.8$$

where  $k \approx 3$ , and  $N$  is the number of counts in a resolution element. Thus, for the observation of a fractional change in intensity of 0.3,  $N$  must be about 100 counts. For the two dimensional counter with its resolution of 7mm FWHM and a detection efficiency of about 6% for 20 keV x-rays, this would be equivalent to a dose of approximately 2 microrads.

One method of reducing the dose requirement of this detector would be to use a krypton/methane filling, as this would raise the detecting efficiency, e.g. for 20 keV x-rays from 6% to 25%.

Almost all of the above work was performed at a fairly low count rate of around  $5 \times 10^2$ /second, but in fact the counter was shown to operate at a count rate of  $2 \times 10^4$ /second with an output from the ratio circuit of  $1.4 \times 10^4$ /second. The resolution at this count rate fell to about 1.5cm, probably due to the effect of pulses lying on top of the overshoots of the previous pulses. As has been mentioned before, double differentiation of the pulses removes this overshoot and should allow count rates of  $2 \times 10^4$ /second to be achieved without any fall of resolution due to electronic effects.

#### Conclusion.

This counter system has been shown to provide accuracy of location and resolution of better than 1.4 mm for alpha particles in both dimensions over an area of 23cm x 23cm. The resolution for 40 keV x-rays, unfortunately, is considerably poorer.

There were some difficulties in the operation of the detector, mainly as a result of the high gas gain necessary to achieve the required signal to noise ratio for good position resolution. For example, sparking was found to occur both across the insulators and inside the volume of the counter. The first effect was reduced by offsetting the potential of the induction wires, as mentioned earlier. It was found that the spurious pulsing in the counter volume was excessive if x-ray energies of a few keV were to be observed at a pulse height from the induction wires of about  $10^7$  electrons. However, it is important that a counter such as this should be able to

operate with soft x-rays and with minimum ionizing particles which deposit about 5 keV per cm in argon at atmospheric pressure. The use of a larger fraction of methane in the mixture did not reduce these spurious effects, but 90% argon/10% propane mixture allowed the 5.9 keV x-rays of iron 55 to be detected at the required counter gain with a negligible background. It has been reported by Charpak et al (1970) that argon/isobutane mixtures will allow output pulses of the order of  $10^8$  electrons to be achieved in multiwire counters without sparking, and it may be that this gas would further improve the performance of the author's detector for low energy x-rays.

It had been hoped that the spurious effects would be reduced by the use of finer anode wire of 10  $\mu\text{m}$  diameter at the same spacing of 3mm. Lower operating voltages were required (e.g.  $\pm 3$  KV instead of  $\pm 3.3$  KV) but it appeared that the spurious pulsing inside the counter volume was worse than before, either due to irregularities on the wire or to dust particles which seemed to adhere very easily to the fine wire and were very difficult to remove.

It is proposed to build another chamber in which more effective guarding of the electrodes will be carried out to reduce the effects of breakdown across the insulators. This should remove the need for the induction electrodes being held away from their correct equipotential between the anode and the cathode, when high counter gain is required. Also it is hoped that, by having a stricter tolerance on the anode wire spacing and planarity and by the assembly of the device in a dust free atmosphere, the existence of areas of high and low gain

and the spurious effects inside the counter volume may be considerably reduced. In order to improve the accuracy of location, the induction wire spacing will be reduced to 3mm and the resistance of the induction electrodes then will be increased by a factor of 2. This should reduce the non-linearity effects, which are present as a result of the coarseness of the wire spacing, and also the electronic noise.

It is interesting to note that with the charge division method of obtaining position information and the same induction wire spacing and counter gain as used in the preceding work, the chamber size could be increased to 1 metre square for a limitation to resolution by electronic noise of 2mm FWHM.

Chapter VII.CONCLUSION.

The work described in this thesis has demonstrated the potential of gas proportional counters for the localisation of ionizing radiation to better than 0.5% of their sensitive lengths or areas and their operation at count rates of up to  $10^4$ /sec.; however, the capability of energy measurement was partially lost as a result of the high gas gain necessary to achieve high position resolution in the author's system.

There have been a number of proportional counter designs reported during the course of this work, but these use different methods of obtaining the position information. For instance, Morgue & Chery (1968) obtained position information in one dimension by measuring the time interval between the signal pulse from an event in the counter reaching each end of the anode, which was constructed as an inductive delay line.

Borkowski & Kopp (1968,70) used the variation with position of the rise time of pulses induced on a high resistance anode to give one dimensional information and extended the idea to give two dimensional data by having a number of parallel anode wires. The readout system for the two dimensions was relatively simple as it only required four preamplifiers and two rise time measurement units.

A proportional counter avalanche emits ultra-violet light and the variation of the intensity with distance of the light reaching a photomultiplier tube has allowed Scobie (1969) to obtain position

information in one dimension. However, this method does not give a linear signal output with position and does not give as high position resolution as the other methods.

An array of parallel anode wires placed between two plane cathodes with each wire behaving as a separate counter was shown by Charpak et al (1968,70) to give position resolution of the order of the anode wire spacing. Each wire can be read out independently or the method of connecting each one to a delay or resistive line can be used (Charpak 1968). Also Charpak et al (1970) have proposed the use of a multiwire cathode or induction electrode, placed between the anode and the cathode, with its wires perpendicular to the anode wires, to allow position location in a second dimension. It must be pointed out that this method is very similar to that used by the author, but did not appear in publication until after the author's system was built and working. Neumann & Nunamaker (1970) have demonstrated a two dimensional counter system similar to that proposed by Charpak.

The available performance data of these detectors is compared with that of the author's in Tables 1 and 2, which include the results from the earlier Geiger and proportional counters. Typical data for semiconductor detectors and spark chambers is also given. From this it can be seen that the proportional counters have the advantage over the semiconductor counters of larger sensitive area or length (with the same order of absolute resolution), over Geiger counters of better position resolution, and over spark chambers of higher count rate. The position resolution of the spark chambers in two dimensions is

TABLE 1 • DETECTORS FOR POSITION SENSITIVITY IN ONE DIMENSION

TECHNIQUE	COUNTER	LENGTH	RADIATION	POSITION RESOLUTION (FWHM)	COUNT RATE CAPABILITY	CAPABILITY FOR ENERGY MEASUREMENT	REFERENCE
propagation of discharge (timing)	geiger	25cm	$\alpha$ particles	2cm	-	no	Frank (1951)
resistive electrode (charge division)	geiger	70cm	1.5MeV $\beta$ particles	2cm	-	no	McDicken (1966)
resistive electrode (charge division)	proportional	30cm	5.3MeV $\alpha$ particles	1.2mm	-	-	Kuhlmann et al (1966)
resistive electrode (charge division)	semi-conductor	5.3cm	5.5MeV $\alpha$ particles	0.57mm	-	yes	Melzer and Pühlhofer (1968)

TABLE 1 (CONTINUED)

TECHNIQUE	COUNTER	LENGTH	RADIATION	POSITION RESOLUTION (FWHM)	COUNT RATE CAPABILITY	CAPABILITY FOR ENERGY MEASUREMENT	REFERENCE
resistive electrode (charge division)	proportional	10cm	5.5MeV $\alpha$ particles	* 0.42mm	$> 10^4$ /sec.	) partial ) ) ) ) )	present work 1967/70
		10cm	6.9keV x-rays	* 0.6mm			
		100cm	5.5MeV $\alpha$ particles	* 1mm			
resistive electrode (rise time)	proportional	20cm	5.3MeV $\alpha$ particles	0.15mm	$10^4$ /sec.	yes	Berkowski and Kopp (1968, 1970)
		40cm	22keV x-rays	0.5mm			
inductive delay electrode	proportional	7.5cm	5.3MeV $\alpha$ particles	1.6mm	-	-	Morgue and Chery (1968)
multewire anode	proportional	arbitrary	370MeV/c protons & pions	depends on anode wire spacing 1-3mm	$10^5$ /sec	yes	Charpak et al (1968, 1970)
attenuation of light from avalanche	proportional	30cm	10.5keV x-rays	3cm	-	yes	Scobie (1969)

\* measured at low count rate (< 100 counts/sec.)

TABLE 2 - DETECTORS FOR POSITION SENSITIVITY IN TWO DIMENSIONS

TECHNIQUE	COUNTER	AREA	RADIATION	POSITION RESOLUTION (FWHM)	COUNT RATE CAPABILITY	CAPABILITY FOR ENERGY MEASUREMENT	REFERENCE
delay (magnetostrictive or acoustic)	spark chamber	typically 50cmX50cm	high energy charged particles	typically 0.7mm	typically ~10 <sup>4</sup> /sec max.	no	e.g. Jones et al (1964) or Perez-Mendez et al (1965, 1967)
multiwire anode and induction electrode (separate amplifier on each wire)	proportional	-	300MeV/c protons	3.3mm (anode) 1.6mm (induction electrode)	-	-	Neumann and Nunamaker (1970)
resistive electrodes (charge division)	semi-conductor	2cmX2cm	5.5MeV $\alpha$ particles	1mm	-	yes	Owen and Awcock (1968)
resistive electrodes (charge division) (induction electrodes)	proportional	23cmX23cm	5.5MeV $\alpha$ particles 40keV x-rays	1.25mm * 7mm *	> 10 <sup>4</sup> /sec	partial	present work (1967/70)
resistive electrode (rise time) - multiwire	proportional	7.5cmX12cm	5.3MeV $\alpha$ particles	0.15mm 3mm	10 <sup>4</sup> /sec	yes	Borkowski and Kopp (1970)

\* measured at low count rate (< 500 counts/sec.)

marginally better but they require external triggering and so are not so adaptable to different experiments.

Further it appears that of the proportional counters, only those of Borkowski & Kopp (1968,70) give better position resolution than the author's; although certain of the others, such as the multiwire chambers of Charpak et al (1970) are able to preserve pulse height, i.e. energy information, at their stated position resolution. Borkowski & Kopp also claim good energy resolution for 20 keV x-rays, but at a lower gain than for optimum position resolution and it is not stated how the energy resolving capability changes as the gain is raised.

The better position resolution obtained in their case is a result of the electronic noise level being lower because of the very high resistance anode wire (10 kilohms per mm) which was used. It can be expected that the use of this material will also reduce the noise in the author's type of counter. This reduction, for the 10cm counter, should be a factor of 35, and the noise limitation to resolution should then be approximately 0.1mm at a counter gain ten times lower than that previously used by the author. At this lower gain it is probable that the limitation to resolution thought to be caused by the spreading of the avalanche would not be so significant, and the counter's resolution might only be limited by the diffusion of the primary electrons, by the electronic noise and by the distance travelled in the gas by photoelectrons or  $\delta$  rays.

#### The Application of Proportional Counters.

The properties of the proportional counters, reported by the

author and others, suggest that these devices will be useful for the detection of charged particles and x-rays in the type of experiments mentioned in the first chapter; e.g. for the measurement of the angular distributions of charged particles, for the focal plane of a charged particle or x-ray spectrometer, or for the image formation of radiation distributions.

The author's work has demonstrated the recording of x-ray shadow images with such a detector, and Borkowski & Kopp (1970) have used their counters for the recording of x-ray diffraction patterns. However, it should be pointed out that the range of the photoelectrons released in the filling gas causes a limitation to the resolution achievable, and that even if a counter which had no other limiting factors - such as electronic noise - could be designed, the resolution would always be poorer than that of a photographic plate for x-ray energies above a few keV.

Multiwire counters of Charpak's design have been used by Amato & Petrucci (1968) for the analysis of the profiles of charged particle beams, and by Koester (1970) for the measurement of the scattering cross section of pions from light nuclei; and there are plans for the utilisation on a large scale of multiwire chambers for the measurement of particle tracks in high energy nuclear physics.

One application, outlined in the first chapter, for which the position sensitive proportional counters reported are not yet suitable, is the recording of x-ray images in the focal plane of a reflecting telescope; position resolution for soft x-rays of about 0.2mm over an

area of  $1\text{cm}^2$  is required and resolution as high as this has not yet been achieved in two dimensions.

A solid state system has been introduced for recording these images for x-ray energies of 1 to 4 keV by Ballas et al (1968). A 1.25cm diameter scintillator crystal was viewed with an image dissector tube which scanned  $48 \times 48$  picture elements, each of 0.25mm diameter, in one second; but this system is rather inefficient, as only the x-ray flux falling on one 0.25mm diameter element at one time is recorded and this is less than 0.1% of the total flux collected by the telescope. However, it is thought that if high resistance wire (10 kilohms per mm) was used for the induction electrodes in the author's type of two dimensional counter, with an induction wire spacing reduced to 1mm, and if an anode of very fine spacing was etched on some suitable material, as proposed by Derenzo et al (1969), a proportional counter giving the required resolution for this application could be constructed. This system would have a considerably higher efficiency for x-rays of 1 to 4 keV than that of Ballas et al.

APPENDIXPOSSIBLE OPERATION OF A PULSE COUNTER  
WITH AN ORGANIC LIQUID FILLING.Introduction

Perhaps the main disadvantage of a gas detection medium is its relatively low density and stopping power for ionizing radiation. This is of importance in several ways in gas filled position sensitive detectors. Firstly, it results in a poor detection efficiency for x and gamma rays (above 20 keV) in the normal size of chamber, and also in a poor position resolution in this case because of the distance travelled by the photoelectrons released in the medium. Secondly, the position resolution for ionizing particles may be limited by the distance travelled by secondary electrons in the gas.

One way of increasing the efficiency for x-rays of such a counter is to raise the pressure of the gas, pressures up to 10 atmospheres being usable. This also has the effect of decreasing the range of the photoelectrons or delta particles (secondary electrons). However, a more effective way would be to utilise a liquid medium, if this were suitable for the detection of radiation.

This appendix describes an attempt by the author to observe pulses resulting from the detection of ionizing radiation in a cylindrical counter filled with an organic liquid. It was hoped that some evidence of pulse amplification as a result of avalanche multiplication of the charge carriers in the liquid would be found.

In order that a pulse counter should operate satisfactorily and

that avalanche multiplication should take place, the mobility of the negative charge carriers must be high, i.e. the carriers must be free electrons as is the case for the liquid noble gases such as argon.

Liquid argon has been used in pulse ion chambers by Hutchinson (1948), Davidson & Larsh (1948,50) and Marshall (1954); but it was only recently that pulses amplified by avalanche multiplication were observed by Derenzo et al (1969) who have been studying the possibility of using a liquid argon filled counter for the space localisation of high energy charged particles. Space charge limited (Geiger type) pulses of up to  $5 \times 10^8$  electrons were obtained from 1 MeV gamma rays with a 4.1mm diameter cylindrical counter in which the electric field at the anode surface was about  $10^6$  volts/cm, but no proportional pulses were observed.

The increase in the conductivity of certain organic liquid when irradiated with x-rays or ionizing particles was noticed by Curie (1902), and this has resulted in the use of current ion chambers, with an organic liquid filling for dosimetry. The negative charge carriers in the liquids were ions of low mobility (about  $10^{-4}$  to  $10^{-5}$  cm<sup>2</sup> per volt per second) and no evidence of pulses from these ion chambers was found by Davidson & Larsh (1948,50). However, Blanc et al (1961) have demonstrated avalanche multiplication in purified liquid hexane for electric fields above  $2 \times 10^4$  volts/cm, and they observed pulses of the order of  $10^{-4}$  volts from 5.3 MeV alpha particles in a parallel plate 'avalanche' chamber. Also Samuel et al (1964) have recorded 20 volt pulses (equivalent to  $6 \times 10^8$  electrons in the avalanche) from

1.3 MeV gamma rays in hexane at lower fields in a parallel plate counter; and they have suggested that the charge carriers in this case are free electrons of mobility between 20 and 200  $\text{cm}^2$  per volt per second. Recent measurements by Minday et al (1969) and Schmidt & Allen (1970) have confirmed the existence of free electron charge carriers in very pure organic liquids.

Therefore, ion chamber and proportional or Geiger counter operation should be possible with a cylindrical counter filled with a very pure organic liquid.

#### Experimental Work.

The following work was carried out in an attempt to observe pulses resulting from the avalanche multiplication of charge carriers in a cylindrical chamber filled with a liquid at room temperature. In order to obtain maximum efficiency for x-rays and stopping power for charged particles it would be best to use a liquid whose molecules had some constituent atoms of high atomic number. However, since avalanche multiplication had previously been observed in hexane, it was decided to use this liquid as the detecting medium.

It would appear that for free electrons to exist, the liquid must have a very low concentration of electron scavenging impurities such as oxygen or water. Therefore, purification is necessary before commercially available liquid can be used. However, chemical purification is a difficult and rather specialised procedure; and in the following work the hexane used was merely fractionally distilled

from a drying agent (lithium aluminium hydride) a number of times before being distilled under vacuum conditions into the test counter.

Two grades of high purity hexane which were available were used :

Hexane, Special for Spectroscopy (B.D.H.)-which is free of unsaturated hydrocarbon impurities

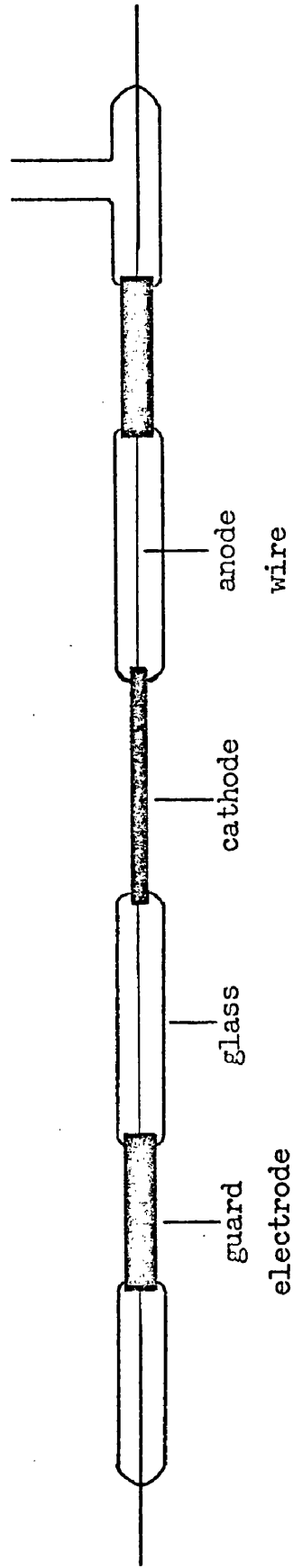
(alkenes, aromatics, etc.) but which according to Kahan & Morant (1965) may be only about 80% n-hexane and 20% of other isomers.

Nanograde Hexane, manufactured by Mallinckrodt.

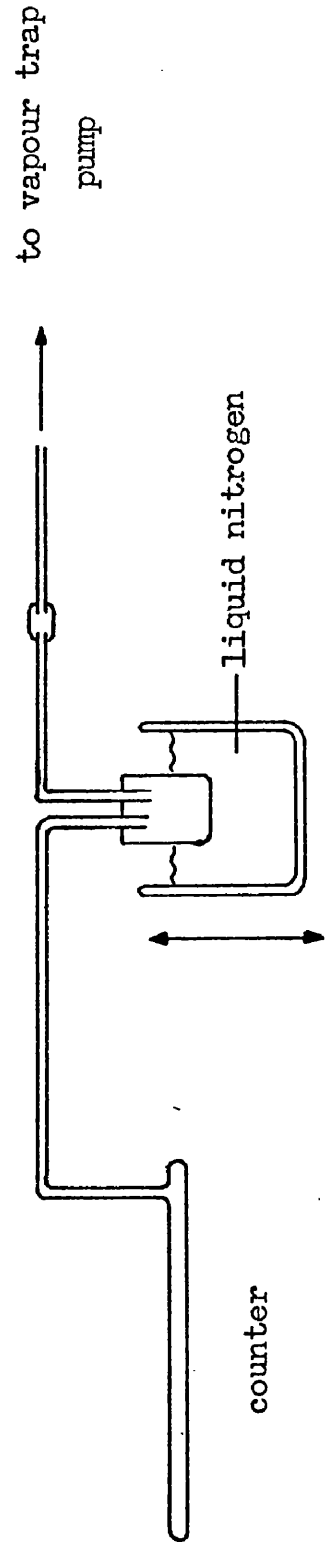
This contains less than 10 nanograms per litre of electron trapping impurities other than oxygen and water. Here also there may be a fairly high percentage of isomers other than n-hexane, but this should not matter for the present work.

The counter was of cylindrical geometry and of a hybrid metal and glass construction as shown in Fig. (a). The cathode, with a 1mm diameter window covered with 5  $\mu\text{m}$  thick mylar, was of 1.5mm diameter palladium tube and the guard rings were of 4mm diameter palladium. A 28  $\mu\text{m}$  diameter gold plated molybdenum anode wire was fitted, being spot welded to lengths of tungsten wire for sealing into the glass envelope. It was found essential to reinforce all the glass metal joints with epoxy cement to avoid vacuum leaks. The counter was joined by a length of glass tubing to a glass bulb of 100cc capacity and through this to a liquid nitrogen vapour trap and rotary vacuum pump, as shown in Fig. (b). The glass tube between the reservoir bulb and

a) CYLINDRICAL COUNTER



b) FILLING SYSTEM

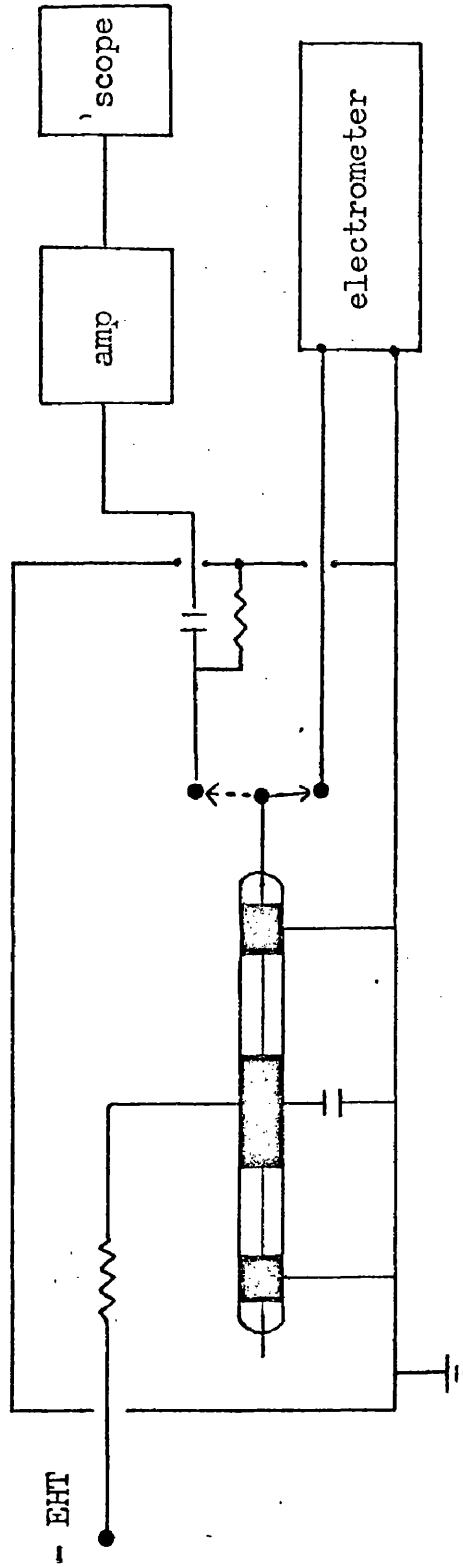


the vapour trap was not continuous but was joined in the middle with a 2cm length of neoprene tubing. This allowed the counter and reservoir to be separated from the vapour trap so that the distilled and dried hexane could be added to the reservoir. Before the addition of the hexane, the system was rinsed with alcohol and acetone, and the counter and reservoir were partially de-gassed by heating with a gas flame while the system was under vacuum. When the hexane was in the reservoir (at a pressure of below 10 microns mercury) the dissolved oxygen content was reduced by carrying out several freeze/thaw cycles with liquid nitrogen. The liquid was then allowed to distil into the counter as the hexane temperature in the reservoir was brought up to the ambient level. When the counter tube was full of liquid the connection to the reservoir was sealed off.

Negative potential of 100 volts to 2.2 kilovolts was applied to the counter cathode and the guard tubes were earthed so that no leakage current across the glass could reach the anode. As shown in Fig.(c), for pulse measurements, the anode was ac coupled to a voltage sensitive amplifier system of 1 microsecond integration time constant and 100 microseconds differentiation time constant; and for leakage current measurements, the anode was directly coupled to an electrometer. The counter itself and its connections were shielded from electrical interference by an earthed aluminium box.

#### Discussion.

No pulses were observed above the noise level for the 5.5 MeV



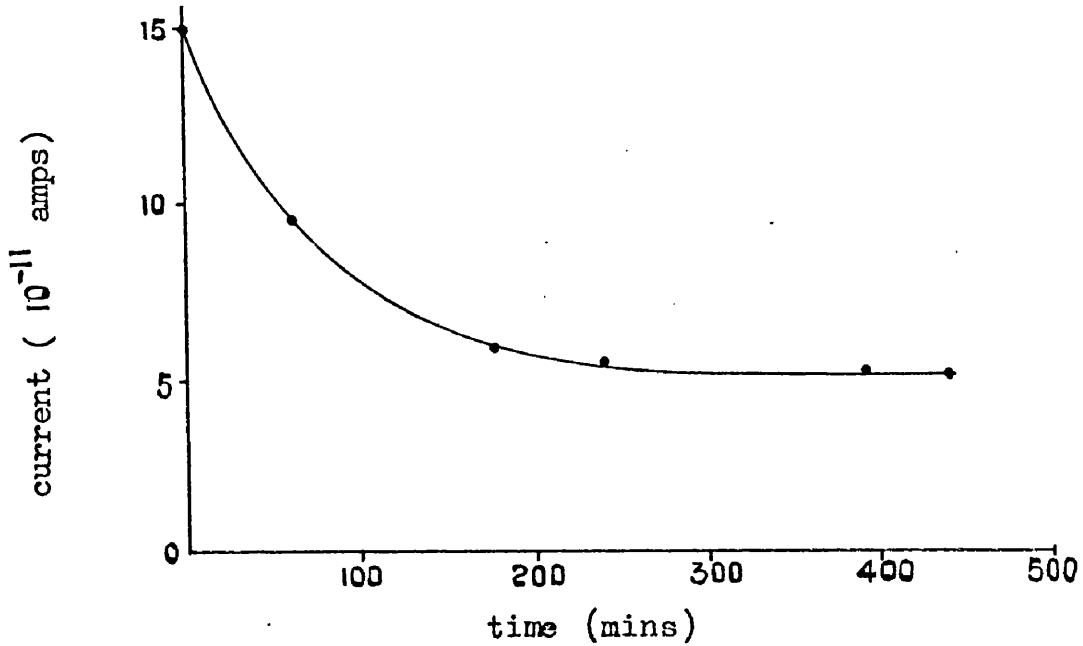
c) BLOCK DIAGRAM FOR LIQUID FILLED COUNTER

alpha particles of americium 241, the 1.33 MeV gamma rays from cobalt 60, or the neutrons of several MeV from a radium beryllium source. The background noise level was high (typically about 100 microvolts rms at 2 kilovolts applied voltage) and appeared to be due to leakage current in the liquid.

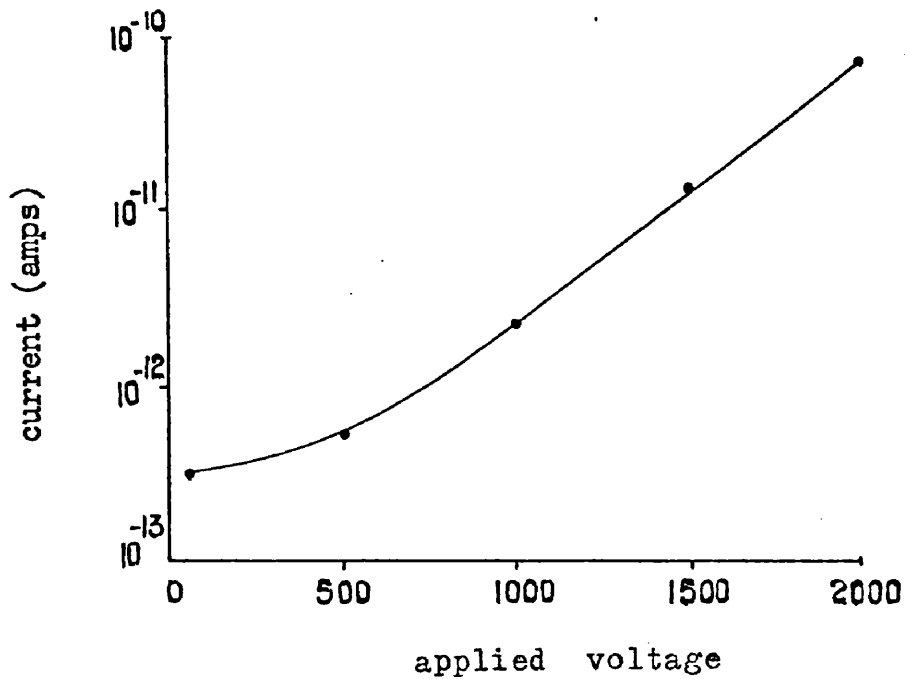
The leakage current in various samples of both grades of liquid was measured as a function of electric field and of time; and it was found that the current seemed to be more dependent on how centrally the anode wire was placed than on the particular sample of liquid. The leakage current was of the order shown in Figs. (d) and (e). The current decreased with time and had an approximately exponential dependence on counter voltage above 500 volts. Electrical breakdown occurred for an applied voltage of about 2.2 kilovolts (equivalent to a field of  $4 \times 10^5$  volts/cm at the anode surface). The current variations in parallel plate liquid filled counters have been studied by Plumley (1941), Ladu et al (1965) and others, and it appears that electrolytic purification of the liquid takes place with time. Ladu et al (1965) found that if the liquid was not of high chemical purity this process could take up to seven days before a residual steady current was reached. It was not possible, however, to leave unattended the cylindrical counter filled with hexane because of the possibility of electrical breakdown and fire, and so the longest purification time used before pulse measurements were made was approximately eight hours.

Thus it is very probable that the hexane was not pure enough for

VARIATION OF THE LEAKAGE CURRENT IN HEXANE  
WITH TIME (2KV APPLIED VOLTAGE)



VARIATION OF THE LEAKAGE CURRENT IN HEXANE  
WITH APPLIED VOLTAGE



the existence of free electron charge carriers. This would prevent the chamber working as a pulse ion chamber and no charge multiplication would take place. Much more elaborate purification using both chemical and electrolytic techniques is probably necessary; but if this was carried out the counter would have to be designed so that no materials which might add impurities - such as mylar or epoxy cement - would be in contact with the liquid.

It appears to the author that research towards the operation of a counter filled with a liquid at room temperature could yield interesting and useful results; however, the necessary experimental conditions of purity must be achieved and maintained over a period of time.

## REFERENCES.

- Alvarez, L.W., 1960, Rev. Sci. Instr., 31, 76.
- Amato, G. and Petrucci, G., 1968, C.E.R.N. Report, 68-33.
- Anger, H.O., 1963, Nucleonics, 21(10), 56.
- Anger, H.O., 1966, IEEE Trans. Nucl. Sci., NS-13(3), 380.
- Ballas, J., Knapp, G., Wiza, J. and Zehnpfennig, T., 1968, IEEE Trans. Nucl. Sci., NS-15(3), 551.
- Bender, M.A. and Blau, M., 1963, Nucleonics, 21(10), 53.
- Bennet, E.F., 1962, Rev. Sci. Instr., 33, 1153.
- Bilaniuk, O.M., 1961, Nucl. Instr. and Meth., 14, 63.
- Blanc, D., Mathieu, J. and Boyer, J., 1961, Nuovo Cimento, 19, 929.
- Bock, R., Duhm, H.H., Melzer, W., Pühlhofer, F. and Stadler, B., 1966, Nucl. Instr. and Meth., 41, 190.
- Borkowski, C.J. and Kopp, M.K., 1968, Rev. Sci. Instr., 39, 1515.
- Borkowski, C.J. and Kopp, M.K., 1970, IEEE Trans. Nucl. Sci., NS-17(3), 340.
- Bunemann, O., Cranshaw, T.E. and Harvey, J.A., 1949, CAN. J. RES., A-27, 191.
- Campion, P.J., 1968, Int. J. Appl. Radiat. Isotopes, 19, 219.
- Charpak, G., 1963, Nucl. Instr. and Meth., 24, 501.
- Charpak, G., Bouclier, R., Bressani, T., Favier, J. and Zupačić, Č., 1968, Nucl. Instr. and Meth., 62, 262; 65, 217.
- Charpak, G., 1968, International Symposium on Nuclear Electronics, Vol.3, Article 1.
- Charpak, G., Rahm, D. and Steiner, H., 1970, Nucl. Instr. and Meth., 80, 13.
- Clark, G., 1963, "The Encyclopedia of x-rays and Gamma Rays", Reinhold.

- Cochran, L.W. and Forester, D.W., 1962, Phys. Rev., 126, 1785.
- Cottrell, T.L. and Walker, I.C., 1965, Trans. Faraday Soc. (G.B.)  
61, (8), 1585.
- Curie, P., 1902, Compt. Rend. Acad. Sci., 134, 420.
- Curran, S.C. and Craggs, J.D., 1949, "Counting Tubes", Butterworth.
- Davidson, N. and Larsh, A.E., 1948, Phys. Rev., 74, 220.
- Davidson, N. and Larsh, A.E., 1950, Phys. Rev., 77, 706.
- Debenham, P.H., Dehnhard, D. and Goodwin, R.W., 1969, Nucl. Instr.  
and Meth., 67, 288.
- Derenzo, S.E., Muller, R.A., Smits, R.G. and Alvarez, L.W., 1969,  
Lawrence Radiation Laboratory Report, U.C.R.L. 19254.
- Doehring, A., Kalbitzer, S. and Melzer, W., 1968, Nucl. Instr. and  
Meth., 59, 40.
- Doehring, A., Kalbitzer, S., Melzer, W. and Stumpi, W., 1969,  
Nucl. Instr. and Meth., 74, 42.
- Elbek, B. and Nakamura, M., 1961, Nucl. Instr. and Meth., 10, 164.
- English, W.N. and Hanna, G.C., 1953, Can. J. Phys., 31, 768.
- Frank, S.G.F., 1951, Phil. Mag., 7s, 42, 612.
- Gelernter, H., 1961, Nuovo Cimento, 22, 631.
- Giacconi, R. and Rossi, B., 1960, J. Geophys. Res., 65, 773.
- Giacconi, R., Reidy, W.P., Zehnpfennig, T., Lindsay, J.C. and Muney, W.S.,  
1965, Astrophysics Journal, 112<sup>2</sup>, 1274.
- Hanna, G.C., Kirkwood, D.H.W. and Pontecorvo, B., 1949, Phys. Rev.  
75, 985.
- Healey, R.H. and Reed, J.W., 1941, "The Behaviour of Slow Electrons  
in Gases", Amalgamated Wireless (Australasia) Ltd.
- Hodby, J., 1970, J. Phys. E. (Sci. Instr), 3, 229.

- Hofker, W.K., Costhoek, D.P., Hobberechts, A.M.E., Dantzig, R., Mulder, K., Oberski, J.E.J., Koerts, L.A., Dieperink, J.H., Kok, E., Runghorst, R.F., 1966, IEEE Trans. Nucl. Sci., NS-13(3), 208.
- Hutchinson, G.W., 1948, Nature, 162, 610.
- Jones, B.D. and Malos, J., 1964, Nucl. Instr. and Meth., 29, 115.
- Kahan, E. and Morant, M.J., 1965, Brit. J. Appl. Phys., 16(2), 943.
- Kalbitzer, S. and Melzer, W., 1967, Nucl. Instr. and Meth., 56, 301.
- Koester, L.J., 1970, IEEE Trans. Nucl. Sci., NS-17(3), 55.
- Kuhlmann, W.R., Lauterjung, K.H., Schimmer, B. and Sistemich, K., 1966, Nucl. Instr. and Meth., 40, 118.
- Kuhlmann, W.R. and Schimmer, B., 1966, Nucl. Instr. and Meth., 40, 113.
- Ladu, M., Pelliccioni, M. and Roccella, M., 1965, Nucl. Instr. and Meth., 37, 318.
- Lansiart, A. and Kellershohn, C., 1966, Nucleonics 24(3), 56.
- Lansiart, A., Morucci, J.P., Roux, G. and Leloup, J., 1966, Nucl. Instr. and Meth., 44, 45.
- Lauterjung, K.H., Pokak, J., Schimmer, B. and Staudner, R., 1963, Nucl. Instr. and Meth., 22, 117.
- Llewellyn-Jones, F., 1966, "Ionization and Breakdown in Gases", Methuen.
- Ludwig, E.J., 1965, Rev. Sci. Instr., 36, 1175.
- McDicken, W.N., 1967, Nucl. Instr. and Meth., 54, 157.
- Maglic, B.C. and Kirsten, F.A., 1962, Nucl. Instr. and Meth., 17, 49
- Maglic, B.C., 1963, Nucl. Instr. and Meth., 20, 165
- Marshall, J., 1954, Rev. Sci. Instr., 25, 232.
- Melzer, W. and Pühlhofer, F., 1968, Nucl. Instr. and Meth., 60, 201.
- Mertz, L., 1965, "Transformations in Optics", Wiley.

- Miller, L.S., Howe, S. and Spear, W.E., 1968, Phys. Rev. 166, 871.
- Minday, R.M., Schmidt, L.D. and Davis, H.T., 1969, J. Chem. Phys., 50, 1473.
- Morgue, M. and Chery, R., 1968, International Symposium on Nuclear Electronics, Vol.1, Article 31.
- Morse, P. and Feshbach, H., 1953, "Methods of Theoretical Physics", Vol.II, McGraw-Hill.
- Neumann, M.J. and Nunamaker, T.A., 1970, IEEE Trans. Nucl. Sci., NS-17(3), 43.
- Owen, R.B. and Awcock, M.L., 1967, A.E.R.E. Report, R 5393.
- Owen, R.B. and Awcock, M.L., 1968, IEEE Trans. Nucl. Sci., NS-15(3), 290.
- Perez-Mendez and Pfab, 1965, Nucl. Instr. and Meth., 33, 141.
- Perez-Mendez, 1967, Nucl. Instr. and Meth., 46, 197.
- Pétin, A., C.E.A. Report, R 3648.
- Plumley, H.J., 1941, Phys. Rev., 59, 200.
- Pullan, B.R., Howard, R. and Perry, B.J., 1966, Nucleonics 24(7), 72.
- Rose, M.E. and Korff, S.A., 1941, Phys. Rev., 59, 850.
- Rossi, B. and Staub, H., 1949, "Ionization Chambers and Counters", McGraw-Hill (National Nuclear Energy Series).
- Samuel, A.H., Halliday, F.O., Keast, A.K. and Taimuty, S.I., 1964, Science, NS-144, 839.
- Schlumbohm, H., 1965, Z. Physik, 182, 306.
- Schmidt, W.F. and Allen, A.O., 1970, J. Chem. Phys., 52, 4788.
- Scobie, J., 1969, Amer. J. Phys., 37, 107.
- Sharpe, 1964, "Nuclear Radiation Detectors", Methuen, Second Edition.
- Strauss, M.G. and Brenner, R., 1965, Rev. Sci. Instr., 36, 1857.
- Tol, T., Oosterkamp, W.J. and Proper, J., 1955, Philips Res. Rep. 10, 141.

Townsend, J.S., 1947, *Electrons in Gases*, Hutchinson's.

Tsukuda, H., 1964, *Nucl. Instr. and Meth.*, 25, 265.

Vorob'ev, A.A. and Korolev, V.A., 1962, *Instrum. Exper. Tech. (U.S.A.)*  
4, 664.

Wilkinson, D.H., 1950, "*Ionization Chambers and Counters*", C.U.P.

Young, N.O., 1963, *Sky & Telescope*, 25, 8.